Nitrogen Transport and Transformation Beneath Stormwater Retention Basins in Karst Areas and Effectiveness of Stormwater Best Management Practices for Reducing Nitrate Leaching to Ground Water
Marion County, Florida

By
Marty Wanielista, Ni-Bin Chang, Zhemin Xuan, Lisa Naujock, and Paul Biscardi

Stormwater Management Academy
Civil, Environmental and Construction Engineering Department
University of Central Florida
Orlando, FL 32816

October 2011

Disclaimer

The opinions, findings, and conclusions expressed in this publication are those of the authors and not necessarily those of the Florida Department of Environmental Protection, the Withlacoochee River Basin Board of the Southwest Florida Water Management District, and Marion County Board of County Commissioners or its employees.

© 2011

EXECUTIVE SUMMARY

This is a research and demonstration project in which the Florida Department of Environmental Protection (www.dep.state.fl.us/water/waters/stormwater) and Marion County (www.marioncountyfl.org) provided funding in partnership with the UCF Stormwater Management Academy, (www.stormwater.ucf.edu), and the Withlacoochee River Basin Board of the Southwest Florida Water Management District (www.swfwmd.state.fl.us). The St. Johns River Water Management District (www.sjrwmd.com) also provided in-kind services. In addition, some of the analytical and field services were conducted by the US Geological Survey (www.fl.water.usgs.gov) through a matching grant. Supplementary publications and presentation materials can be obtained from the Stormwater Management Academy at the University of Central Florida in Orlando, Florida and by accessing their web site at www.stormwater.ucf.edu.

Information in this report provides science and engineering data and explanations for the fate of nitrogen in the ground water beneath stormwater retention basins. The basins for the data collection are located in Marion County, Florida. Two retention basins constructed in two distinctly different types of soils are measured for their pollution retention capacity. The bottom soils in one retention basin, namely the South Oak (SO) basin, were found to remove nitrogen in the vadose zone or shallow ground water before it entered the deeper ground water flow system. While the other retention basin, namely the Hunters Trace (HT) basin, did not remove nitrogen. The Hunters Trace basin had a desirable design feature of infiltrating the stormwater at a faster rate than the South Oak basin and thus would reduce land for a retention basin compared to a slower infiltrating retention basin. Thus the physical, biological and chemical conditions at the

South Oak basin that contributed to the removal of nitrogen while not significantly decreasing the infiltration rate are determined and reported.

Within this publication is information that demonstrates a design using soil augmentation with Biosorption Activated Media (BAM) for the removal of nitrogen in water retention (infiltration) basins. The BAM constitutes a 1.0:1.9:4.1 mixture (by volume) of tire crumb (to increase sorption capacity), silt+clay (to increase soil moisture retention and sorption), and sand (to promote sufficient infiltration).

Water quality measurement data after HT basin modification shows a pollution control area that does remove nitrogen before it enters the ground water. Phosphorus removal was also measured. Data on infiltration rates, water volumes and depth in the basin, and water quality effectiveness were continued through October 2011 and shown that the effectiveness and infiltration rate did not change over a 24 month time period.

The HT retention basin is also permitted for flood control by the St. Johns River Water Management District. An integrated pollution and flood control design is attained that can function to remove nitrogen within existing retention basins in the Marion County, Florida area. For newly constructed integrated flood and pollution control retention basins, the design details for soil augmentation using BAM presented in this report can also be used.

Furthermore, BAM for nitrogen removal can be used with the goal of pollution control at a separate site or integrated with flood control. The idea of soil augmentation may be used in the bottom of on-site retention systems, such as those know as Low Impact Development (LID) methods. It is anticipated that the soil augmentation will better protect ground water as well as

surface water quality by enhancing nitrogen removal, as well as to demonstrate cost savings relative to other methods.

Another benefit of the soil augmentation used in this report is the use of Florida naturally occurring soils and blending them with recycled materials. The process is also deemed economical as the initial conversion cost for the Hunters Trace basin was only about $6.00 per square foot of basin bottom. This cost did not include profit and permit fees. There is minimal to no additional operation and maintenance cost, and operation, maintenance, and repairs are similar to those expected with existing retention systems.

Scientific and engineering data in this report are continuous measurements of hydrologic and hydraulic conditions and discrete samples for soil, basin water, soil gas, soil water, and shallow groundwater that are analyzed for multiple biogeochemical indicators, including denitrifier activity by quantitative real-time polymerase chain reaction (qPCR), major ions, nutrients, dissolved and soil gases, and stable isotopes. Comparison of nitrate/chloride (NO_3^-/Cl) ratios for the shallow groundwater indicate that prior to using BAM, NO_3^- concentrations were substantially influenced by nitrification or NO_3^- input increases with isolated periods of conservative movement. In contrast, the biogeochemical and qPCR data with post-BAM NO_3^-/Cl ratios indicate NO_3^- loss. This ratio and biogeochemical data suggest NO_3^- losses are occurring in the amended layer before the water is measured in the well. After construction, denitrifying bacteria gradually acclimated to the new environment and exponentially increased in the BAM layer concurrent with the drop in DO level and then NO_3^- losses became significant in about 9 months or in August 2010. The water chemistry, soil and dissolved gas, isotopic, and real-time PCR analyses suggest that most NO_3^- losses are attributable to denitrification, which

likely is intermittent; whereas soil chemistry results suggest possible NO_3^- losses due to dissimilatory nitrate reduction to ammonium. Intermittent denitrification is likely occurring in anoxic microsites and sustained by the soil moisture conditions within the BAM layer and resultant reductions in surface/subsurface oxygen exchange. For the specific design of the augmentation soils, a total nitrogen removal up to about 50% is achieved. A stable NOx/Cl ratio during the 8-month verification period in 2011 suggests NO_3^- losses in the BAM layer were similar to those occurring in August 2010. Concentrations of total dissolved phosphorus and orthophosphate (PO_4^{3-}) were reduced by greater than 70% in vadose zone soil water likely caused by sorption in the BAM layer. Post-BAM PO_4^{3-}/Cl ratios for shallow groundwater indicate PO_4^{3-} was predominantly moving conservatively or removal of PO_4^{3-} occurred at shallower depths (likely in the BAM layer). Also, during the 8 month verification time period, the pollution control basin continues to function at the same infiltration rate and to remove both nitrogen and phosphorus species.

Given a target level capture of annual runoff volume equal to 85% for a pollution control retention basin with augmented soils and a limiting infiltration rate of 0.25 in/hr, the recommended pollution control basin size in Marion County should be calculated based on 3 inches of rainfall. For the HT basin, the pollution control basin is sized on the runoff from 3 inches over the Effective Impervious Area (EIA). From a simulation of two years (2004-2005) of rainfall, the capture runoff is 86% of the runoff amount. These years had more than the average rainfall (about 57 inches per year compared to about 50 inches per year). For an average rainfall volume in a year, the capture is about 88% of the annual runoff.

Using the continuous pond depth data after a runoff event, an average infiltration rate is measured at 0.37 in/hr during the verification time period. Also, a double ring infiltrometer embedded 2 inches into the upper layer of soil and an embedded ring infiltrometer into the parent soil beneath the amended layers is used to estimate limiting infiltration rates. Each method estimated a limiting infiltration rate of about twice the actual operating basin infiltration rate. Thus, it is recommended that the limiting infiltration rates obtained from either a double ring or embedded ring into parent soil should be reduced by at least one-half to estimate the actual limiting operating infiltration rate. Furthermore, it is recommended that a limiting infiltration rate of 0.25 in/hr be used for design and simulations. It is noted that the HT basin is over 25 years old, and compaction appears to be at the maximum in the pollution control and flood control areas of the basin.

The berm for an integrated basin design must be protected against erosion to provide the operational pollution control volume. The depth of the pollution control HT basin is 2.5 feet and is used to provide the volume for retention in the pollution control basin. The pollution control basin will completely empty in 120 hours at a 2.5 feet depth and a limiting infiltration rate of 0.25 in/hr. Visual observation during two storms which over-topped the berm showed that the pollution control basin drain time varied from 60 to 120 hours. Using an average infiltration rate from the storage depth data during measured runoff events after the integrated design, the average rate of infiltration is about 0.35 inch/hour, thus the 2.5 foot deep pollution control basin will empty in 86 hours.

Results of the extensive field testing demonstrate the pollutant removal effectiveness and infiltration capacity of using the functionalized soil amendment which is a Biosorption Activated

Media (BAM). Not every mix will perform as well and thus, the amended material mix must have data sheets on soil moisture retention, removal effectiveness, and infiltration rates before approved for application.

The design provides a passive and economical stormwater nutrient-treatment technology. It is recommended that the information in this report be used to improve the design of stormwater treatment systems to remove nitrogen, especially where the site location is feasible to use BAM. The installation of soil augmentation is not difficult and common existing construction methods are used. The design information should also be used to educate builders, engineers, scientists, private citizens, government officials, and students on the benefits of BAM and in particular the design used at Hunters Trace Basin.

ACKNOWLEDGMENT

Table of Contents

LIST OF FIGURES

LIST OF TABLES

CHAPTER 1: INTRODUCTION

Introduction

In Marion County Florida, two retention basins are studied to document the removal of nitrogen as stormwater infiltrated into the ground water beneath the basins. Marion County is located in north-central Florida and in a Karst region. The location of the two retention basins is shown in Figure 1 along with a record of ground water nitrate concentrations.
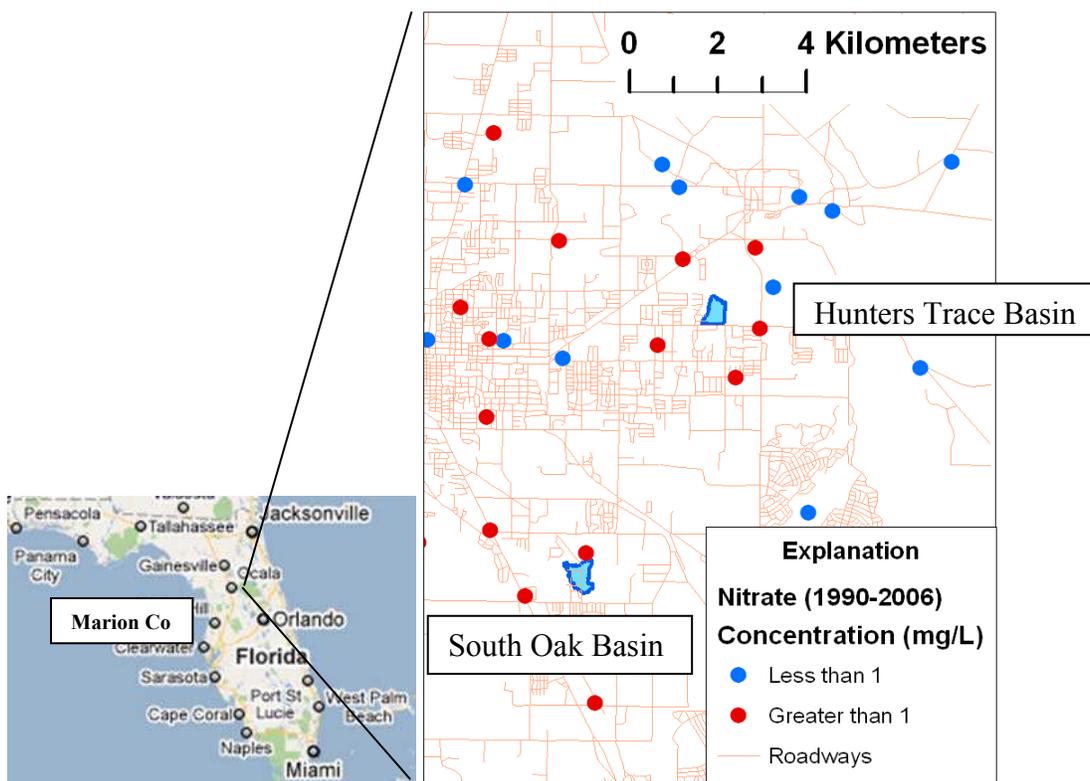
Figure 1 Locations of retention basins studied in Marion County, Florida. Ground water nitrate concentrations as reported by O'Reilly et al. (2007).

The nitrogen levels in some springs in Florida have been steadily increasing throughout the past 30 years and have had an impact on the economy of the region and especially on water based tourism and local resident activities in surface waters.

Nitrate concentrations have increased in many Upper Floridan aquifer springs since the 1950s, exceeding 1 mg/L in recent years at some springs (Spechler and Halford, 2001; Phelps, 2004). The Upper Floridan aquifer is particularly vulnerable to impacts from land-use activities in Karst/high recharge areas, where the aquifer is not confined or only thinly confined, such as exist throughout much of Marion County. Phelps (2004) reported that nitrate concentrations ranged from less than 0.02 to 12 mg/L, with a median of 1.2 mg/L, for 56 Upper Floridan aquifer wells sampled in Marion County during 2000–2001. Stormwater runoff is one possible source of nitrogen, among others such as septic tanks and land-based application of reclaimed water or fertilizer, which can contribute to elevated nitrate concentrations in the Upper Floridan aquifer. St. Johns River Water Management District (2005) has identified "sensitive Karst areas" in Alachua and Marion Counties where potential contamination of the Upper Floridan aquifer from stormwater is greater than in areas where the overburden layer is thicker.

As a State-wide unified rule for stormwater is developed there is a need to quantify using field and laboratory data the effects on the aquifer from stormwater retention basins. Schiffer (1988), Harper and Herr (1993), Wanielista and Hulstein (2006), and Wanielista et al. (2006) collected water-quality data on the effects of various stormwater best management practices (BMPs) on ground water quality. However, in general, little research is available for a quantitative process-based understanding of the effects of stormwater on ground water or the fate

of nitrogen. This research will provide data and interpretative analysis to assist in this quantification.

Objectives

The objectives of this study are to:

(1) Measure nitrogen concentrations associated with ground water beneath two stormwater retention basins;

(2) Identify and evaluate the natural processes (physical, chemical, and biological) that control the nitrogen cycle in soil and ground water beneath the retention basins;

(3) Identify an alternative design for infiltration best management practices (BMPs) that could reduce the impact of nitrogen in stormwater on ground water; and

(4) Compare nitrogen transport and transformation and nitrate removal for both existing stormwater management designs and an alternative design.

Roadmap for Report

Chapter 1 is an introduction to the study objectives. Also, a roadmap to the report is presented. In Chapter 2, results of background monitoring results from both basins are compared and contrasted, and interpretations are made regarding denitrification and other biogeochemical processes. In Chapter 3, information is presented on the development of the integrated pollution and flood control design at the Hunters Trace basin. In Chapter 4, an evaluation of the performance of the integrated pollution and flood control design at the Hunters Trace basin is

presented, and interpretations are made regarding nitrate transport and fate. A summary with conclusions and recommendations is presented in Chapter 5.

Scope and Limitations

This study focuses on ground water recharge and nitrogen transport and transformation beneath stormwater infiltration (dry) basins. Nitrogen impacts on ground water up-gradient and down-gradient of each basin are investigated. The selected stormwater infiltration basins are in the Karst/high recharge areas of Marion County, Florida. These areas are representative of similar environmental settings elsewhere in Florida where the underlying aquifer system is vulnerable to impacts from land use activities. Specific results presented herein are limited to the two retention basins studied, however the general principles elucidated in this study will be transferable to many similar environmental settings both within and outside Florida.

Existing and alternative infiltration BMP design criteria are studied. The existing design criteria for a typical stormwater infiltration basin is natural soil, unmodified except by possible incidental compaction during the construction process, and the addition of vegetation on the sides and bottom such as sod. Alternative design criteria focus on different media (natural soil and amendment mixtures) that could facilitate nitrate removal. Success of this technique has been demonstrated in a saturated ground water setting in the context of contaminant remediation (Schipper and Vojvodic, 2000; Schipper and Vojvodic, 2001; and Schipper et al., 2004). Shaddox (2004) reported no nitrate leaching with the use of surfactant-modified amendments in golf course putting greens. Wanielista and Hardin (2006) have also reported substantial nitrate removal with select media used in a green roof system with a cistern.

CHAPTER 2: EXISTING RETENTION BASINS in MARION COUNTY

Introduction

Marion County is about the size of the State of Rhode Island. The environmental protection from stormwater pollutants results in the use of many stormwater management methods. Many of these methods are considered retention basins, and sometimes are called infiltration basins because under current rainfall and runoff conditions, the basins will infiltrate the runoff waters from storms up to those characterized as occurring once every 100 years. Retention basins are a commonly used stormwater management practice in Marion County for runoff quantity and quality control. Or as other options, retention can be promoted near the source. Using retention source control, such as bioretention or bioswales, or regional retention basins, a great majority of the stormwater finds its way to the ground water. If nitrogen and other pollutants are not removed before gaining access to the ground water, some compounds, such as nitrate (a form of nitrogen) may continue to exist and make its way to adjacent springs or become part of well waters.

Within this chapter of the report are data on two retention basins that were instrumented to measure the fate of nitrogen and other pollutants transported to the ground water from storage within the two basins. Physical, biological, and chemical measures were taken to define the conditions which may affect the fate and transport.

Objectives

Within this chapter the data collected at the South Oak and Hunters Trace retention basins during 2007–2009 are used to characterize the hydrologic and water quality conditions for

the existing retention basin designs. Next, these results are interpreted in order to identify and evaluate the natural processes (physical, chemical, and biological) that control the nitrogen cycle in soil and ground water beneath the retention basins. Lastly, some discussion of the factors controlling biogeochemical processes at both sites is presented.

Data Collection

The project called for the selection of two dry retention basins in a karst environment in Marion County. Basins were to be located in a residential land use; one basin could be located in a commercial land use if possible. The Hunters Trace and South Oak basins (Figure 1) were selected using a multistep process:

1) Marion County staff initially screened a large number of basins and selected about two dozen basins.

2) Marion County and Stormwater Management Academy staff visited each basin to assess suitability.

3) A subset of candidate basins was selected for further review.

4) Four candidate basins were selected. Marion County contracted Andreyev Engineering Inc. to conduct a continuous standard penetration test and lithologic description at each candidate basin.

5) Based on the standard penetration test results, the two final basins were selected

Several criteria were used during the selection process:

1) Site access: drill rig access, utility locations, property ownership, and local homeowner concerns.

2) Geologic conditions: lithology of shallow sediments, depth to limestone, and sinkhole presence/active karst activity.

3) Hydrologic conditions: well-defined watershed, water-table depth, and infiltration capacity.

Due to the concern of potential sinkhole presence/active karst activity, the Stormwater Management Academy contracted Subsurface Evaluations, Inc. to perform a ground penetrating radar survey at both the South Oak and Hunters Trace sites. The radar signal was attenuated and did not penetrate to the top of limestone because of the prevalence of fine-grained sediments at each site. Nevertheless, these fine-grained sediments served as subsurface reflectors for the radar signal, and results indicated no active karst activity at either site as inferred from the absence of truncated or dramatically down warped subsurface reflectors (Figure 2). Therefore, these two basins were selected for intensive monitoring.

South — Hunters Trace pond - east berm — North

0 ft — 0 ns

20 ft

Approx. depth, in feet bls

Two-way travel time, in nanoseconds

Top of 30-in culvert

Possible water table and/or clay layer

360 ns

0 ft — Distance — 140 ft
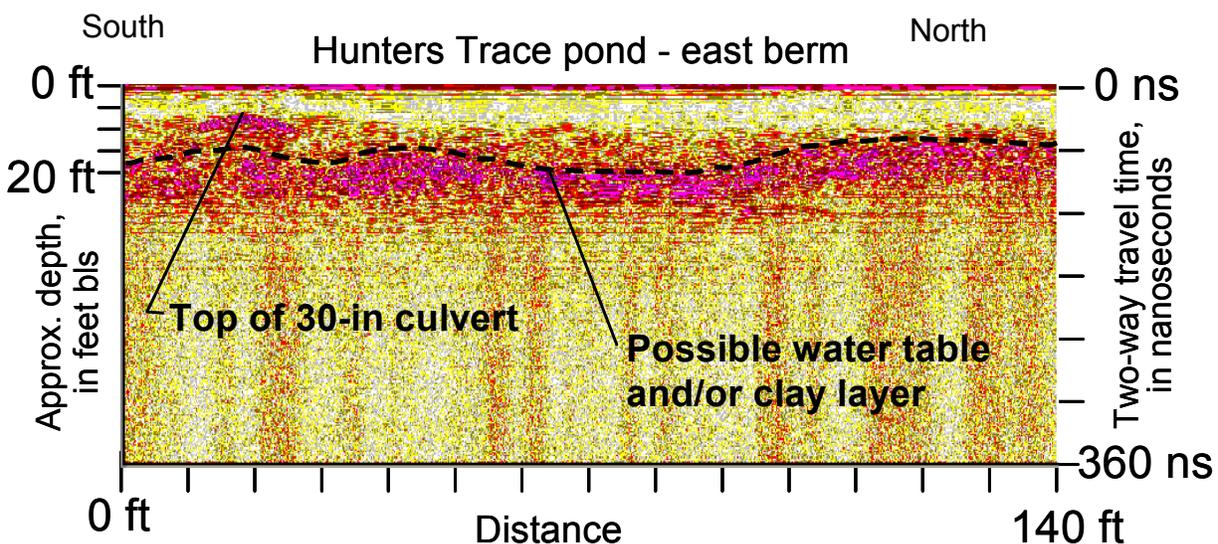
Figure 2 Ground penetrating radar profile along part of the east berm of the Hunters Trace basin.

Both the South Oak and Hunters Trace retention basins are located in the Silver Springs springshed and were monitored during 2007–2009 to identify subsurface biogeochemical processes (Figure 1). The Silver Springs springshed is characterized by karst topography consisting of predominantly internal drainage into closed depressions or diffuse seepage into the highly permeable surficial sediments (Phelps, 2004). Climate of the area is humid subtropical, with hot, rainy summers and cool, relatively dry winters (Phelps, 2004). Long-term (1901–2008) rainfall averages about 1360 mm/yr (53.5 inches) and daily air temperature averages about 22°C at the National Oceanic and Atmospheric Administration (NOAA) Ocala station (station index number 6414) approximately 7 and 13 km south of the two retention basins. For 2007–2009, annual average rainfall ranged from 1120 to 1400 mm/yr; minimum daily air temperature averaged about 15°C; and maximum daily air temperature averaged about 28°C. Potential

evapotranspiration averages about 1250 mm/yr (49.2 inches) (1996–2009) as computed by the Priestley-Taylor equation for a 2-km pixel covering the NOAA Ocala station according to the methodology of Jacobs et al. (2008).

Both retention basins are located in watersheds that have transitioned from rural to residential land use during 1973–1990. The basins were designed to retain the runoff from a 100 year storm event. The South Oak (SO) basin is 1600 m^2 (17,000 ft^2) in bottom area with a watershed of 29 ha (72 acres); the Hunter's Trace (HT) basin is 2800 m^2 (31,000 ft^2) in bottom area with a watershed of 23 ha (56 acres). Both basins function as infiltration basins without surface outlets. The SO basin occupies a natural land surface depression and was excavated to a depth of about 1 m, although it overflows during prolonged or intense storm events and remains confined to the natural depression. The HT basin was excavated to a depth of about 3 m in a relatively flat terrain and remains confined to the basin boundaries even during extreme storm events. In the HT basin watershed, the stormwater conveyance system consists of curb-and-gutter roadway; whereas, in the SO basin watershed roadside swales are the primary system used to convey runoff to the basin. Given the karst, well drained terrain, the majority of each retention basin's watershed probably does not contribute runoff to the basin except perhaps during extreme, prolonged storm events.

Hydrologic monitoring consisted of the following: rainfall, basin stage, ground water level, subsurface temperature, and volumetric moisture content (Figure 3). Rainfall was measured with a tipping bucket gage; basin stage and ground water level were measured with submersible pressure transducers, temperature was measured using thermistors, and volumetric water content was measured using time domain reflectometry (TDR). TDR measurements were

adjusted, as necessary, based on gravimetric measurement of volumetric moisture content on undisturbed soil cores at field and saturated moisture contents. Data were recorded at 5-minute intervals from December 2007 through October 2010.

Monitor wells were installed at each site by hollow-stem auger in March 2007. The wells consisted of a 5.1-cm-diameter polyvinyl chloride casing with a 1.5-m-length screen. Wells were screened in the shallow surficial aquifer system (within 4 m below the water table) with the exception of one well at each site which was screened approximately 15 m deeper in the surficial aquifer system. At the SO site, one shallow well was installed inside the basin, and seven wells were installed around the perimeter of the basin (Figure 3a). At the HT site, one shallow and one deep monitor well were installed inside the basin, and four wells were installed around the basin perimeter (Figure 3b). Well construction details are provided in Table 1. Suction lysimeters (20 cm long porous cup, 1.1 L volume) were installed at each site by hand excavation at depths of 0.5, 0.9, and 1.4 m (1.3 m at HT) inside the basin adjacent to the well (Figure 3). TDR and thermistor probes were installed adjacent to the lysimeters by hand excavation and insertion into the undisturbed excavation wall at depths of 0.3, 0.6, and 0.9 m.
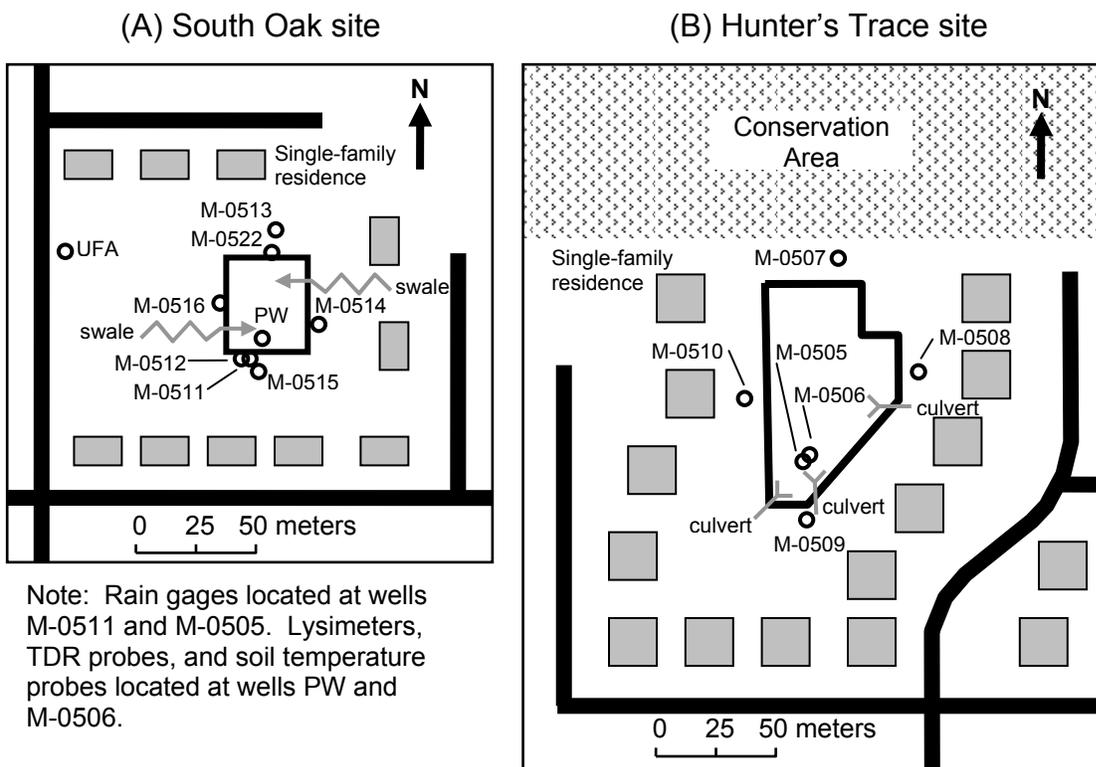
Figure 3 Locations of monitoring sites at the (a) South Oak basin, and (2) Hunter's Trace basin.

Table 1 Monitoring wells construction details. Well locations shown in Figure 3.

Name	Well Dia. (in)	Total Depth (ft bls)	Screen Length (ft)	Wellhead Completion
M-0505 HT Basin deep	2	30.7	5	3.7-ft stickup
M-0506 HT Basin shallow	4	15.2	5	3.7-ft stickup
M-0507 HT Perimeter N	2	30.6	5	8-in manhole
M-0508 HT Perimeter E	2	30.3	5	8-in manhole
M-0509 HT Perimeter S	2	30.2	5	8-in manhole
M-0510 HT Perimeter W	2	31.5	5	8-in manhole
M-0511 SO Basin deep	2	29.7	5	5.7-ft stickup
M-0512 SO Basin shallow	4	7.9	5	5.7-ft stickup
M-0513 SO Perimeter N	2	20.6	5	3.9-ft stickup
M-0514 SO Perimeter E	2	10.4	5	5.2-ft stickup
M-0515 SO Perimeter S	2	10.9	5	2.9-ft stickup
M-0516 SO Perimeter W	2	10.2	5	5.4-ft stickup
M-0522 SO Perimeter N2	2	10.2	5	5.3-ft stickup
PW SO Basin Well shallow #2	2	8.8	5	6.8-ft stickup
UFA (unused domestic well)	4	84.5	1.5	0.8-ft stickup

11

A variety of soil physical, mineralogical, and chemical properties were measured on samples collected at both sites. Soil samples were collected at depths ranging from 0.1 to 32 m in both the surficial aquifer system and intermediate confining unit. Soil physical property measurements consisted of particle size gradation, bulk density, particle density, soil moisture retention curve (SMRC), and saturated hydraulic conductivity. Soil mineralogical and chemical analyses were performed at the University of Florida Soil Core Laboratory in Gainesville, FL under the direction of Dr. W.G. Harris. Samples were analyzed for silt and clay mineralogy by x-ray diffraction, iron (Fe) and aluminum (Al) oxyhydroxides using acid-ammonium oxalate extraction (AAO) and citrate-dithionite-bicarbonate-extraction (CDB), phosphorus by CDB extraction, pH, electrical conductivity, cation-exchange capacity (CEC), anion exchange capacity (AEC), soil solids N and C contents, and extractable N and C contents. Soil solids were analyzed for organic carbon (OC), total carbon (TC), and total nitrogen (TN). Both KCl and water extractions were performed and analyzed for NH_4^+, NO_3^- plus NO_2^- (denoted NO_x), and NO_3^-; water extractions were additionally analyzed for OC, TC, and TN.

Water samples were collected for atmospheric deposition samples (wet and bulk), stormwater, soil water (suction lysimeters), and ground water (wells). Water samples were collected following standard USGS protocol (U.S. Geological Survey, 1998). Monitor wells were purged until at least three casing volumes of water were removed, and field parameters (temperature, specific conductance, pH, dissolved oxygen, and redox potential) had stabilized. Field parameters were measured at all well sites using YSI 556MPS multiparameter sonde (prior to May 2008) and YSI 6920 V2 multiparameter sonde (May 2008 and later) in a flow-through chamber. Sondes were calibrated daily against known standards according to standard USGS

protocols (Wilde and Radtke, 1998). Stormwater samples were collected from water at five locations within each basin and composited by stirring. Soil-water samples were collected by first purging the lysimeter and then applying a pressure of −60 kPa and allowing the lysimeter to fill for 6−48 hours, depending on ambient soil moisture content. Atmospheric air was used to apply a pressure to force the water into a 1 L amber glass bottle from which water was withdrawn by peristaltic pump for filtration and bottle filling. Atmospheric deposition samples (wet and bulk) were obtained by collection in an 8 L plastic bucket from which water was withdrawn by peristaltic pump for filtration and bottle filling. Alkalinity was determined for all samples by incremental titration with 0.16 N or 1.6 N sulfuric acid. Water samples were collected for laboratory analysis of major elements, trace elements, nutrients, and organic carbon. All major element, trace element, nutrient, and organic carbon samples were shipped to the USGS National Water-Quality Laboratory in Denver, Colorado. Analytes and laboratory reporting limits are listed in Appendix A.

In addition to the standard wet chemistry analyses, dissolved gas and isotopic analyses were also performed. Ground water samples were analyzed for major dissolved gases (Ar, N_2, O_2, CO_2, and CH4) by gas chromatograph according to the methods of Busenberg et al. (2001) by the USGS Chlorofluorocarbon Laboratory in Reston, VA. Isotopic values are reported using standard delta (δ) notation (Clark and Fritz, 1997) as follows:

$$\delta R_{sample} = \left[\left(R_{sample}/R_{standard} \right) - 1 \right] \times 1000$$ for $\delta^{15}N$, R = $^{15}N/^{14}N$; for $\delta^{18}O$, R = $^{18}O/^{16}O$; and for δ^2H, R = $^2H/^1H$. Results are reported in parts per thousand (per mil, ‰). N isotopes are reported relative to N_2 in air; O and H isotopes are reported relative to Vienna Standard Mean Ocean Water (VSMOW). $\delta^{15}N$ values of NO_3^- and dissolved N_2, $\delta^{18}O$ values for NO_3^- and H_2O, and

δ^2H for H_2O were determined. Isotopic analysis of NO_3^- and H_2O samples was performed by the USGS Reston Stable Isotope Laboratory in Reston, VA. NO_3^- samples were analyzed by bacterial conversion of NO_3^- to nitrous oxide and subsequent measurement on a continuous flow isotope ratio mass spectrometer (Sigman et al., 2001; Casciotti et al., 2002; Coplen et al., 2004; Revesz and Casciotti, 2007). $\delta^{18}O$ of H_2O was determined using the CO_2 equilibration technique (Epstein and Mayeda, 1953; Revesz and Coplen, 2008b). δ^2H was determined using a hydrogen equilibration technique (Coplen and others, 1991; Revesz and Coplen, 2008a). Isotopic analysis of N_2 samples was performed by the research lab of J.K. Bohlke (U.S. Geological Survey, Reston, VA) based on the method outlined by Bohlke et al. (2004).

Quantitative real-time polymerase chain reaction was applied to gain insight into denitrifier activity by measuring NO_2^- reductase gene density in the soil. Analyses were performed by Z. Xuan under the direction of N. Chang at the University of Central Florida according to the methods described by Xuan et al. (2009). Since the reduction of NO_2^- to nitric oxide is the core step in the dissimilative denitrification process, the two NO_2^- reductase genes, *nirK* and *nirS*, encoding the cd1 and copper nitrite reductase, respectively, were regarded as the key denitrifying enzyme, and most used to measure the denitrification in this area. Braker et al. (1998) validate the suitability of the method for the qualitative detection of denitrifying bacteria by using *nirK* and *nirS* targeted primer in environmental samples.

Results of hydrologic monitoring and water and soil sampling are presented in the following sections. Isotope, dissolved gas, and soil sampling were concentrated primarily from March−December 2008; hydrologic monitoring and water sampling were conducted prior to this

period; and hydrologic monitoring and water and soil sampling were conducted following this period.

Hydrologic and Soils Data

The 5-minute hydrologic monitoring data were composited into daily values (summed for rainfall and averaged for all other values) for 2008−2009 (Figure 4). Annual rainfall was slightly higher at the SO site than the HT site, but was close to the long-term average and similarly distributed in time at both sites. Two particularly large rainfall events occurred in August 2008 (Tropical Storm Fay) and May 2009, resulting in substantial and prolonged water holding in both basins. Substantial differences are apparent in the magnitude and frequency of water holding at each site, which are indicative of lower infiltration rates at the SO basin. Infiltration rates were estimated by analysis of basin stage recession curves for several storm events in 2008−2009. For 46−155 mm (1.8−6.1 inches) rainfall events (5−33 h duration), infiltration rates were 14−29 mm/d (0.55−1.1 in/d) at the SO basin, while at the HT basin infiltration rates were 170−260 mm/d (6.7−10.2 in/d).

(A) South Oak site

(B) Hunters Trace site
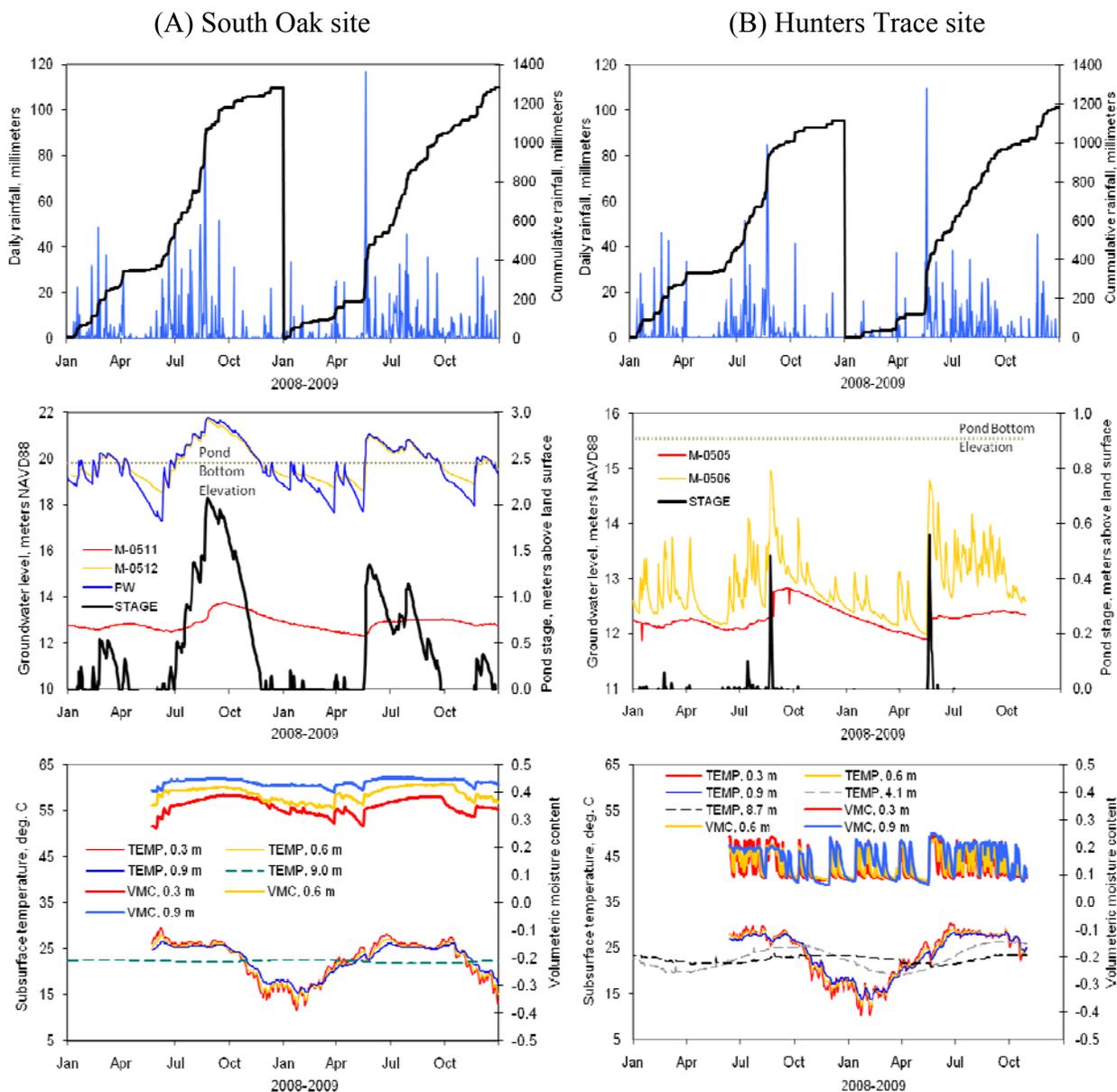
Figure 4 Hydrologic monitoring of rainfall, basin stage, ground water level, soil moisture content, and subsurface temperature at the (a) South Oak stormwater infiltration basin, and (b) Hunter's Trace stormwater infiltration basin.

The response of all the hydrologic variables to climatic forcing (rainfall and air temperature) is clear, showing good hydraulic communication between the surface and

subsurface environments at both sites. The hydraulic communication is considerably more subdued at the SO site compared to the HT site. The highly attenuated response of well M-0511 at the SO site is due to a prevalence of fine-grained sediments leading to large vertical head gradients of 0.90−1.3 m/m between M-0511 (9.1 m deep) and M-0512 (2.5 m deep), indicating a perched water table beneath the basin at times. The two wells inside or at the edge of the typical water holding area (M-0512 and PW, Figure 3a) tap the shallow water table that responds rapidly to runoff events; subsequently, water percolates slowly through the sandy silts and clays to the regional water table tapped by well M-0511. The nearly constant temperature signal at a depth of 9 m (measured in M-0511) further indicates the attenuating effects of the shallower fine-grained sediments forming the shallow water table. Despite this thick soil profile, much of the important chemical evolution of the infiltrated stormwater occurs in the shallow vadose and water-table zones. In contrast, at the HT basin the relatively well drained soils led to more rapid surface-subsurface transmission of climatic forcing as indicated by relatively small vertical head gradients of 0.014−0.57 m/m between M-0505 (9.4 m deep) and M-0506 (4.6 m deep). Distinct sinusoidal temperature signals are evident throughout the soil profile, even at a depth of 8.7 m (measured in M-0505), further indicating more rapid movement of ground water beneath the HT basin compared to the SO basin.

Hydrogeologic conditions at each basin are quite different. Soils at the SO site generally are finer textured than those at the HT site (Figure 5a). Textural differences contributed to substantial difference in SMRCs and other soil properties (Figure 5b). The greater moisture retention characteristics of the soil at the SO site support the wet to nearly saturated conditions that existed beneath the basin even during prolonged dry periods; whereas, the relatively coarse

textured soil at the HT site dried rapidly after infiltration events (Figure 4b). As a result of these differences in soil physical properties, the water table typically was less than 1 m deep at the SO basin and less than 3 m deep at the HT basin (Figure 4).
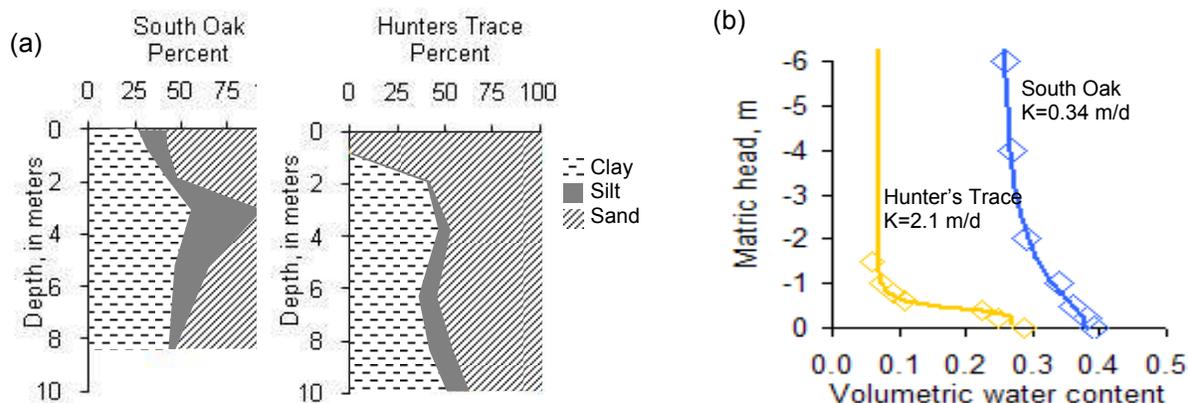
Figure 5 Soil properties at the infiltration basins: (a) textural variations with depth; (b) soil moisture retention curves reported by Naujock (2008) for undisturbed cores collected from 0.3 m depth (K, saturated hydraulic conductivity).

Samples at well M-0506 (0.8 m depth) and M-0508 (8.2 m depth) at the HT basin are typical of weathered Florida sandy soils with respect to mineralogy, showing the common suite: hydroxyl interlayered vermiculite, kaolinite, gibbsite, and quartz (Harris et al., 1987). The shallow soils at the HT site are predominantly sandy at depths up to approximately 2 m below the bottom of the basin (approximately 5 m below surrounding natural land surface). At the SO site, substantial silt and clay generally are present throughout the soil profile. Most of the clay mineralogical components of soils at both sites are consistent with Miocene phosphorites or the soils forming in those materials (Wang et al., 1989), including the phosphate mineral apatite,

along with smectite and kaolinite. Smectite was particularly prevalent at the SO basin. Silt fractions are dominated by quartz and/or apatite.

P, Fe, and Al concentrations generally were greater at the SO site than the HT site (Appendix B). High P contents at certain depths at both sites are due to the prevalence of phosphate minerals. Fe and Al concentrations are important due to the high sorption capacity of the oxyhydroxides of these metals. AAO extractable Fe was quite high compared to typical Fe content of most Florida soils, exceeding 1% (>10,000 mg/kg) for 5 of the 22 samples analyzed. Furthermore, AAO extracted nearly as much Fe as did CDB, and in some cases more, suggesting that most of the Fe present in the material was noncrystalline. Amorphous Fe generally has greater sorption capacity than crystalline forms.

Soils at the SO site generally have high CEC of 7−52 cmol$_c$/kg, further indication of favorable sorption conditions; whereas CEC of soils at the HT site were lower, 1.1−19 cmol$_c$/kg (Appendix B). Smectite is a secondary expansible phyllosilicate group mineral with high surface area conducive to a high CEC. AEC was relatively low at both sites, ranging from 0.4 to 5 cmol$_c$/kg (Appendix B).

Soil solid and extractable N and C concentrations indicate important differences between sites and temporal variations at each site (Figures 6 and 7). At the SO site, results indicate different N and C characteristics in the late winter/spring (March and May) before the prolonged summer wet period compared to autumn (November and December) after the prolonged summer wet period (Figure 4a). Soil solids analyses indicate slightly lower OC concentrations in autumn compared to spring, although TN concentrations generally were similar (Figure 7). Results of soil water extractable analyses generally indicate increases in water extractable OC and IC

concentrations from spring to autumn at depths less than 1.3 m, but were generally unchanged below this depth (Figure 7). The increases in water extractable OC compared to the decreases in soil solids OC are consistent, at least qualitatively, with mass transfer of OC between solid and aqueous phases. Increases in water extractable IC from spring to autumn may be indicative of a zone of active biogeochemical processes in the shallow soil zone 0–1.3 m deep. Because OC is the preferred electron donor for a wide variety of redox reactions, such as NO_3^-, Mn, or Fe reduction, increases in IC may be caused by mineralization of OC substrates to CO_2 and HCO_3^-. Substantial reductions in soil solid IC may also explain the increases in water extractable IC. The near absence of NO_x in water extractable samples in autumn is suggestive of denitrification or dissimilatory nitrate reduction to ammonium (DNRA) during the summer wet season (Figure 6). NO_x comprises primarily NO_3^-; samples analyzed for both NO_3^- and NO_2^- indicate that NO_2^- was typically less than 10% of NO_3^-. The increased NH_4^+ concentrations in November may be due to DNRA, whereas the decreased NH_4^+ combined with slight NO_x concentrations in December likely is due to nitrification in uppermost soil layers as the basin dried and denitrification in the portions of the underlying soil zone that remained saturated (Figures 4 and 6).

(A) South Oak
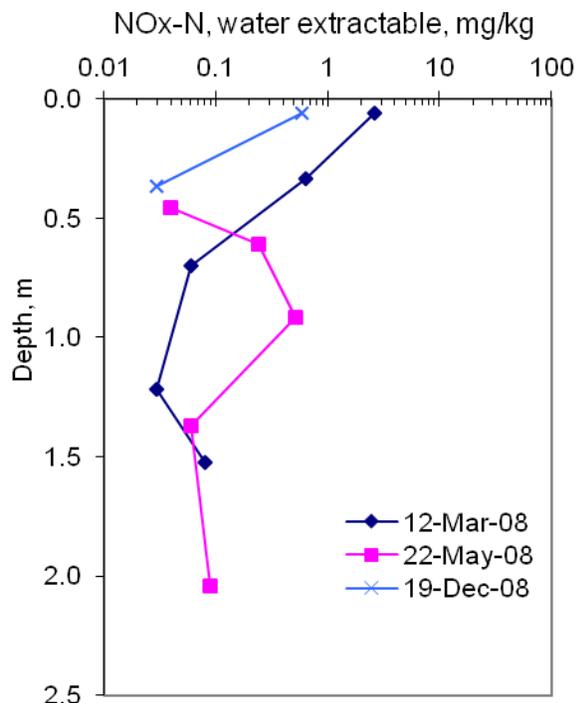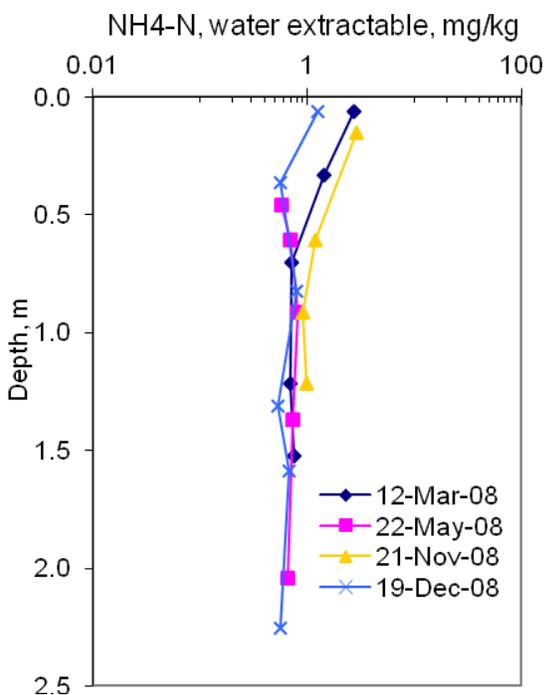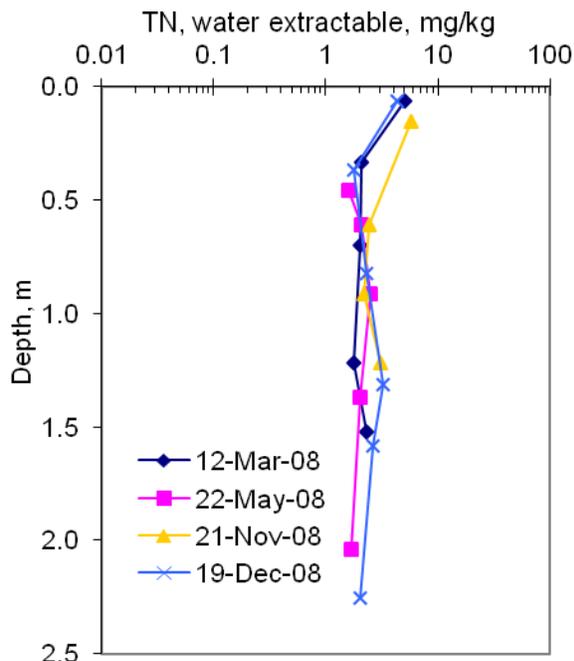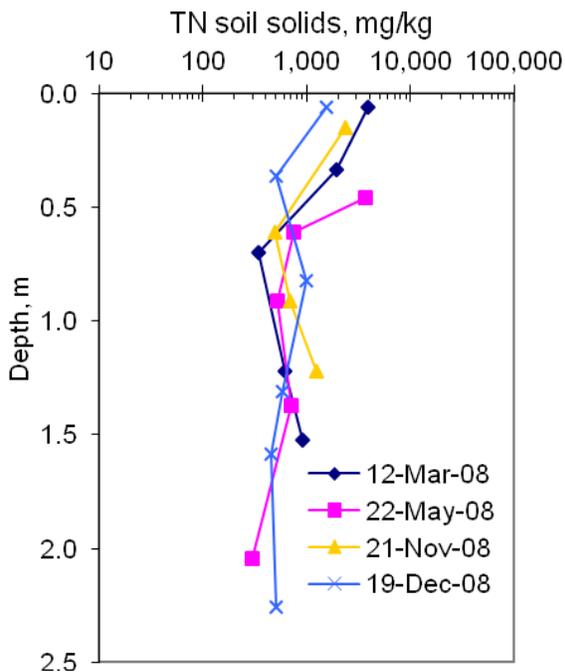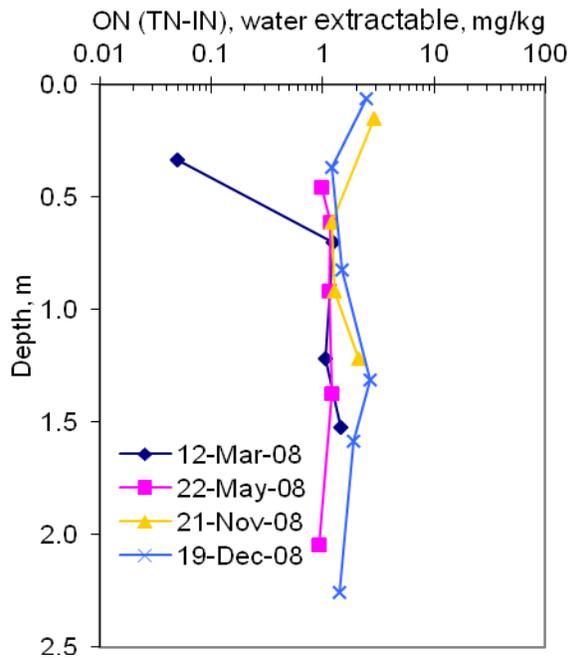
Figure 6a Soil solid and water extractable total nitrogen (TN) and soil water extractable ammonium nitrogen (NH$_4^+$), nitrate plus nitrite (NO$_x$), and organic nitrogen (ON) at the South Oak stormwater infiltration basin.
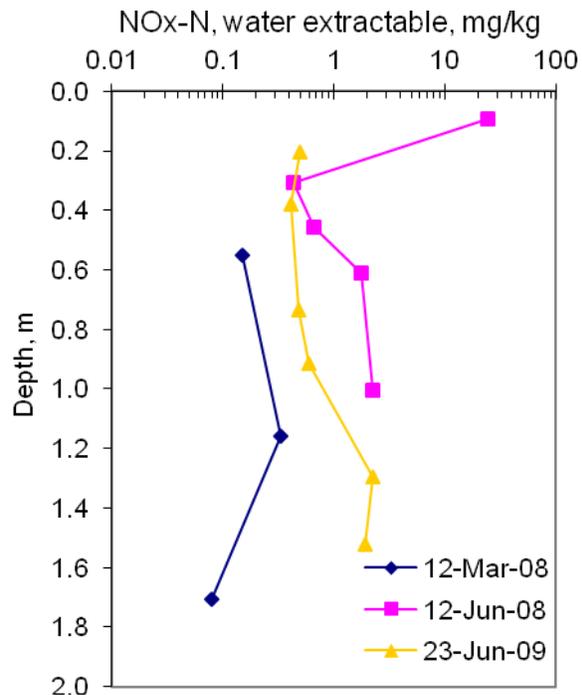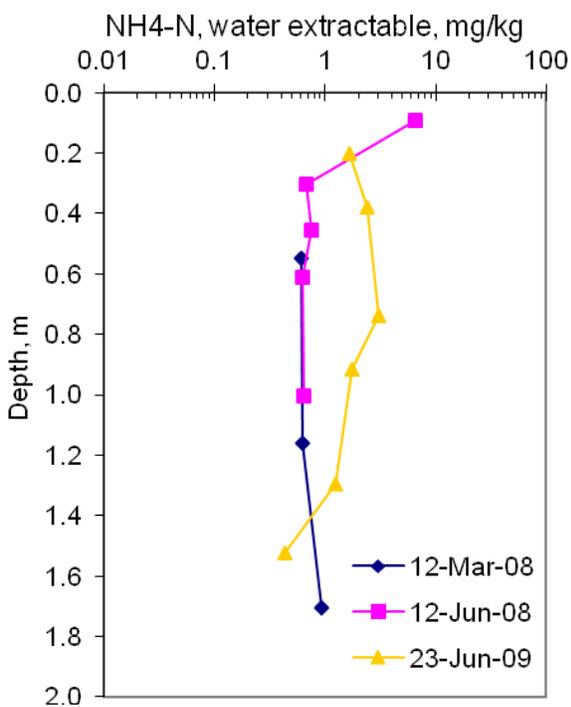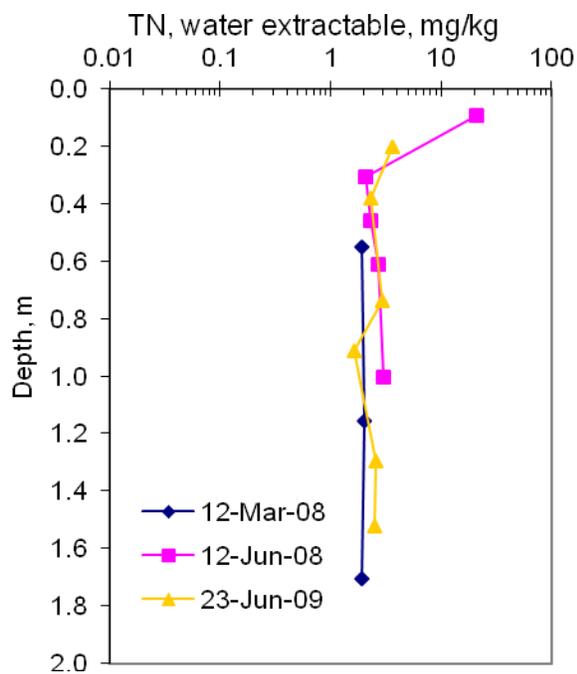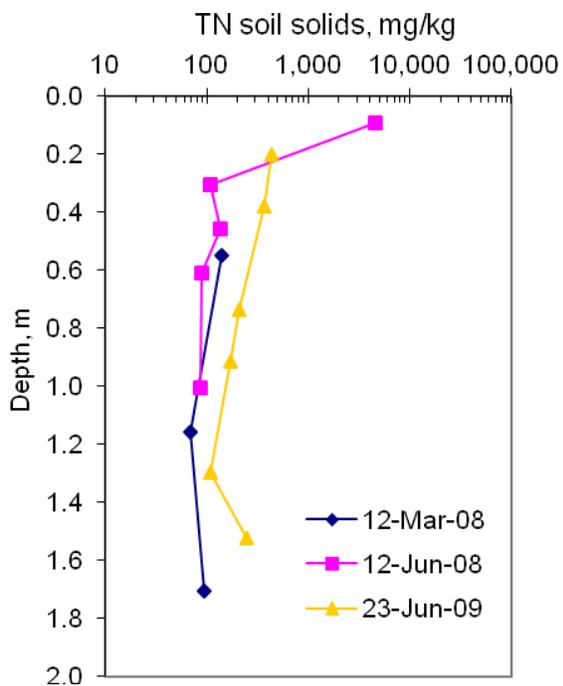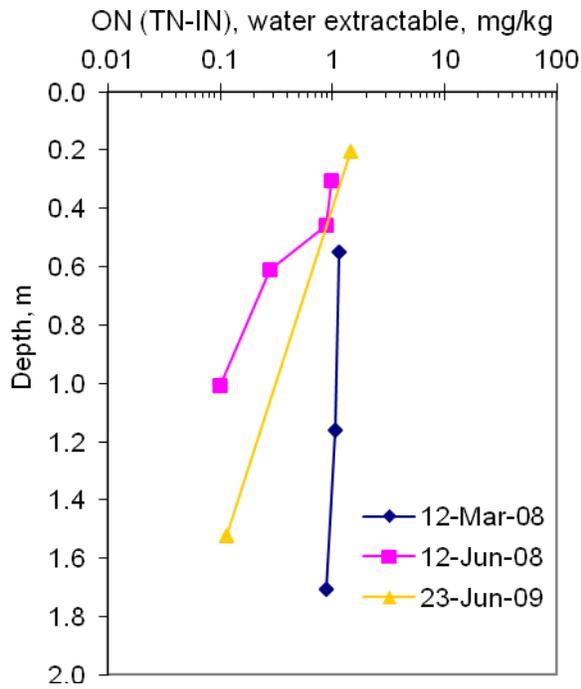
(B) Hunters Trace

Figure 6b Soil solid and water extractable total nitrogen (TN) and soil water extractable ammonium nitrogen (NH$_4^+$), nitrate plus nitrite (NO$_x$), and organic nitrogen (ON) at the Hunter's Trace stormwater infiltration basin.

(A) South Oak
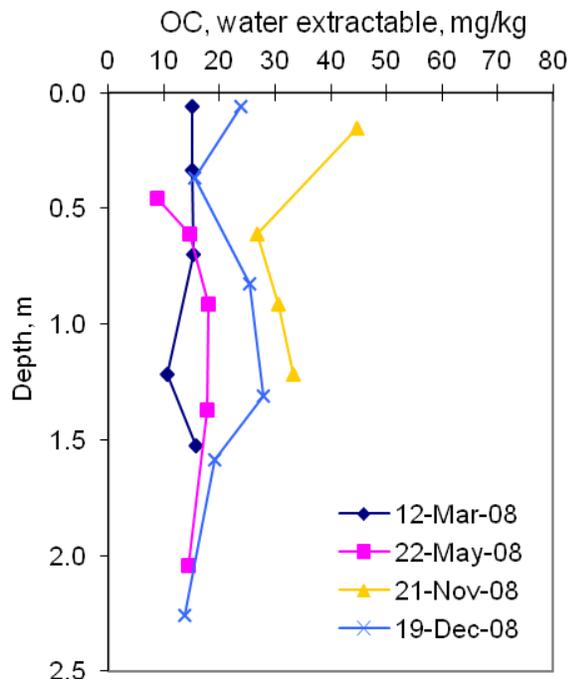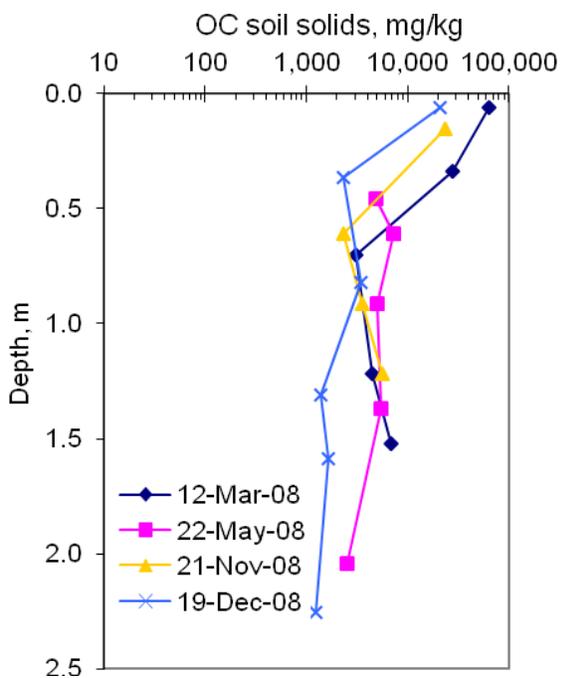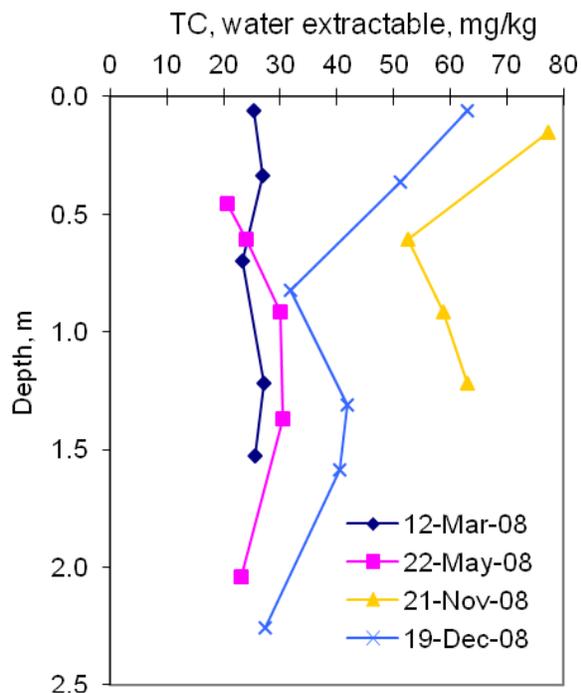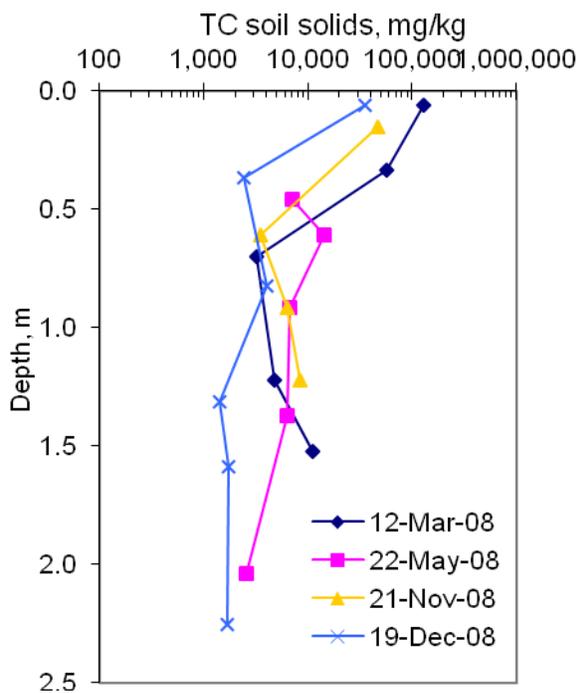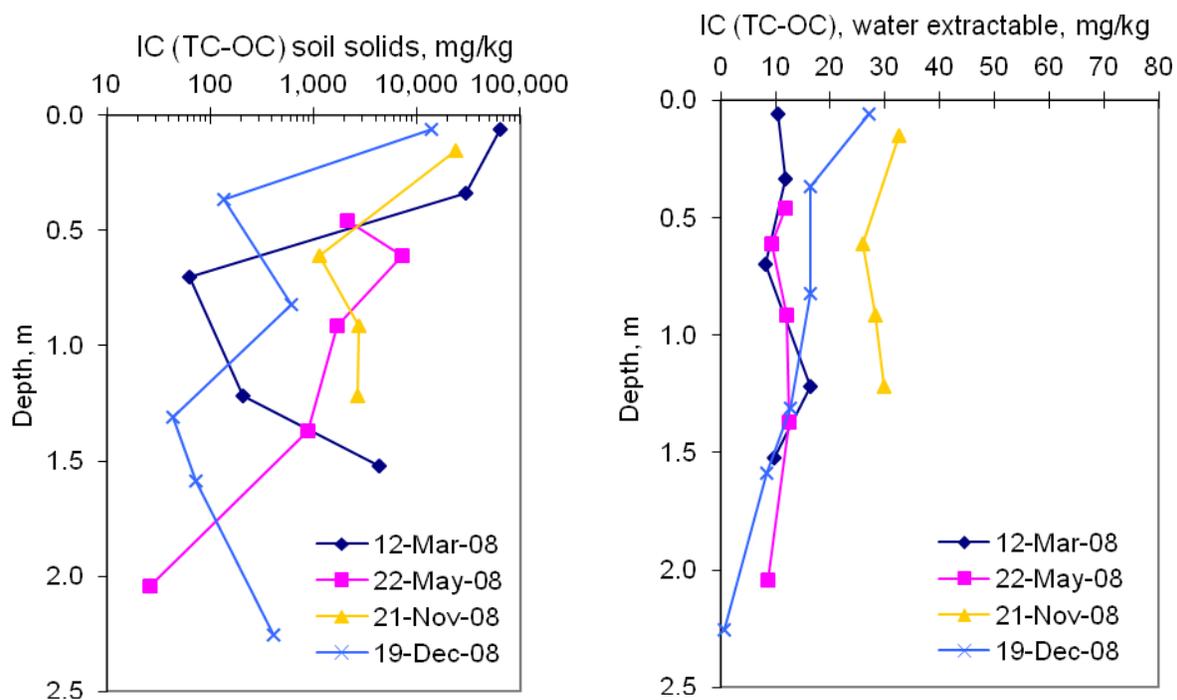
Figure 7a Soil solid and water extractable total carbon (TC), organic carbon (OC), and inorganic carbon (IC) contents at the South Oak stormwater infiltration basin.

(B) Hunters Trace

TC soil solids, mg/kg

TC, water extractable, mg/kg

OC soil solids, mg/kg

OC, water extractable, mg/kg
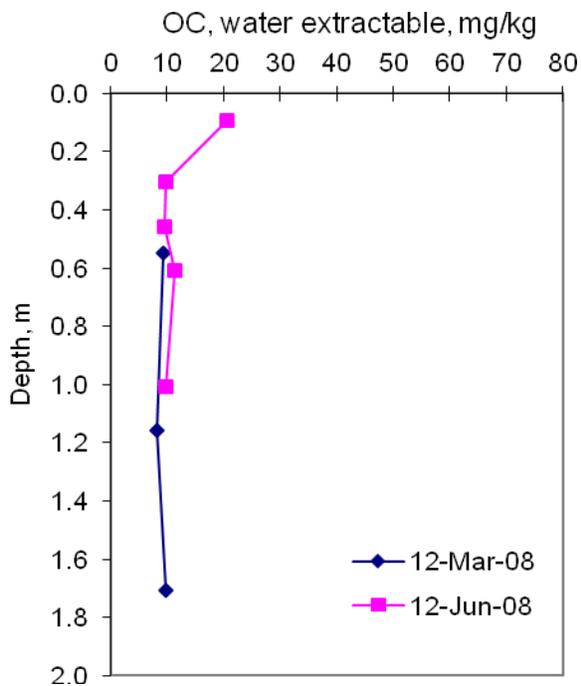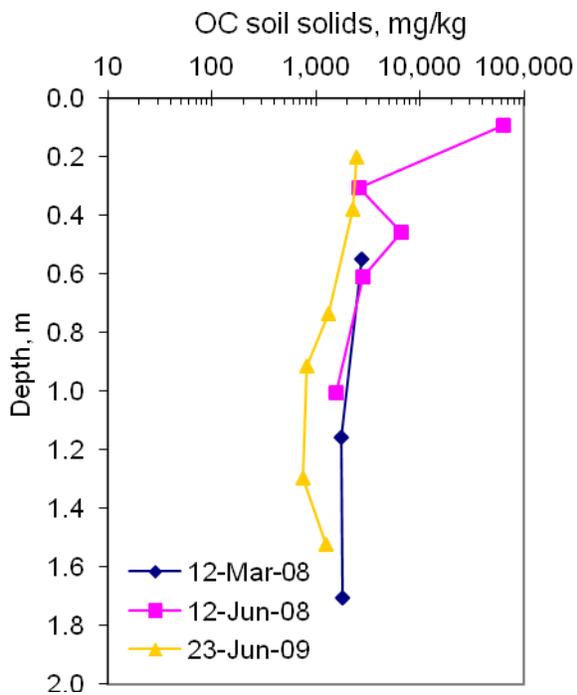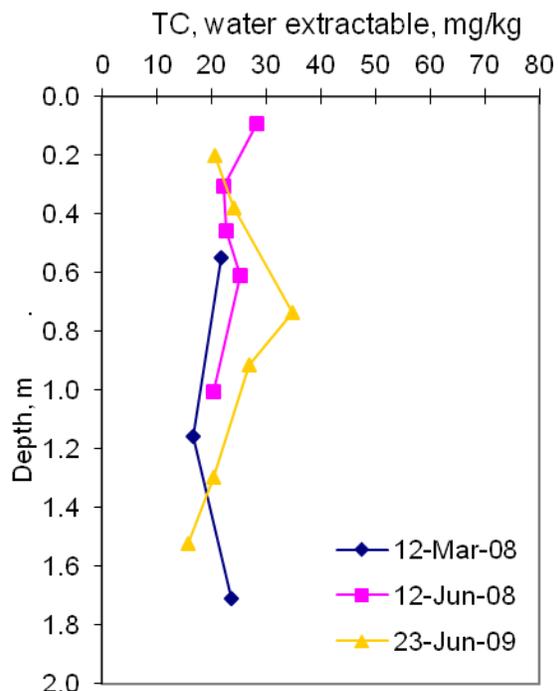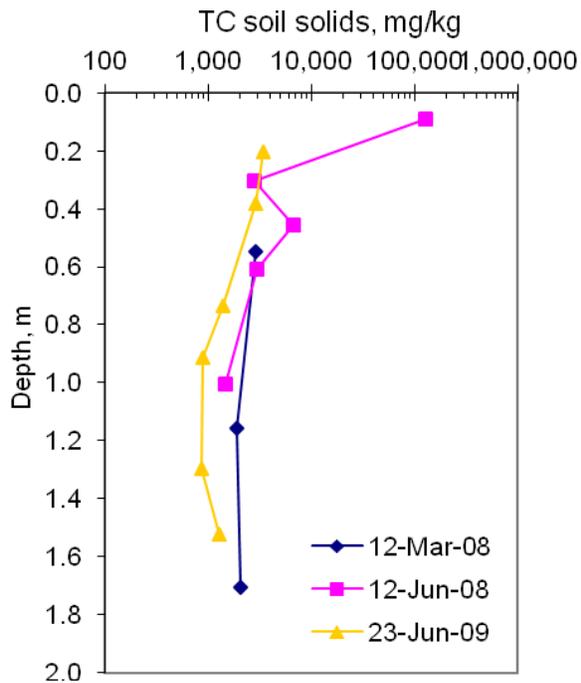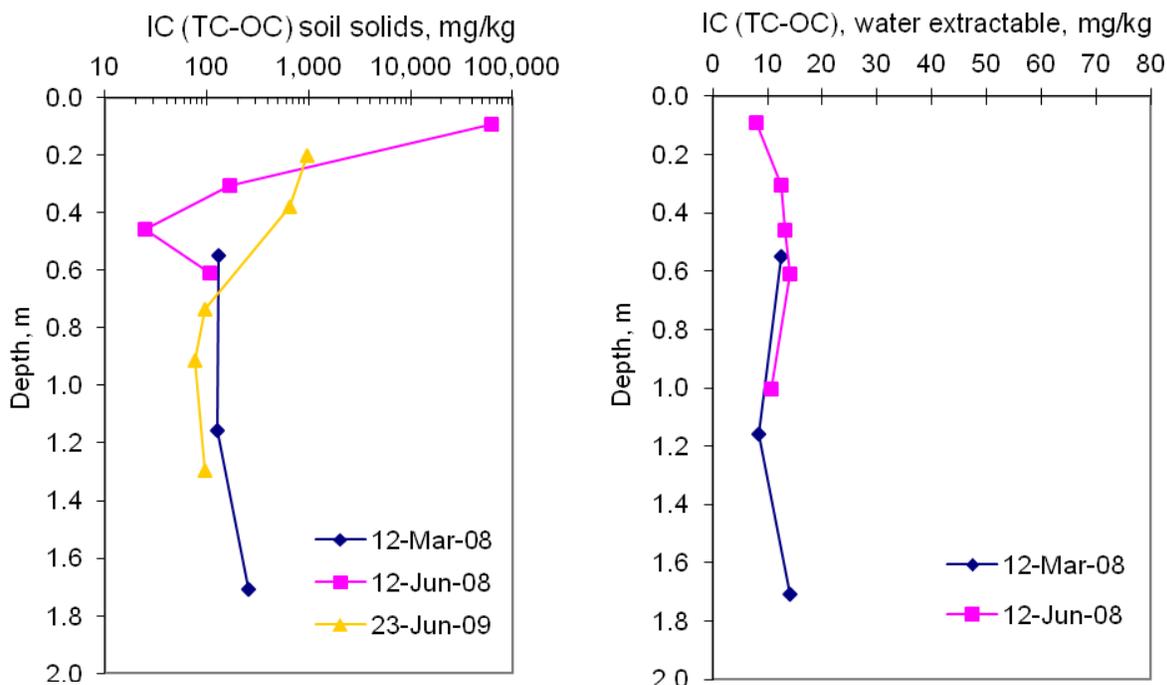
Figure 7b Soil solid and water extractable total carbon (TC), organic carbon (OC), and inorganic carbon (IC) contents at the Hunter's Trace stormwater infiltration basin.

At the HT site, soil solid OC generally was lower than at the SO site and accordingly soil solid TN was lower as well (Figures 6 and 7). Soil water extractable TN was similar to that at the SO site; however N was predominantly in the NO_3^- form at HT and in the NH_4^+ and organic forms at SO. Generally decreasing OC and increasing IC with depth (Figure 7) combined with well drained soils (relatively low moisture contents in the vadose zone, Figure 4b) is consistent with aerobic oxidation of soil organic matter.

Water Quality Data

Comparing nitrogen species for the water ponding in HT and SO show total nitrogen concentrations were similar between basins, varying from 0.49 to 1.3 mg/L with a mean of 0.88 mg/L (10 samples) at SO and varying from 0.23 to 1.4 mg/L with a mean of 0.64 mg/L (5 samples) at HT. However, Water chemistry profiles beneath the SO and HT basins indicate variations with depth and time relevant to a variety of biogeochemical processes and demonstrate substantial differences between the two sites (Figures 8 and 9). TN is generally greater at HT (high of 7.3 mg/L) than SO (high of 3.3 mg/L) and is predominantly in the form of organic N (ON) at SO and NO_3^- at HT. NH_4^+-N concentrations were less than 0.1 mg/L at the SO site and not detectable (less than 0.02 mg/L) at the HT site. DOC was generally greater at the SO site than at the HT site with large decreases occurring in the vadose zone at HT. The zone of largest DOC depletion (between 0.5 and 1.3 m depths) at the HT basin coincides with increased alkalinity, suggesting oxidation of DOC (Figure 9). Given the measured pH values, which were generally less than 7.6 (Figure 9), carbonate alkalinity was predominantly in the HCO_3^- form. DOC oxidation likely is coupled with O_2 reduction in the vadose zone, which probably is aerobic given the coarse-grained texture of the soil at depths less than 1.6 m (Figure 5a) and relatively low moisture contents in the vadose zone (Figure 4b). Additionally, shallow ground water was perennially aerobic at the HT basin (Figure 10b). In contrast, shallow ground water commonly was anoxic at the SO basin (Figure 10a), inhibiting aerobic DOC oxidation contributing to relatively constant or only slightly decreasing DOC concentrations with depth (Figure 8).
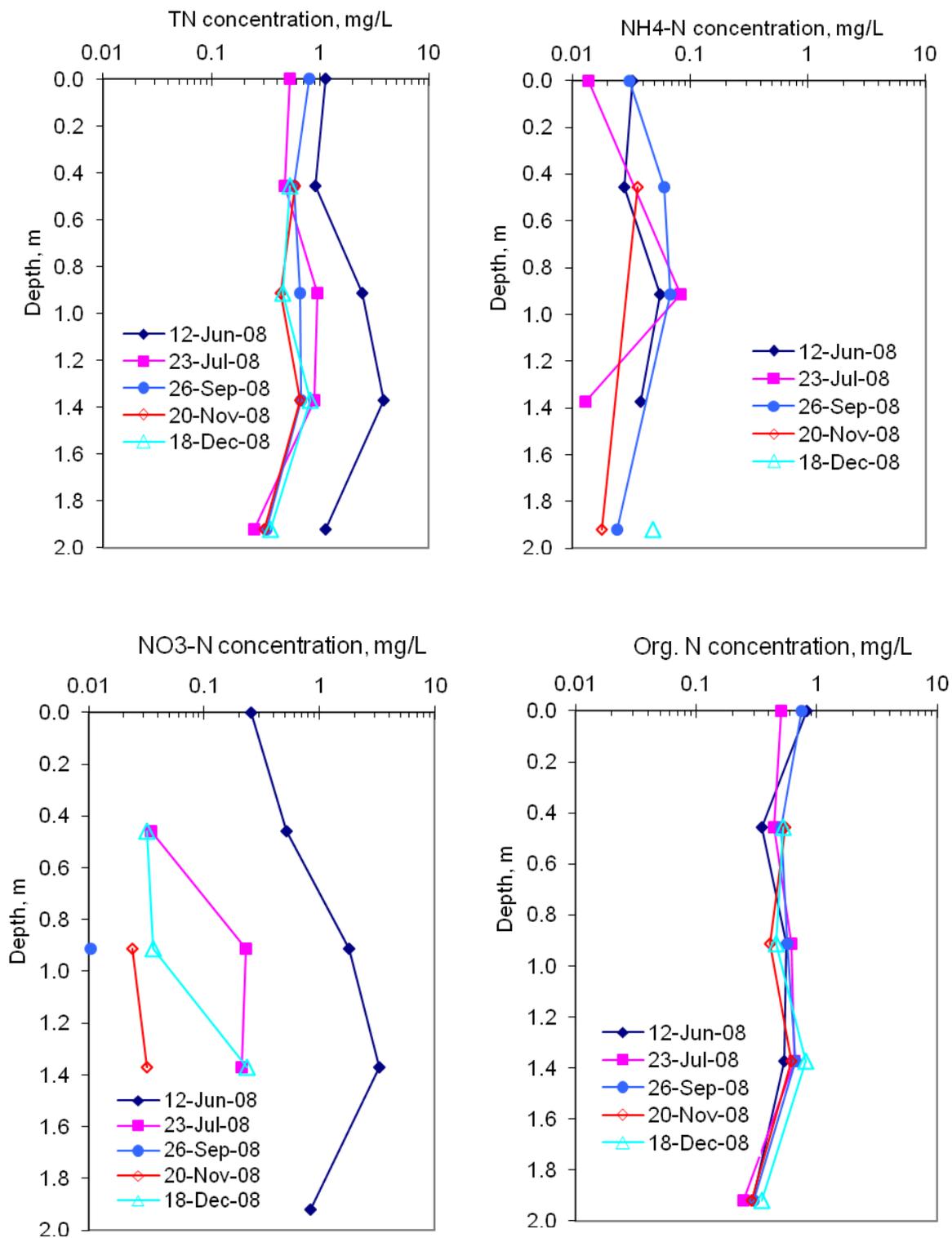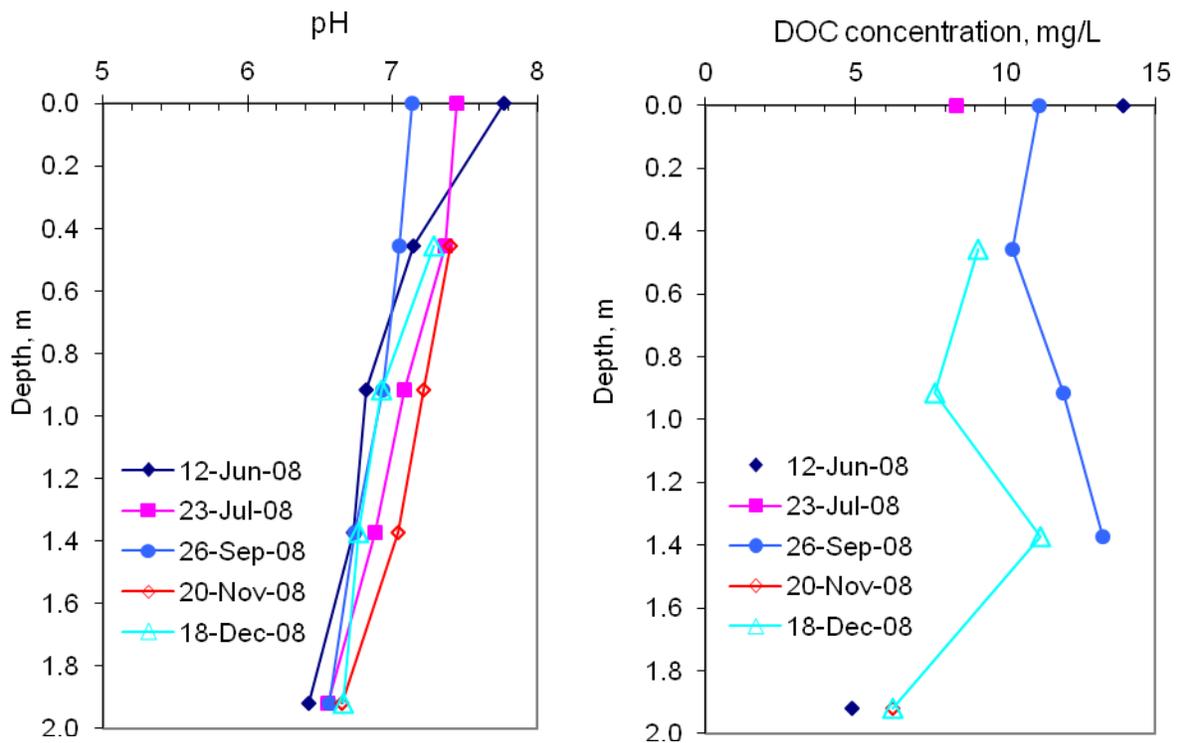
gure 8 **Soil-water and ground water chemistry profiles beneath the South Oak stormwater infiltration basin (continued on next page).**
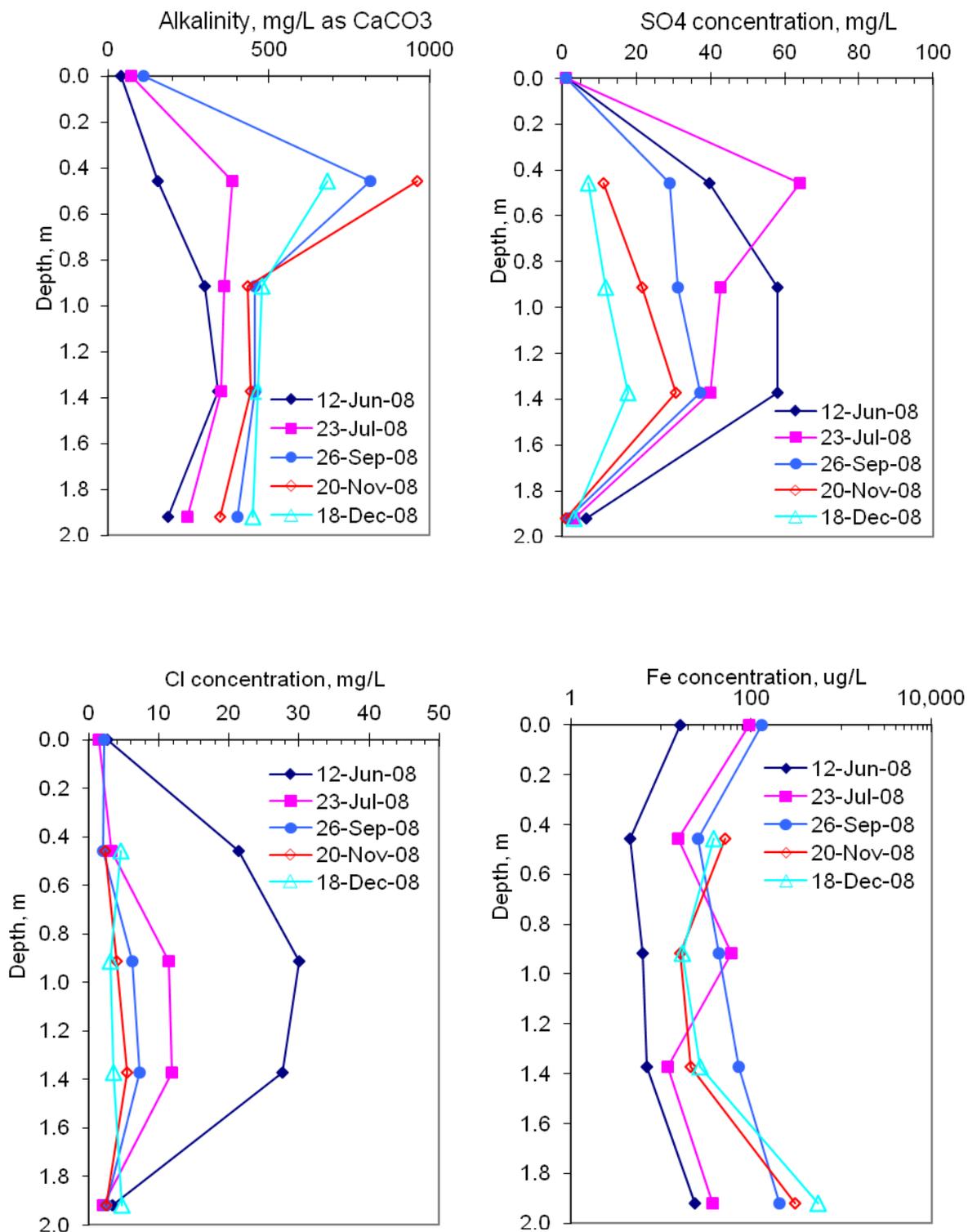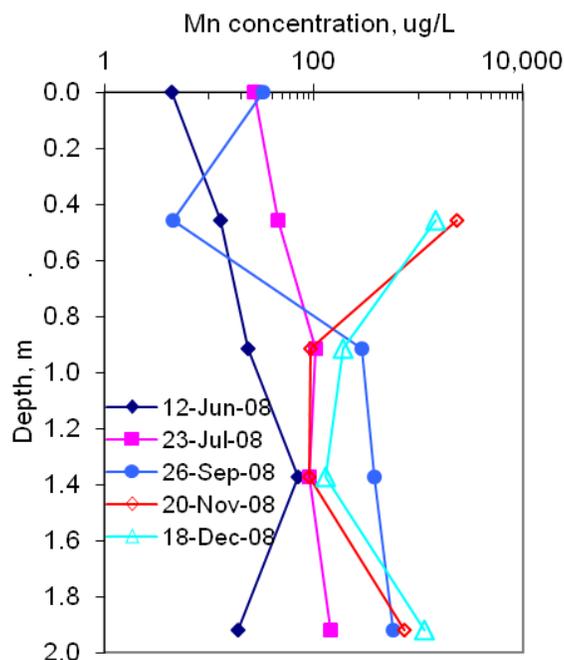
Figure 8 (continued) Soil-water and ground water chemistry profiles beneath the South Oak stormwater infiltration basin.

Data at 0-m depth represent stormwater samples; data at 0.5, 0.9, and 1.4-m depths represent lysimeter samples; data at 1.9-m depth represent well PW. Data is not available at every depth for every sampling event due to lack of sample (stormwater), lack of analysis for that sample (DOC), or non-exceedence of detection limit (TN, NH4-N, NO3-N). NO2-N was typically below the laboratory reporting limit of 0.002 mg/L for all soil-water and ground water samples, with the exception of June and July samples at 0.5 and 0.9 m depths where NO2-N varied 0.0027–0.0072 mg/L.
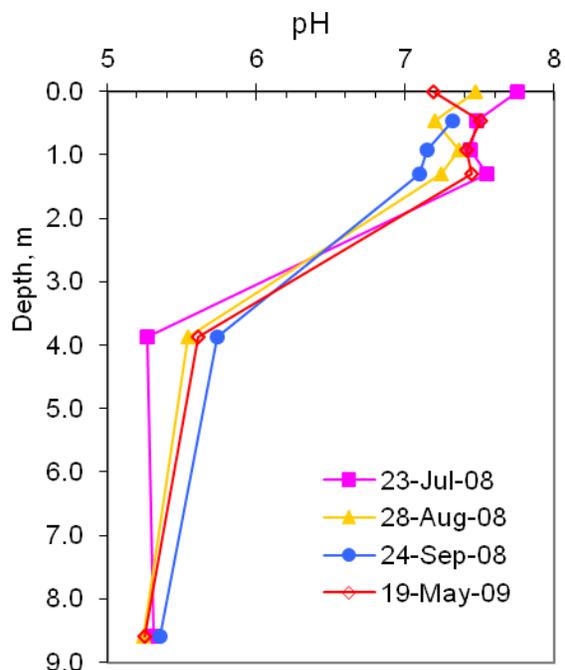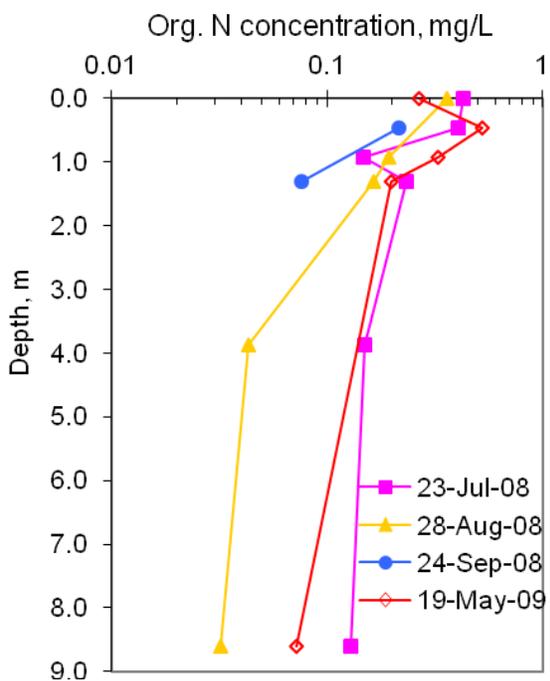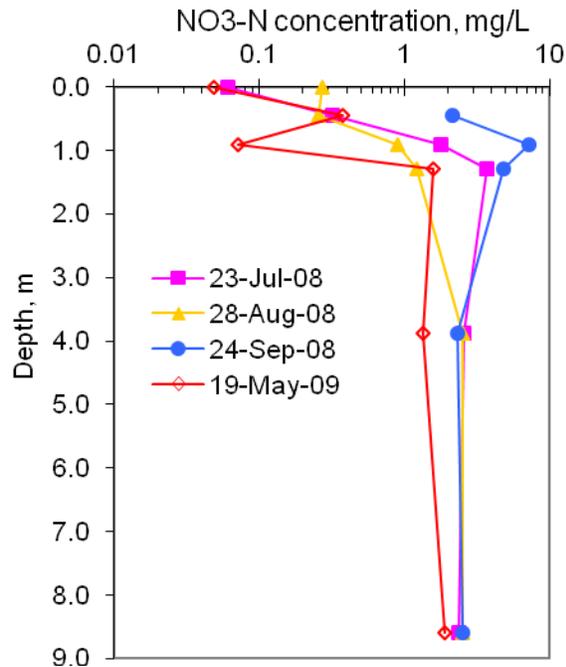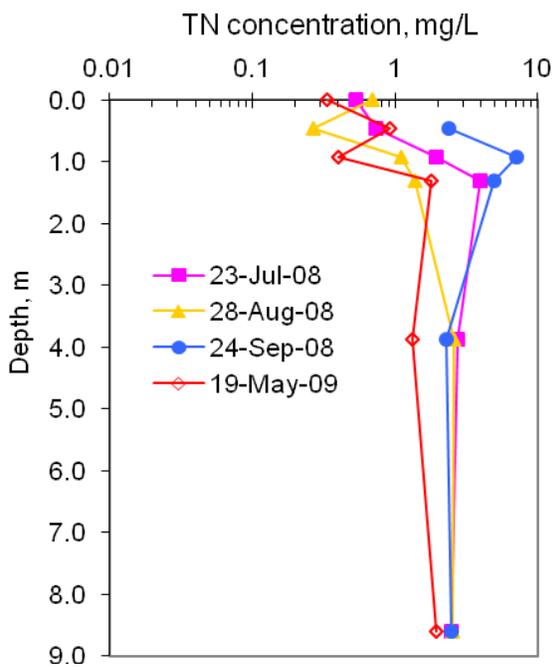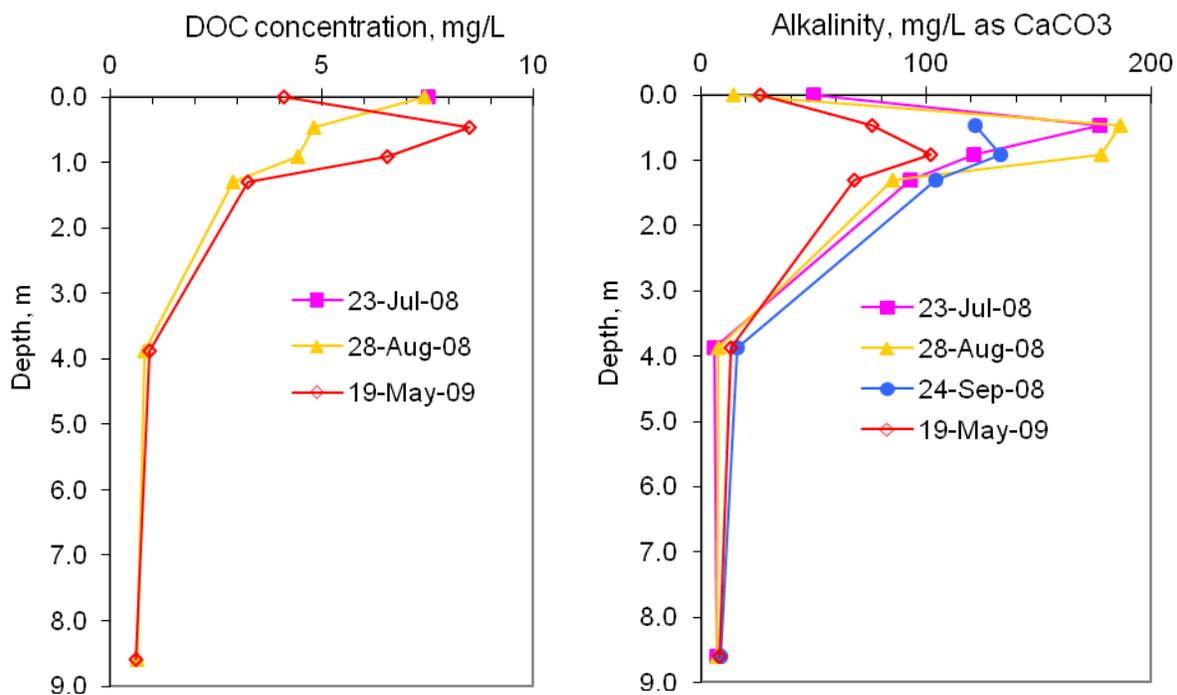
Figure 9 Soil-water and ground water chemistry profiles beneath the Hunter's Trace stormwater infiltration basin (continued on next page).
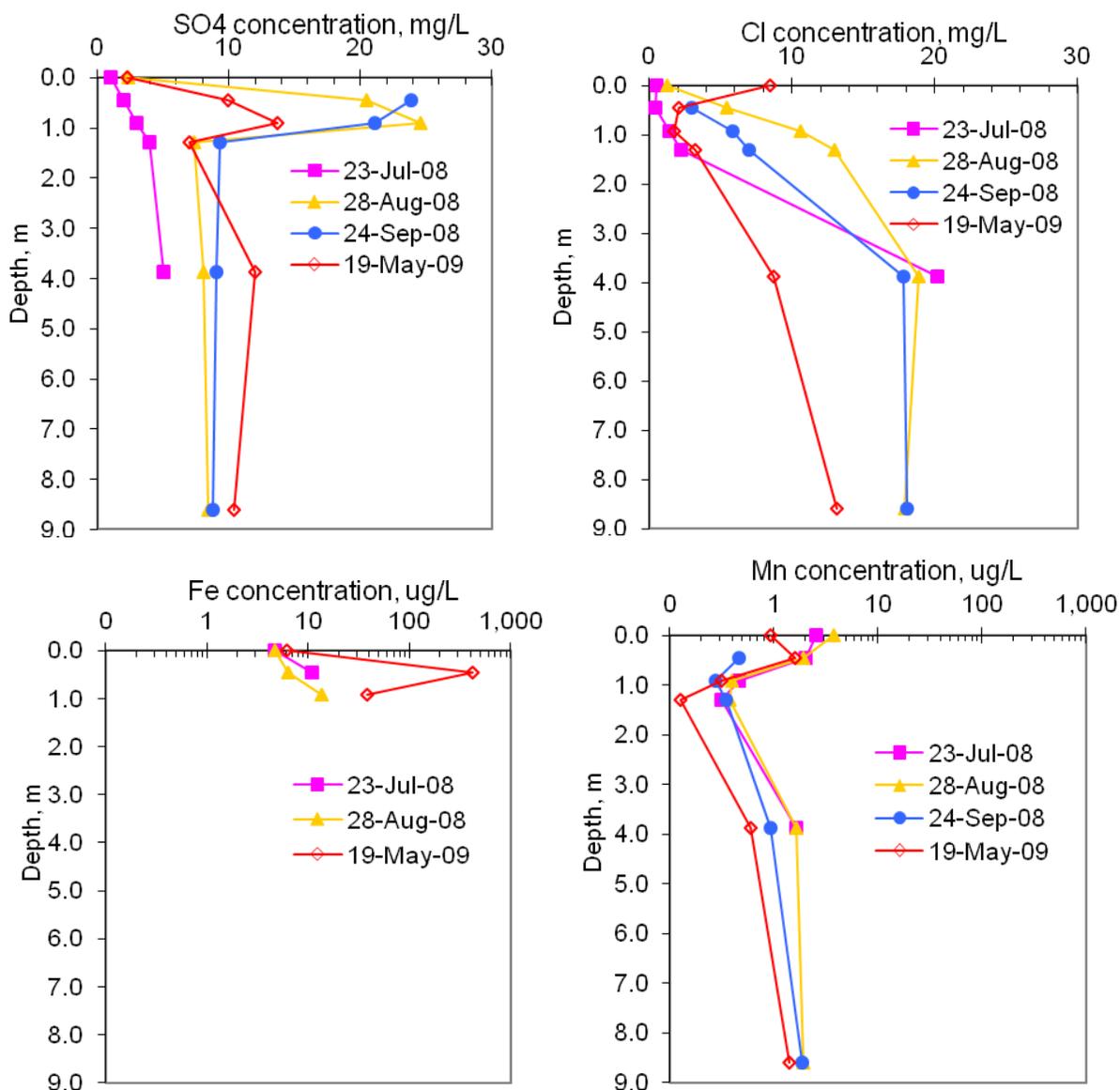
Figure 9 (continued) Soil-water and ground water chemistry profiles beneath the Hunter's Trace stormwater infiltration basin.

Data at 0-m depth represent stormwater samples; data at 0.5, 0.9, and 1.3-m depths represent lysimeter samples; data at 3.9 and 8.6-m depths represent wells M-0506 and M-0505, respectively. Data is not available at every depth for every sampling event due to lack of sample (stormwater and well M-0505), lack of analysis for that sample (DOC), or non-exceedence of detection limit (TN, NO3-N, ON). NH4-N was below the laboratory reporting limit of 0.02 mg/L for all soil-water and ground water samples. NO2-N was below the laboratory reporting limit of 0.002 mg/L for all soil-water and ground water samples except the May 2009 soil-water sample at 0.5 m depth which had NO2-N of 0.0031 mg/L.

(A) South Oak well PW

(B) Hunters Trace wells M-0505 and M-0506
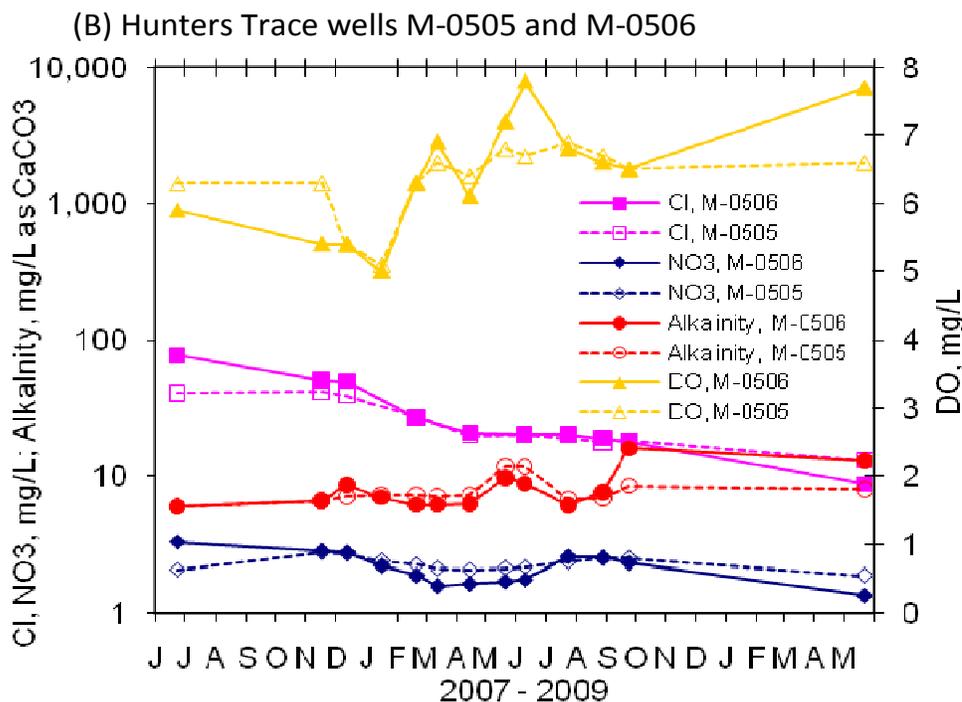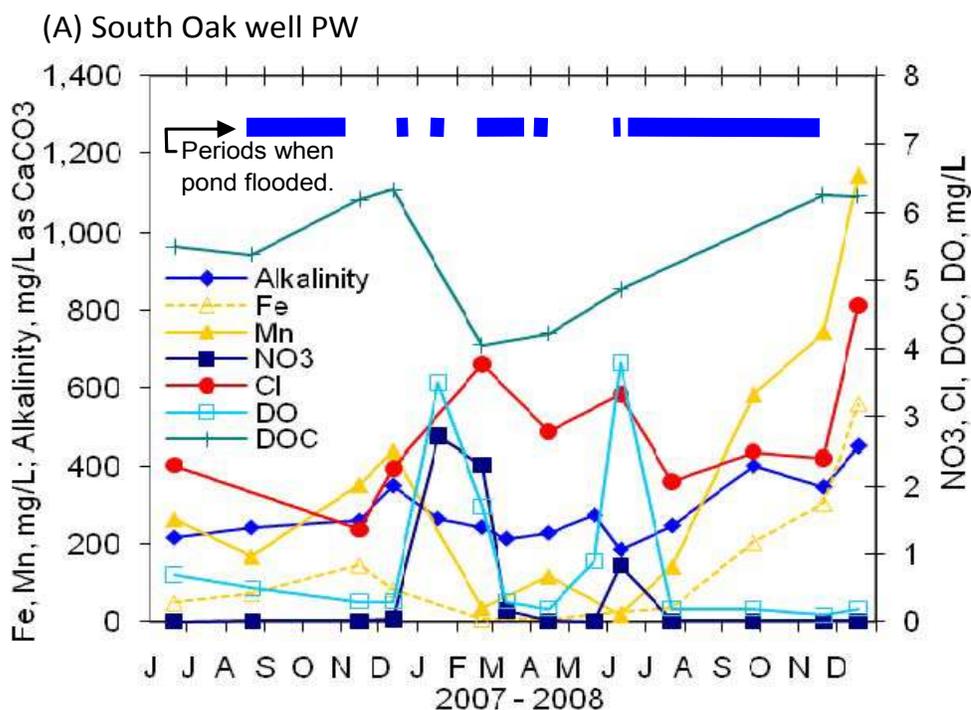
Figure 10 Temporal ground water quality variations beneath the (A) South Oak stormwater infiltration basin, and (B) Hunter's Trace stormwater infiltration basin.

Subsurface O_2 contents likely played a key role in controlling biogeochemical processes beneath both basins. At the SO basin, cyclic variations in ground water chemistry are evident in many important redox sensitive constituents, such as DO, NO_3^-, Mn, Fe, and DOC (Figure 10(A)). These cyclic variations coincided with generally wet and dry hydroclimatic conditions, with oxidizing conditions (January, February, and June 2008) at the beginning of wet periods upon the infiltration of aerobic stormwater followed by reducing conditions. Concomitant peaks in DO and NO_3^- concentrations likely indicate short periods of nitrification (Figure 10(B)). The reducing conditions enabled the loss of NO_3^- and increases in Mn and Fe. At the HT site, ground water DO concentrations showed some variations but were always greater than 5 mg/L, thus NO_3^- likely was transported conservatively or not removed before it reached the well measuring point, which is further supported based on very similar NO_3^- and Cl variations (Figure 10b).

DO was measured during each sample event, but additional dissolved gas samples (Ar, N_2, CO_2, CH_4) were collected during the spring, summer, and autumn 2008 to better understand biogeochemical activity and its seasonal variation, particularly denitrification, focusing primarily on the SO site where biogeochemical activity appeared to be most active. Dissolved gas samples collected from the shallow ground water beneath the SO basin illustrate in more detail a transition from oxic conditions at the beginning of the summer wet season to anoxic conditions during the remainder of the wet season (Figure 11). The DO level had a strong influence on the biogeochemistry of N. NO_3^--N of 3.3 mg/L was measured in the lysimeter at a depth of 1.4 m and 0.84 mg/L from well PW (mid-screen depth 1.9 m) in June 2008 (Figure 8) when DO was 3.8 mg/L, but NO_3^--N remained below the lab reporting limit (0.016 mg/L) for the remainder of

the wet season while DO remained 0.1–0.2 mg/L (Figures 10a and 11). From July through late November 2008, the basin remained flooded continuously (up to 2.1 m deep) due to heavy summer rainfall and Tropical Storm Fay; the basin was dry again in late November and December 2008 (Figure 3a). Increased CO_2 concentrations (Figure 11), as well as increasing alkalinity (Figure 10a); suggest that OC was being mineralized during the wet season, thus likely serving as the predominant electron donor for a variety or redox reactions. Therefore, when NO_3^- was present, denitrification occurred, yet when NO_3^- was not present and increasingly reducing conditions prevailed, other sequential redox reactions occurred—Mn and Fe reduction and methanogenesis. After NO_3^- was depleted and DO was low by July 2008, Mn and Fe concentrations steadily increased (Figure 10a). Presumably, the Mn and Fe concentrations consist of the reduced valance states of Mn^{2+} and Fe^{2+}; soil chemical analyses indicate Fe oxides contents as high as 20,000 mg/kg (Appendix B) that may be serving as the source of Fe^{3+}, and Mn oxides are often associated with Fe oxides in subsurface sediments (Schulze, 2002). Methane (CH_4) concentrations start to increase in August 2008 (Figure 11), lagging the Mn and Fe increases as expected based on thermodynamic considerations. CH_4 concentrations increase until peaking in November, and finally drop after the basin was dry again in December (Figure 11). The elevated CH_4 concentrations likely are the result of methanogenesis, typically the final step in biodegradation of organic matter under anoxic highly reducing conditions. The concurrent decreases in CO_2 and alkalinity when CH_4 peaks in November are consistent with methanogenesis, as the reduction of either CO_2 or HCO_3^- is the most thermodynamically favorable methanogenic reaction.
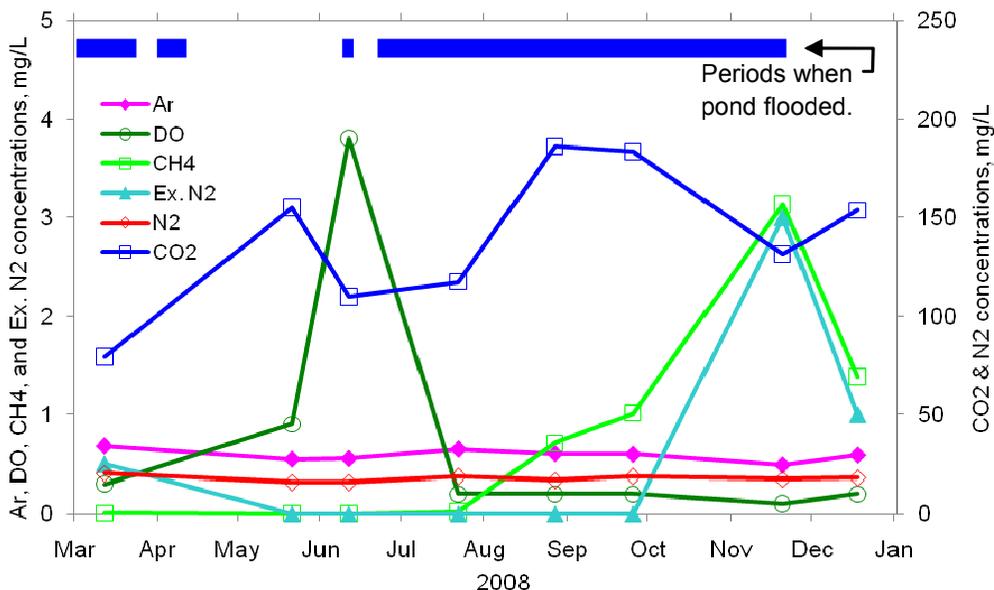
Figure 11 Dissolved gas concentrations in ground water beneath the South Oak stormwater infiltration basin.

All samples were collected from well PW, except the August sample which was collected from well M-0512. Dissolved gas concentrations are expected to be comparable at these two wells at this time due to extensive flooding of the basin (2.0 m deep at PW and 1.0 m deep at M-0512) and similar well depths (mid-screen depths of 1.9 m for PW and 1.7 m for M-0512).

Further evidence of denitrification is indicated by the presence of N_2 dissolved in the ground water. N_2 and other atmospheric and biogenic gases can be present in the saturated zone in aqueous form or as gas phase bubbles (Vogel et al., 1981). Analysis of dissolved gas concentrations, in particular N_2 and Ar, in the ground water beneath the retention basins permits estimation of the amount of excess air and excess N_2. Excess air is the dissolved atmospheric gas in excess of that attributable to atmospheric equilibration of the water during infiltration and transport through the vadose zone (Aeschbach-Hertig et al., 2008). Excess air commonly occurs when air is entrained in infiltrating water or air bubbles are trapped in the shallow water-table

zone. The amount of N_2 dissolved in ground water attributable to atmospheric equilibration is estimated based on Ar concentration because Ar is an inert noble gas and the Ar/N_2 ratio of atmospheric air is well established for a given temperature and pressure. Excess N_2 is that fraction of dissolved N_2 in excess of that attributable to atmospheric solubility equilibrium and thus can be attributed to denitrification.

Excess N_2 was present in ground water beneath the SO basin for samples collected in March, November, and December (Figure 11), suggesting that denitrification was occurring at these times or had occurred prior to these times. For the March sample, the low NO_3^- concentration (0.17 mg/L) possibly represented residual nitrate that had not been denitrified (Figure 10a). In contrast, NO_3^- concentrations were below the laboratory reporting limit (0.016 mg/L) for the July through December samples (Figure 10a), calling into question the location of the source of NO_3^- for denitrification. One possible explanation is the NO_3^- was present in the shallow soil zone above the screened interval of well PW (1.2–2.7 m). Samples collected from the lysimeters (depths of 0.5, 0.9, and 1.4 m) indicate NO_3^- concentrations ranging from 0.024 to 0.24 mg/L in November and December (Figure 8). Nitrification occurring as the basin dried and the water table dropped below land surface in late November, forming a thin aerobic zone near land surface, is a likely source of NO_3^-. Soil water-extractable analyses indicated a NO_x concentration of 0.59 mg/kg at a depth of 0.1 m in December (Figure 6a), corresponding to a NO_3^- concentration of 1.37 mg/L. Subsequently, the nitrified water entered a saturated or nearly saturated soil zone (and consequently was probably anoxic) at shallow depths above 1.2 m. This shallow soil zone is the likely location of active denitrification. Increases in water-extractable IC from spring to autumn (before, during, and after the summer wet period) for soil samples

collected between depths of 0–1.3 m (Figure 7a) are suggestive of biogeochemical processes, such as denitrification, whereby IC is generated by mineralization of OC substrates to CO_2 and HCO_3^-. Excess N_2 produced in this zone subsequently could have been transported further downward below the water table by the prevailing hydraulic gradient into the screened interval of well PW (Figure 11).

Isotopes of nitrogen ($^{15}N/^{14}N$) and oxygen ($^{18}O/^{16}O$) of NO_3^- in ground water can indicate the enrichment of ^{15}N and ^{18}O and nitrogen isotopes ($^{15}N/^{14}N$) for the dissolved N_2 in ground water can indicate depletion of ^{15}N, all of which can provide further evidence of denitrification when considered in combination with other data (Böttcher et al., 1990; Bohlke, 2002). These isotopic fractionations occur due to the preference of bacteria to metabolize isotopically light organics and oxidizers (Clark and Fritz, 1997). Therefore, reactants (such as NO_3^-) become isotopically heavier (enriched in ^{15}N), whereas products (such as N_2) become isotopically lighter (depleted in ^{15}N). Additionally, isotopic analysis of NO_3^- can indicate whether the contamination source is inorganic (for example, NO_3^- or NH_4^+ based fertilizer) or organic (for example, manure or septic tank leachate) (Kendall, 1998). Isotopes of hydrogen ($^2H/^1H$) and oxygen ($^{18}O/^{16}O$) of water can elucidate ground water/surface water interactions by providing insight into the sources of infiltration, degree of evaporation infiltrating water has undergone, and tracking of individual infiltration events.

Results of the N and O isotopic analysis of NO_3^- for precipitation, stormwater, soil water, and ground water samples collected at the HT and SO sites provide insight into the sources of NO_3^- and differences in NO_3^- biogeochemistry (Figure 12). Typical NO_3^- source outlines delineated in Figure 12 are based on those reported by Kendall and Aravena (2000). The

stormwater samples are indicative of atmospheric NO_3^-, fertilizer NO_3^-, nitrification of atmospheric or fertilizer derived NH_4^+, or perhaps most likely a mixture of these sources. Many ground water and soil-water samples (primarily at the HT site) are indicative of nitrification of either atmospheric or fertilizer derived NH_4^+ or organic waste (manure or septic). Many ground water samples and one soil-water sample (primarily at the SO site) are indicative of nitrification of either soil nitrogen (organic or NH_4^+) or organic waste (manure or septic). It is important to note that denitrification can confound NO_3^- source identification, as explained later in this section. N contamination from organic waste sources is believed to be limited or negligible at both sites. Both watersheds drain residential areas with no large-scale agricultural pollution (manure). Residences within each watershed and immediately surrounding each retention basin (Figure 3) are served by septic tanks. Septic tank leachate possibly could impact ground water at the wells sampled at each retention basin, however hydraulic gradients indicate this potential is very limited at the SO site and negligible at the HT site. Water-table gradients at the SO site were toward the basin at times, yet were more than an order of magnitude smaller than vertical gradients; whereas at the HT site, water-table gradients were nearly always outward and similarly small relative to vertical gradients. Therefore, the source of NO_3^- at both sites likely is fertilizer impacted stormwater runoff and nitrification of soil N.
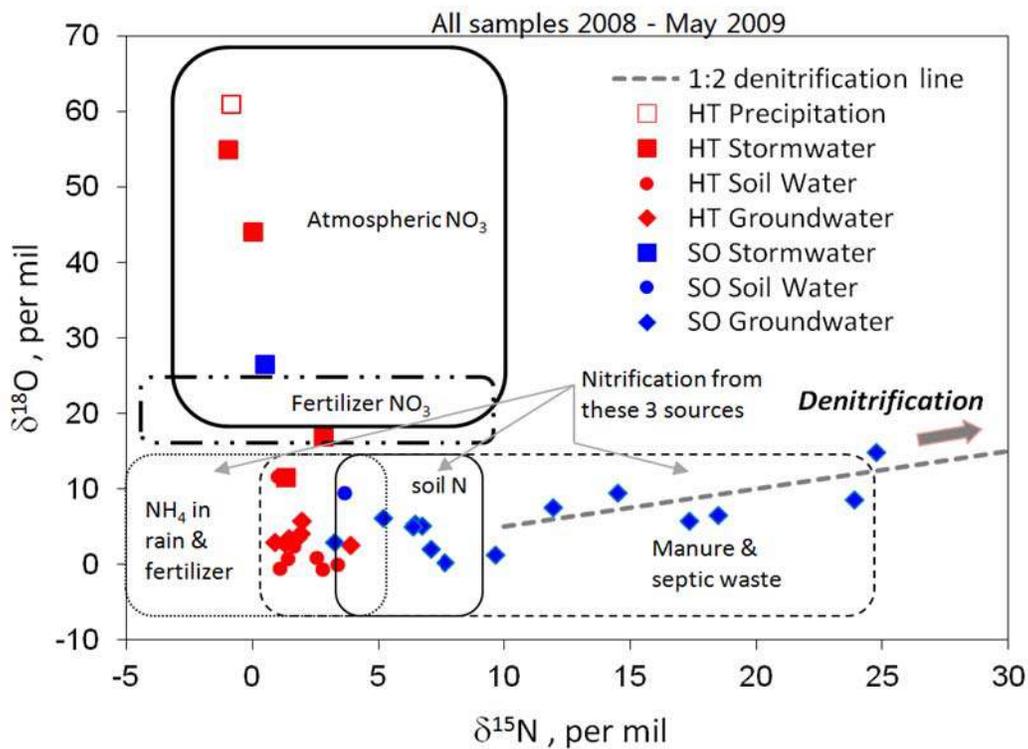
(A) South Oak pond
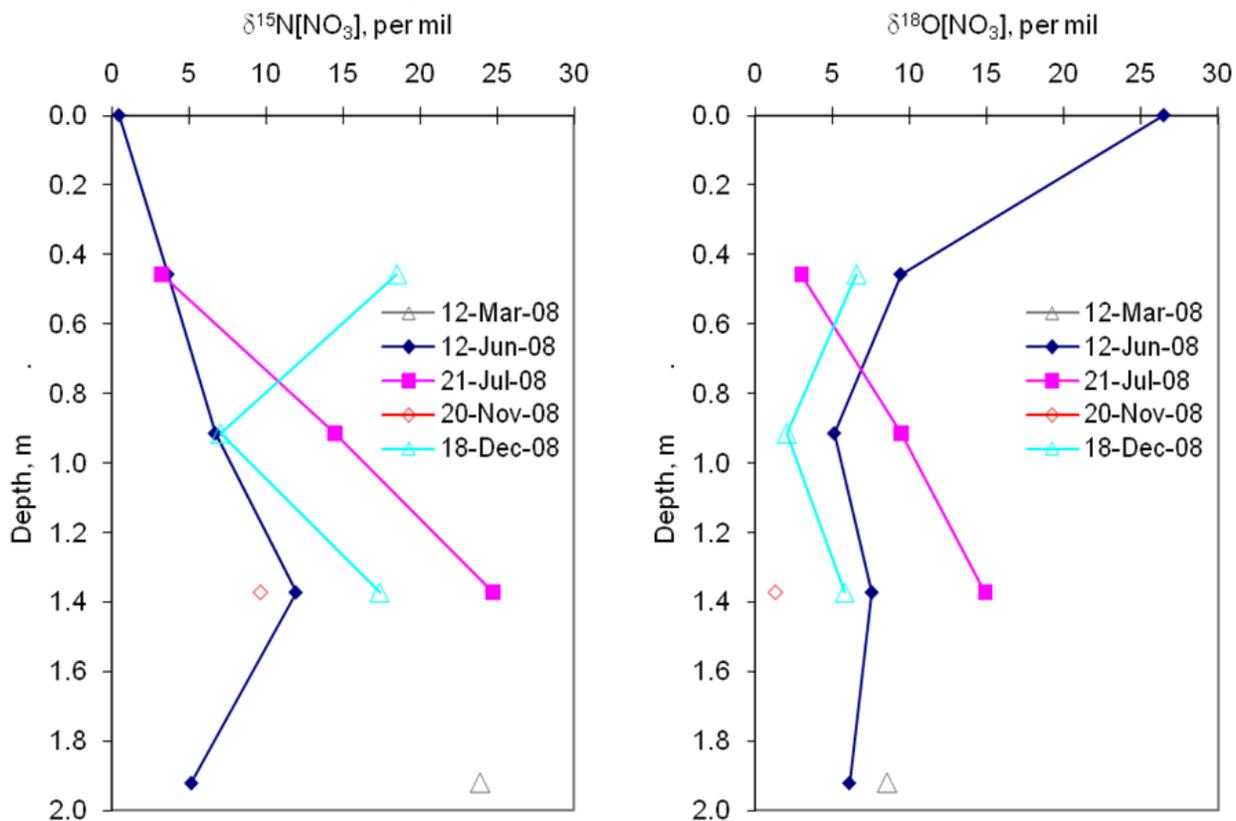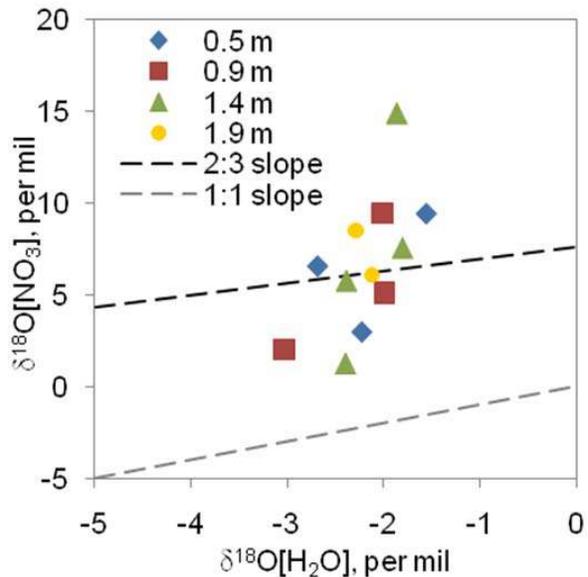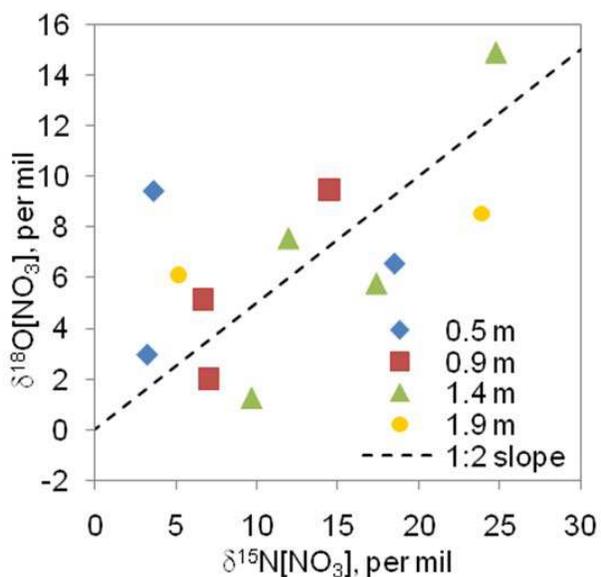
(B) Hunter's Trace pond
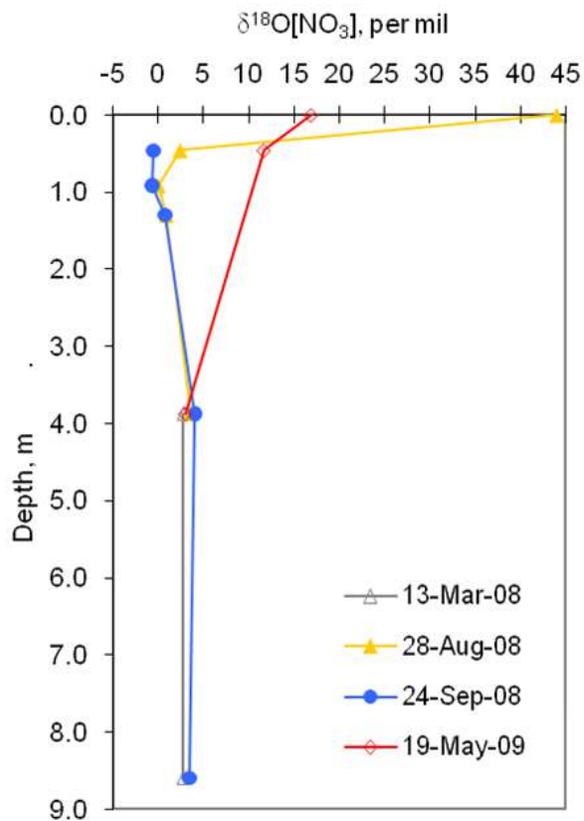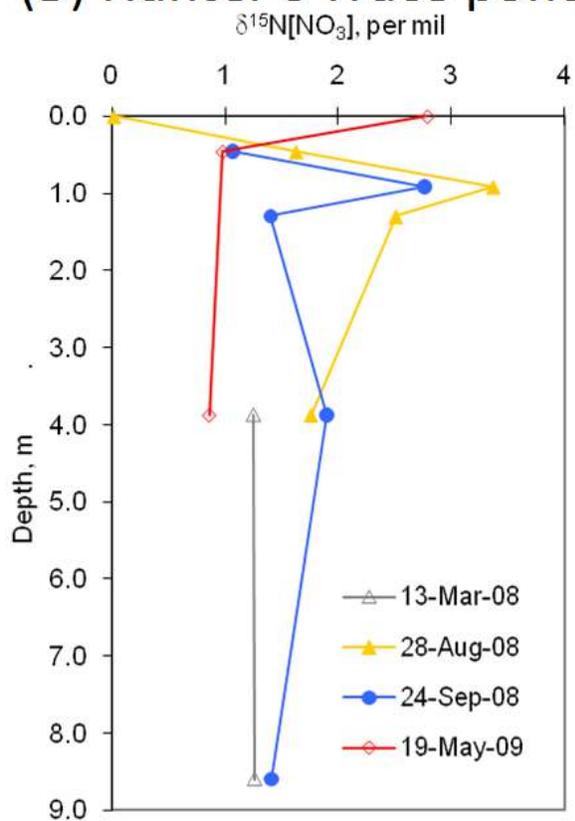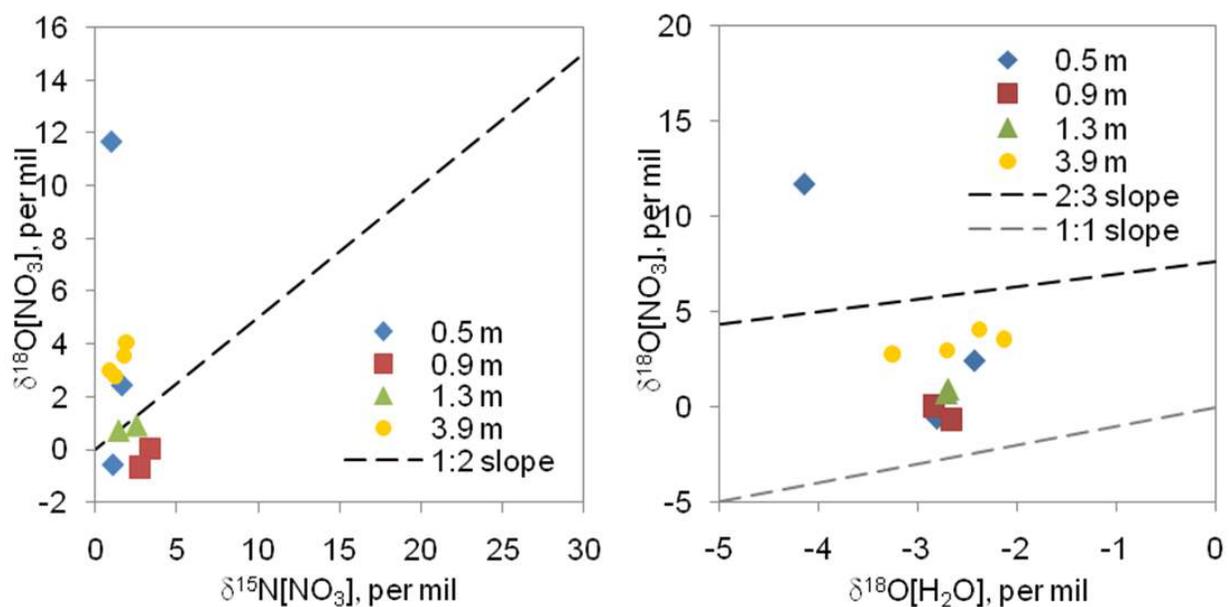
Figure 12 δ^{15}N and δ^{18}O of NO_3^- in precipitation, stormwater, soil water, and ground water at the South Oak and Hunter's Trace stormwater infiltration basins.

Research has indicated that nitrification derives oxygen from water molecules and O_2 in a predictable manner according to the two-step microbial mediated reactions: (1) NH_4^+ oxidation to NO_2^- by Nitrosomonas uses one oxygen from water and one from O_2; and (2) NO_2^- oxidation to NO_3^- by Nitrobacter uses one oxygen from water (Kendall, 1998). If the process occurs without fractionation, the δ^{18}O[NO_3^-] can be computed simply as 2/3 δ^{18}O[H_2O] + 1/3 δ^{18}O[O_2] (Kendall, 1998). Figure 12 shows isotopic results in relation to the 2:3 slope line and assuming δ^{18}O[O_2] of 23‰ characteristic of atmospheric O_2 (Kendall, 1998) and a 1:1 slope line indicating the trend if all oxygen during nitrification were derived from water. Distinct differences are evident between the HT and SO samples with all but one HT sample plotting within this range. Values that plot above the 2:3 slope line indicate either enriched δ^{18}O[O_2] was being used (values of δ^{18}O[O_2] of soil air can be as high as 60‰ caused by respiration derived fractionation

(Kendall, 1998)) or $\delta^{15}N[NO_3^-]$ had been fractionated by denitrification. In the latter case, examination of the $\delta^{18}O[NO_3^-]$ will confirm whether denitrification had occurred.

The effects of denitrification can confound use of $\delta^{15}N[NO_3^-]$ for source identification. Denitrification results in enrichment of $\delta^{15}N[NO_3^-]$, thus an inorganic NO_3^- source can appear to be an organic source after denitrification and enrichment of $\delta^{15}N[NO_3^-]$ from, say, 0–5‰ to 10–25‰. The dual-isotope approach was used to help discern an organic NO_3^- source from denitrification effects. Enriched values of $\delta^{15}N[NO_3^-]$, and to a lesser degree of $\delta^{18}O[NO_3^-]$, occur during bacteriological denitrification with a ratio of $\delta^{18}O : \delta^{15}N$ about 1:2 (Kendall, 1998; Kendall and Aravena, 2000). Six ground-water samples fall closely along this line and are more highly enriched ($\delta^{15}N[NO_3^-] > 10‰$) relative to the other ground water samples; these samples likely indicate denitrification rather than an organic waste source (Figure 12). Other SO samples with $\delta^{15}N[NO_3^-] < 10‰$ also follow this trend. In contrast, all HT samples have $\delta^{15}N[NO_3^-] < 5‰$ and show no trend with $\delta^{18}O[NO_3^-]$. All samples indicative of denitrification were from the SO site. All ground water and soil-water samples at the HT site are indicative of nitrification.

Water undergoing denitrification will experience an increase in $\delta^{15}N[NO_3^-]$ with decreasing NO_3^-, but increases in $\delta^{15}N[NO_3^-]$ also can result from two-component mixing of waters of different isotopic composition. Marotti et al. (1988) describe that denitrification will result in an exponential increase in $\delta^{15}N[NO_3^-]$ while dilution (by water with low or zero nitrate concentration) results in a hyperbolic increase in $\delta^{15}N[NO_3^-]$, thus reaction-based changes in NO_3^- can be discerned from dilution-based conservative transport. $\delta^{15}N[NO_3^-]$ results shown in Figure 12 were plotted with respect to $\ln(NO_3^-)$ and $(NO_3^-)^{-1}$, where a linear relation would indicate denitrification and mixing, respectively. No linear relations were evident, although this

is likely due to the timescale of the relevant hydraulic and biogeochemical processes relative to sampling frequency. Due to the episodic nature of stormwater runoff generation, subsequent infiltration and ground water recharge processes occur at the timescale of hours to days depending on the intensity and duration of the storm event, resulting in a highly dynamic shallow ground water flow system. These conditions probably result in relatively rapid fluctuations in ground water quality that is continuously adjusting to changing inputs. In order to estimate mixing ratios or denitrification rate constants from $\delta^{15}N[NO_3^-]$ data at either site, multiple sampling of individual stormwater infiltration events at the daily timescale likely would be required. Because the intent of this study was to ascertain seasonal variations in ground water quality to ascertain more long-term behavior, samples were collected at monthly or longer frequencies in order to maximize the variety of hydroclimatic conditions sampled.

Excess N_2 produced during denitrification will be depleted in $\delta^{15}N$ relative to the NO_3^- from which it was formed. All $\delta^{15}N[N_2]$ values (ranging from 0.4 to 1.1‰, Figure 13) were less than the $\delta^{15}N[NO_3^-]$ values (ranging from 3.2 to 24.7‰, Figure 12) for ground water samples at the SO site. However, $\delta^{15}N[N_2]$ values between 0 and 0.8‰ may be indicative of isotope abundances typical of N_2 in air or air-saturated water, depending on temperature and the Ar/N_2 molar ratios. Figure 13 shows several samples that plot above the air/air-saturated water line and are indicative of possible generation of isotopically lighter N_2 via denitrification. All these samples were collected at the SO site during or shortly after hydroclimatic wet periods when other data indicate other reductive biogeochemical processes were occurring.

(A) South Oak and Hunter's Trace
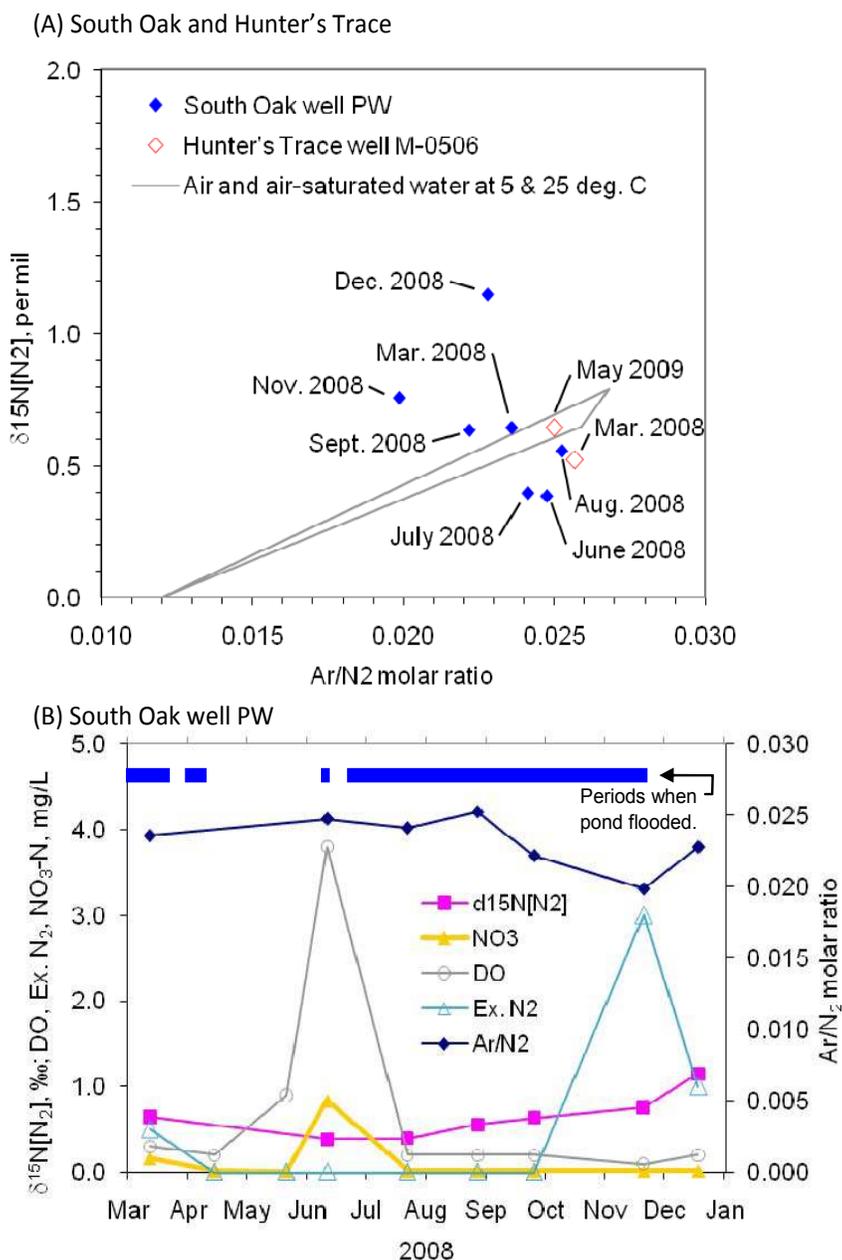
(B) South Oak well PW

Figure 13 $\delta^{15}N$ of dissolved N_2 in ground water beneath the South Oak and Hunter's Trace stormwater infiltration basins.

All samples at the SO site were collected from well PW, except the August sample which was collected from well M-0512. Dissolved gas concentrations are expected to be comparable at these two wells at this time due to extensive flooding of the basin (2.0 m deep at PW and 1.0 m deep at M-0512) and similar well depths (mid-screen depths of 1.9 m for PW and 1.7 m for M-0512).

Samples that plot below the air/air-saturated water line reflect excess air effects (Figure 13a), such that gas excess above atmospheric solubility equilibrium occurs (Aeschbach-Hertig et al., 2008). Some SO and all HT samples (including four samples not plotted in Figure 13a collected at wells M-0505, M-0508, and M-0509) have δ^{15}N[N_2] suggesting N_2 was from excess air not excess N_2 from denitrification. These conditions likely are common beneath a retention basin where infiltration is rapid and the ground water system is highly dynamic. Examination of the volumetric moisture content data indicates a gradual but prolonged rise in moisture content from early July through mid-September 2008 after flooding of the SO basin during the summer wet period (Figure 3a). This phenomenon is most pronounced at the two shallowest soil moisture probes (0.3 and 0.6 m below the basin bottom) in 2008, but similar behavior is also apparent when the basin was flooded during summer 2009. These moisture content variations likely are due to a combination of factors, including air bubble entrapment and subsequent dissolution, generation of subsurface biogenic gases (such as CO_2, N_2, or CH_4) via biogeochemical processes, and degassing due to lowered hydrostatic pressure as the basin stage drops from late summer to early autumn. Such biogenic gas production is consistent with results of dissolved gas sampling (Figure 11).

A time-series plot of dissolved gas and isotopic data at well PW provides further evidence of denitrification beneath the SO basin (Figure 13b). δ^{15}N[N_2] values are lowest and near 0‰ (δ^{15}N[N_2] of atmospheric air) for the June 2008 sample (collected 27 hours after a 26 mm storm event resulting in water retention up to 0.28 m deep). At this time, a high DO and an elevated NO_3^- concentration of 0.84 mg/L indicative of nitrification (δ^{15}N[NO_3^-] of 5.2‰ and δ^{18}O[NO_3^-] of 6.1‰, Figure 12) was measured. As the basin remained flooded July through late

November, DO dropped sharply to 0.2 mg/L and $\delta^{15}N[N_2]$ rose steadily. Excess N_2 was detected in March, November, and December and $\delta^{15}N[N_2]$ was enriched over that during aerobic conditions, (albeit slightly, exceeding 0.64‰ for all three samples), providing supporting evidence of denitrification during or prior to these times.

Predictable relations exist between $\delta^{18}O$ and $\delta^{2}H$ for fresh surface waters, the most common of which is that published by Craig (1961) based on a synthesis of data from around the world. This linear relation is commonly called the global meteoric water line (GMWL): $\delta^{18}O = 8\delta^{18}O + 10$ (in ‰). As water moves through the hydrologic cycle, it is partitioned from rainfall to ground water through runoff, evaporation, and transpiration processes. Of these processes, only evaporation imparts a significant isotopic fractionation yielding $\delta^{18}O$ and $\delta^{2}H$ values plotting to the right of the GMWL (Clark and Fritz, 1997; Coplen et al., 2000). Thus water isotopes may be used to assess the degree of evaporation, discriminate surface water from ground water, and provide insight into ground water recharge processes.

Analysis of the water isotope data indicate little isotopic enrichment (relative to the GMWL) of ground water at the HT site suggesting little evaporative losses, whereas slight enrichment occurred at the SO site suggesting some evaporative losses as indicated by the linear equation fit to the ground water samples (Figure 14). These results are consistent with hydraulic analyses indicating a high infiltration rate at the HT basin and a low infiltration rate at the SO basin. Also, the relatively shallow water table at the SO basin increases the likelihood of direct evaporation from the water table.

South Oak Groundwater
$\delta^2H = 5.78\ \delta^{18}O + 2.87$
$R^2 = 0.77$

(A) South Oak pond
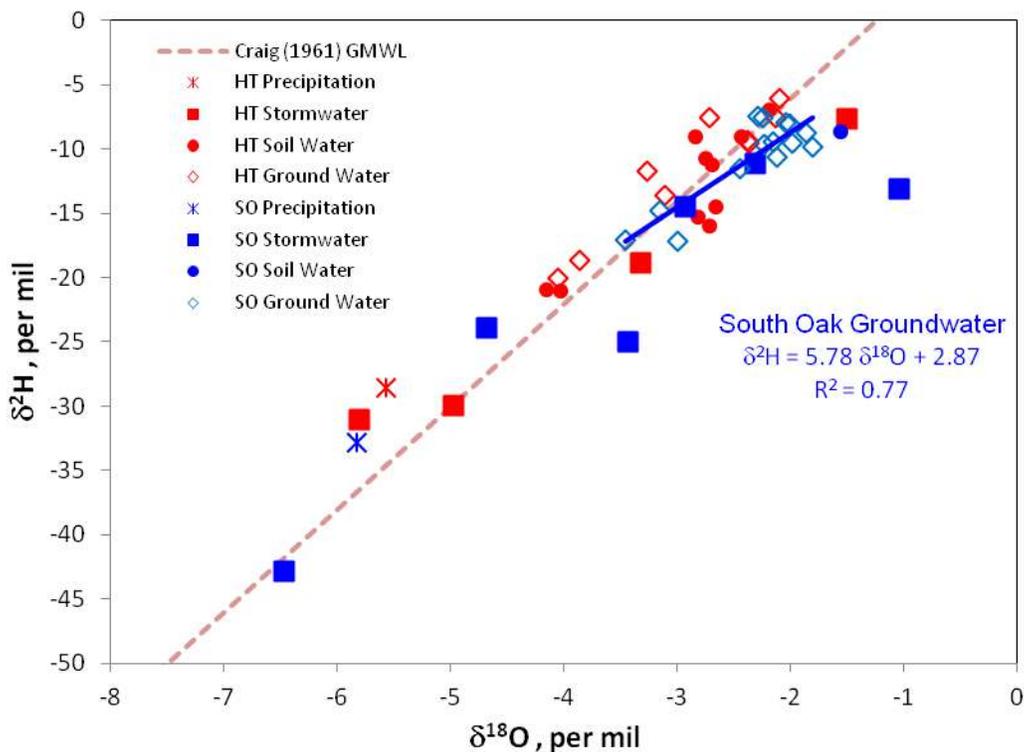
(B) Hunter's Trace pond
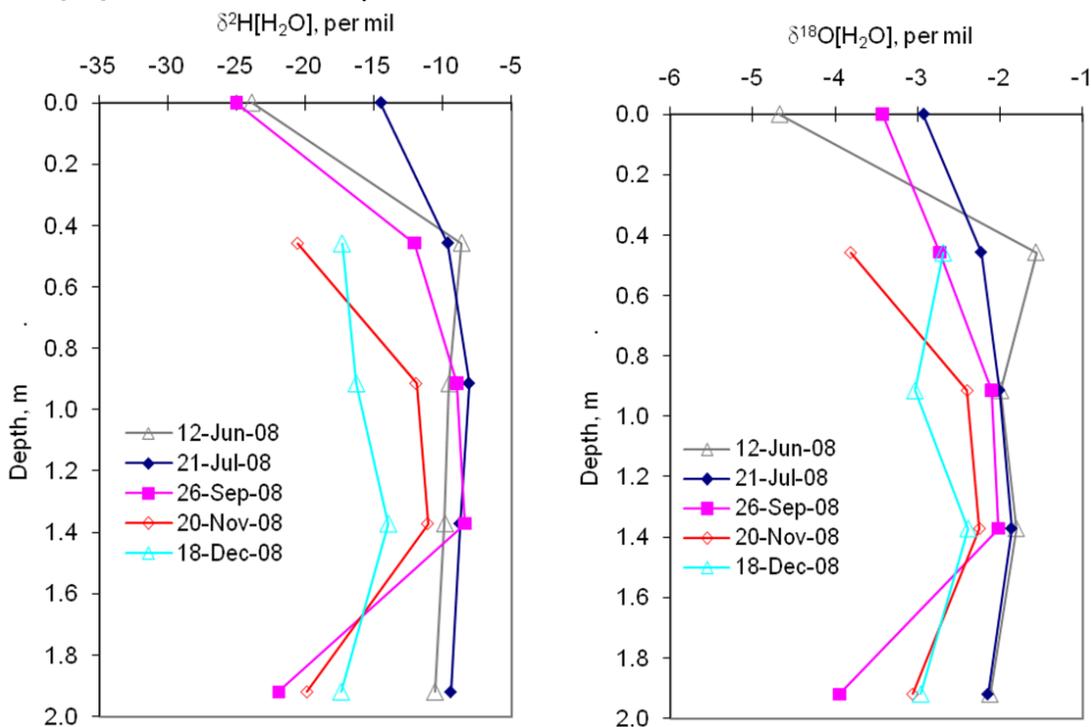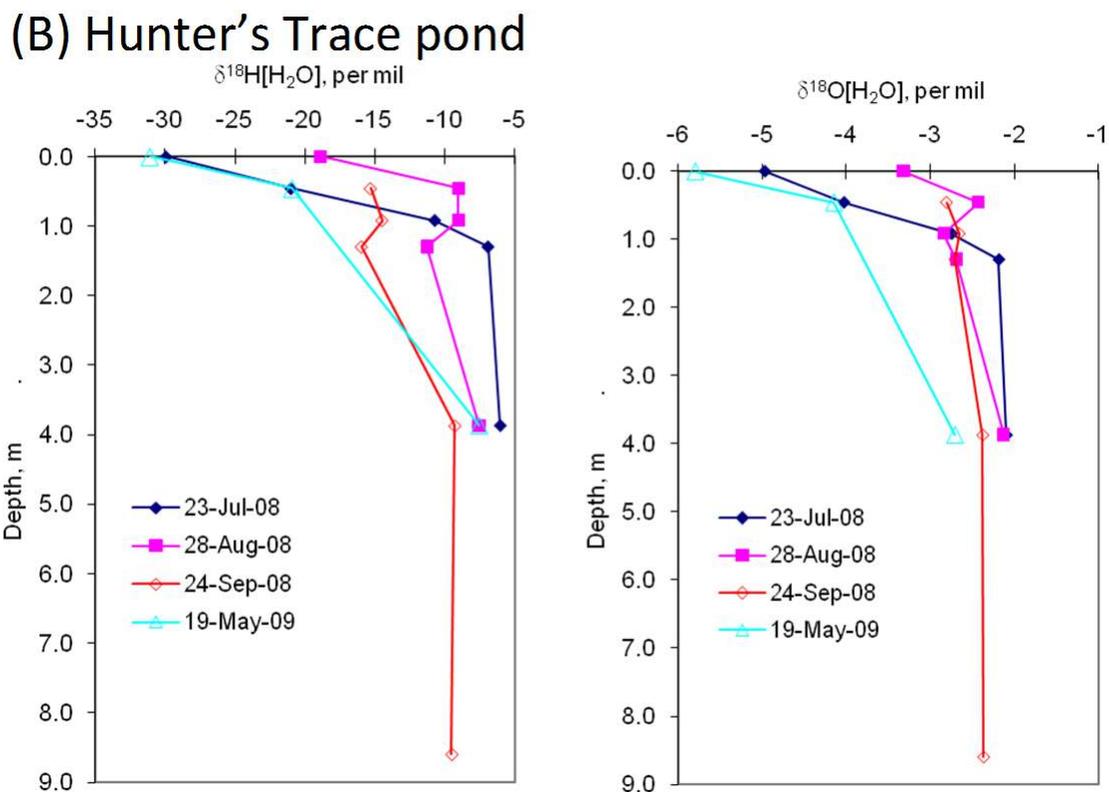
Figure 14 δ2H and δ18O of precipitation, stormwater, soil water, and ground water at the South Oak and Hunter's Trace stormwater infiltration basins.

In Figure 14, stormwater samples that plot far to the right of the GMWL represent stormwater that likely had undergone considerable evaporation during runoff or as it remained in the basin during infiltration.

Differences in the profiles with depth of $\delta^{18}O$ and δ^2H between the two sites likely indicate differences in travel time of recharge through the vadose and shallow saturated zones and the degree of evaporation that the water is subject to during this process (Figures 14A and 14B). Enrichment of $\delta^{18}O$ and δ^2H occurs at both sites up to a depth of about 1 m likely due to evaporation induced fractionation. Normal seasonal and storm intensity induced variations in

$\delta^{18}O$ and δ^2H decrease with depth at both sites as expected due to hydrodynamic dispersion, but with two important differences: (1) beneath the SO basin, an increase in $\delta^{18}O$ and δ^2H variations occurred at the 1.9 m depth (well PW), which is indicative of the effects of preferential flow pathways (Clark and Fritz, 1997); and (2) beneath the HT basin, considerable variations in $\delta^{18}O$ and δ^2H persist below 1 m, which is indicative of faster flow paths compared to the SO site. Visual observation of the soil profile during collection of soil samples and installation of monitoring equipment confirmed the presence of such preferential flow paths at the SO basin, possibly caused by macro-organisms, root pathways, or soil shrink/swell cycles due to the prevalence of smectite. Such a dual-porosity flow system may have also contributed to the evolution of the SO_4^{2-} and Cl profiles from June–December 2008 (Figure 8), where elevated concentrations at the three lysimeters slowly decreased yielding a largely flat profile by December. The sandy cohesionless soil at the HT site is less conducive to preferential pathway development than the fine-textured cohesive soil at the SO site. Nevertheless, the $\delta^{18}O$ and δ^2H results confirm shorter travel times, on average, of recharge beneath the HT basin, consistent with higher infiltration rates, compared to the SO basin.

Biological Data

Results of real-time PCR analyses provide valuable insight into denitrifier activity as inferred from NO_2^- reductase gene density. Interpretation of the real-time PCR results is based on the assumption that the presence of the *nirK* and *nirS* genes in bacterial DNA also indicates the bacteria are actively producing the Nir enzyme required for this denitrification step. However, Wallenstein et al. (2006) indicate that only the presence of denitrifying genes in mRNA is a direct indicator of gene expression. Nevertheless, quantification of *nirK* and *nirS*

genes in DNA does provide another independent line of confirmatory evidence when considered in combination with other denitrification indicators. The greatest denitrifier activity was in the shallow soil zone at depths above about 1.4 m and was fairly consistent for all five sample dates (Figure 15a). This generally corresponds with the zone of fine textured soil (silt+clay content > 40%, Figure 15a). Such fine-textured soil would maintain high moisture contents based on SMRC (Figure 5b) even as the water table drops, increasing the likelihood for anoxic conditions to develop and thus denitrification to occur. Additionally, specific surface area generally is much greater for soils with appreciable amounts of clay minerals and organic matter (Pennell, 2002), and denitrifiers more commonly adhere to soil solids than occur freely in soil pore water or ground water (Mariotti et al., 1988). Thus a fine-textured soil likely provides more favorable conditions for denitrifier growth than a sandy soil. There is no apparent relation between denitrifier activity and soil N or C contents (Figures 6 and 7) or soil-water/ground water N or C concentrations (Figures 8 and 9). However, soil water-extractable OC and IC results at the SO site suggest C cycling consistent with OC oxidation coupled with biogeochemical reduction processes in the same shallow soil zone at depths above 1.3 m (Figure 7).

(A) South Oak pond

(B) Hunters Trace pond
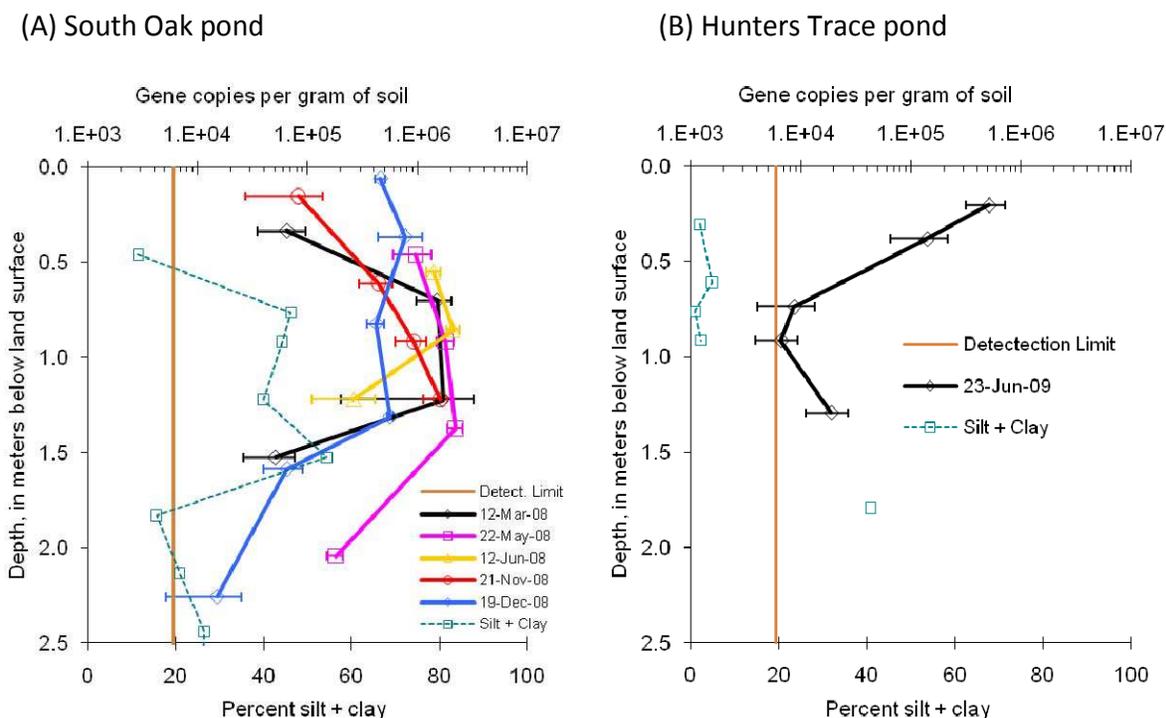
Figure 15 Nitrite reductase gene density profiles beneath the (A) South Oak stormwater infiltration basin, and (B) Hunter's Trace stormwater infiltration basin. Error bars indicate ±1 standard deviation.

Only one set of soil samples from the HT basin were analyzed because denitrification was assumed to be very limited based on water chemistry, dissolved gas, and isotopic analyses. Denitrifying activity was unexpectedly high in the aerobic shallow soil zone (less than 0.5 m depths), falling within the range of values measured at the SO basin (Figure 15B). Denitrification in aerobic vadose zones likely occurs intermittently when soil is wet or saturated and the bulk soil becomes anoxic (Christensen et al., 1990a,b) and in anoxic microsites in an otherwise aerobic bulk soil (Parkin, 1987; Koba et al., 1997). Under such dynamic conditions, net water quality effects would be related to the intensity and duration of intermittent denitrification and

mixing ratios with non-denitrified water. The water chemistry, dissolved gas, and isotopic analyses at the HT site suggest that denitrification is infrequent, rates are low, or both.

At the HT site there is no apparent relation between denitrifier activity and silt+clay content (Figure 15B), soil N contents (Figures 6 and 7), or soil-water N concentrations (Figure 9). There appears to be some relation between denitrifier activity and soil solids OC content (Figure 7b) and soil-water DOC (Figure 9). Soil solid and water-extractable OC (Figure 7b) was highest for the same two samples with the greatest denitrifier activity. Soil-water samples were not collected in June 2009, but previous results indicate DOC is greatest at depths above 1 m. This increased OC content may be due to infiltrating particulate OC or DOC from stormwater and increased OC leaching from the thin root zone. The root zone at HT is only about 0.1 m thick, but OC content is high (see 12-Jun-08 samples, Figure 7b). Interestingly, there is no similar relation at the SO site. Soil OC and soil-water/ground water DOC is higher at SO, so perhaps there is a threshold value above which denitrifier activity is not related to OC, and below which denitrifiers are sensitive to OC content.

Denitrification and Other Biogeochemical Processes

Hydroclimatic conditions and soil properties can play an important role in controlling denitrification and other subsurface biogeochemical processes in subtropical environments. Due to their close proximity, both retention basin sites investigated during this study experience similar climatic forcing, such as precipitation and temperature (Figure 3), and both are located in similar residential settings. However, results of soil and water sampling clearly demonstrate profoundly different physical, chemical, and biological conditions in the subsurface at each site. What, then, might be causing such substantial differences? Data presented herein support the

hypothesis that interactions between similar climatic and land use conditions with different soil conditions result in the different hydrologic and biogeochemical conditions observed at each site. These contrasting biogeochemical conditions have important implications for potential NO_3^- pollution impacts on local and down gradient ground water resources and provide an opportunity to glean insight that may be applied toward alternative stormwater infiltration BMPs.

The approach applied in this study to identify denitrification is largely inferential based on a "preponderance of evidence" concept using numerous indicator methods: hydrologic data, soils data, water chemistry, dissolved gas, isotopes, and PCR. Denitrification can be more directly measured, such as in a controlled field experiment, but this would require high frequency sampling during discrete infiltration events. Because the intent of this study was to monitor seasonal variations in ground water quality to ascertain more long-term behavior, samples were collected at monthly or longer frequencies in order to maximize the variety of hydroclimatic conditions sampled. It is believed that the methods for identifying denitrification in the field were significant, relatively independent, and mutually corroborating. The expense of high-frequency sampling during a controlled field experiment would have precluded monitoring for seasonal variations.

Evolution of subsurface water quality along a flow path from infiltration to eventual discharge commonly is influenced by reduction/oxidation (redox) reactions. Water chemistry changes resulting from redox reactions, which are commonly mediated by subsurface microorganisms as they use the energy produced during electron transfer for growth, interact with the solid phase of aquifer materials in a variety of biogeochemical processes. These biogeochemical processes proceed according to a sequence defined by microorganisms

competitively using combinations of available electron acceptors and electron donors to derive the maximum amount of energy (McMahon and Chapelle, 2007). OC commonly serves as an electron donor due to its relative prevalence in the subsurface and is coupled to the following sequence of electron acceptors—$O_2 > NO_3^- > Mn(IV) > Fe(III) > SO_4^{2-} > CO_2$—referred to as the ecological succession of terminal electron-accepting processes (TEAPs) (McMahon and Chapelle, 2007; Chapelle, 1995). Many of these processes were identified beneath the SO basin but few were identified beneath the HT basin. Of particular interest were the first two processes, O_2 and NO_3^- reduction, due to the desire to mitigate NO_3^- impacts from stormwater infiltration basins.

Four conditions are required for dissimilatory NO_3^- reduction (denitrification): (1) NO_3^- present, (2) DO very low or absent (commonly considered to be <0.2 mg/L (Seitzinger et al., 2006), although higher values are not uncommon and possibly are due to mixing of aerobic water with denitrified water from anoxic zones or microsites (McMahon and Chapelle, 2007)) (3) electron donor present (typically an OC compound), and (4) a population of denitrifying bacteria producing the necessary enzymes for each of the reductive steps $NO_3^- \rightarrow NO_2^- \rightarrow NO \rightarrow N_2O \rightarrow N_2$ (Tiedje, 1994). If conditions 3 and 4 are present in large enough quantities to not be rate limiting, denitrification likely will occur rapidly. Conditions 2–4 are typically met at the SO site such that NO_3^- presence is short lived, being lost to denitrification as indicated by water chemistry changes, isotopic fractionations, and excess N_2 generation. At the HT site, condition 1 is perennially met; condition 3 is met, although OC contents are less than at SO; and condition 4 is likely met as well. Real-time PCR results indicate denitrifying bacteria are ubiquitous in the soil, even under aerobic conditions at the HT site. Since denitrifiers are facultative anaerobes

they will switch to respiring NO_3^- as O_2 decreases (Korom, 1992). Therefore, condition 2—anoxic conditions—probably is the critical component missing at HT effectively truncating the ecological succession of TEAPs at O_2 reduction and precluding further reductive biogeochemical processes other than possibly ephemeral denitrification.

At the SO site, water chemistry changes (Figures 10a and 11) indicated that a temporal succession of TEAPs occurred, including O_2 reduction, denitrification, Mn and Fe reduction, and methanogenesis. The progression of TEAPs to methanogenesis provides solid evidence that NO_3^-, when present, would be denitrified.

Cyclic variations in ground water chemistry are evident in many important redox sensitive constituents, such as DO, NO_3^-, Mn, Fe, and DOC (Figure 10). These cyclic variations are prominent in all constituents at the SO site; at the HT site, relatively subtle variations occur in DO and NO_3^-. Variations generally coincide with wet and dry hydroclimatic conditions because stormwater runoff results in infiltration of oxygenated water with potentially elevated N concentrations. At the SO basin, substantial and prolonged ponding of stormwater runoff occurred (Figure 4a). In contrast, at the HT basin significant water depths only occurred after unusually large storm events and soil moisture varied cyclically at high frequency due to the well drained sandy soil (Figure 4b). The prolonged water retention and perennially high moisture contents at the SO basin contributed to the depletion of O_2 in the subsurface leading to reducing conditions allowing the ecological succession of TEAPs to proceed to denitrification and beyond.

Subsurface O_2 levels are critical as aerobic conditions preclude the reduction of electron acceptors other than O_2. Therefore, O_2 depletion appears to be the most probable critical process

inhibiting denitrification. O_2 is commonly consumed in the subsurface by respiration of micro/macro organisms in the soil by oxidizing OC and reducing O_2. Since photosynthesis does not occur in the subsurface, O_2 can only be replenished by atmospheric O_2 diffusion into the subsurface. O_2 diffusion is severely limited by moisture content of a soil, being orders of magnitude less in saturated soil than dry soil. Accordingly, anoxic conditions will develop in the subsurface if (1) the soil stays wet, (2) O_2 respiring micro/macro organisms are present, and (3) sufficient organic matter is present. All these conditions existed at the SO basin, while the first condition often was not met at the HT basin. Median volumetric gas-phase contents were about 0.25 (66% of pore space for average porosity of 0.38) beneath the HT basin, but typically were 0.04 or less (10% of pore space for average porosity of 0.40) beneath the SO basin.

The presence of subsurface O_2 was a key factor controlling the biogeochemical processes, such that when O_2 was present the C cycle was limited to aerobic oxidation of OC and the N cycle was effectively limited to ammonification, nitrification, and assimilation. However, once DO was depleted, the O_2 cycle was truncated thus allowing anoxic conditions to prevail and anaerobic oxidation of OC. Therefore, DOC provided by a large solid-phase reservoir of OC served as the predominant electron donor for such TEAPs as NO_3^-, Mn, and Fe reduction, even progressing to methanogenesis during highly reducing conditions caused by prolonged water retention. At the HT site, advection-dominated transport of NO_3^- prevailed due to the persistent aerobic conditions and permeable soils.

The presence or absence of O_2 in the subsurface at the SO site was strongly controlled by soil texture. The fine-grained soil maintained a generally high water table, and even as the underlying water table dropped the vadose zone remained wet or nearly saturated during

prolonged dry periods (saturations exceeding 70%). A fine textured soil that remains wet during prolonged dry periods will promote anoxic conditions because: (1) the diffusion coefficient of O_2 through water is 10^4–10^5 times less than through air; and (2) the gas diffusion coefficient in soil is proportional to the square of the volumetric gas-phase content (Jin and Jury, 1996). A fine-grained soil remains wet for extended periods because of capillary wicking and adhesion of soil water in the narrow pores (Koorevaar et al. 1983). Based on the measured soil moisture contents and SMRCs at each site, soils that maintain a water saturation greater than 90% (that is, 90% of the soil void space filled with water) are expected to significantly inhibit surface/subsurface O_2 exchange, thus helping to produce denitrifying conditions.

CHAPTER 3: DESIGN of an INTEGRATED POLLUTION and FLOOD CONTROL BASIN

Introduction

The contrasting conditions at the SO and HT sites provide valuable insight into natural biogeochemical processes beneath stormwater infiltration basins and the important factors that control these processes. Hossain et al. (2009) describes the application of functionalized soil amendments for mitigating ground water quality impacts of stormwater infiltration basins, with emphasis on reducing NO_3^- leaching. The alternative design implemented at the HT basin is based on combining such soil amendments to replicate the soil and subsequent biogeochemical conditions documented at the SO site. This design involves integrating pollution and flood control basins into a single retention basin. Several important criteria were outlined and the integrated design was developed to meet these:

1) Maintain the flood control capacity of the original retention basin;

2) Reduce the nitrate loading to ground water by implementing a passive pollution control technology that promotes potentially self-sustaining natural biogeochemical processes for nitrate removal; and

3) Maximize economic feasibility by minimizing design and construction costs and keeping operation and maintenance costs comparable to existing retention basin designs.

Objectives

In this chapter information on the development of the integrated pollution and flood control design at the Hunters Trace basin is presented. First, the new integrated design is described. Next, the hydraulic design methodology is presented, followed by model simulated predictions of basin flood control performance. Lastly, a short description of field construction activities at the HT basin is provided.

New Integrated Design

The HT basin has a 56 acre watershed, consisting of 3.4 acres of curb-and-gutter roadway, 34.9 acres of residential lots (1/4 to 1/3 acre each), and 17.7 acres of undeveloped conservation area. The basin has a bottom area of approximately 31,000 ft^2, a bottom elevation varying from about 50.7 ft NAVD88 to 51.4 ft, and a top elevation varying from 60.3 ft to 62.1 ft (Figure 16a). Based on these elevations, which were surveyed by Marion County in 2007, the basin is considered to have maximum depth of 9 ft before overtopping. Runoff enters the basin through three culverts; the west and south culverts are 42-inch corrugated metal pipes (CMP) and the east culvert is a 30-in CMP (Figure 16a).

The alternative design developed for the HT basin consists of dividing the basin into two approximately equal sub basins: the south basin functions as the pollution control basin and the north basin functions as the flood control basin (Figure 16a). The pollution control basin was formed by excavating 22 inches of native soil, placing a 4-inch thick coarse sand filter layer followed by a 12-inch thick amended soil layer, and backfilling with a 6-in thick layer of the native topsoil that was originally on the bottom of the basin (Figure 16b). The remaining excavated soil was used to create at 2.5-ft high berm forming the north side of the pollution

control basin. To minimize erosion, the berm side slope was constructed at 10:1 (H:V) or milder

slope and a soil erosion blanket was used and covered with grass seed.

(A) Plan View

(B) Section A-A'

Notes: 4 inches of coarse sand, 12 inches of amended media and 6 inches of native soil
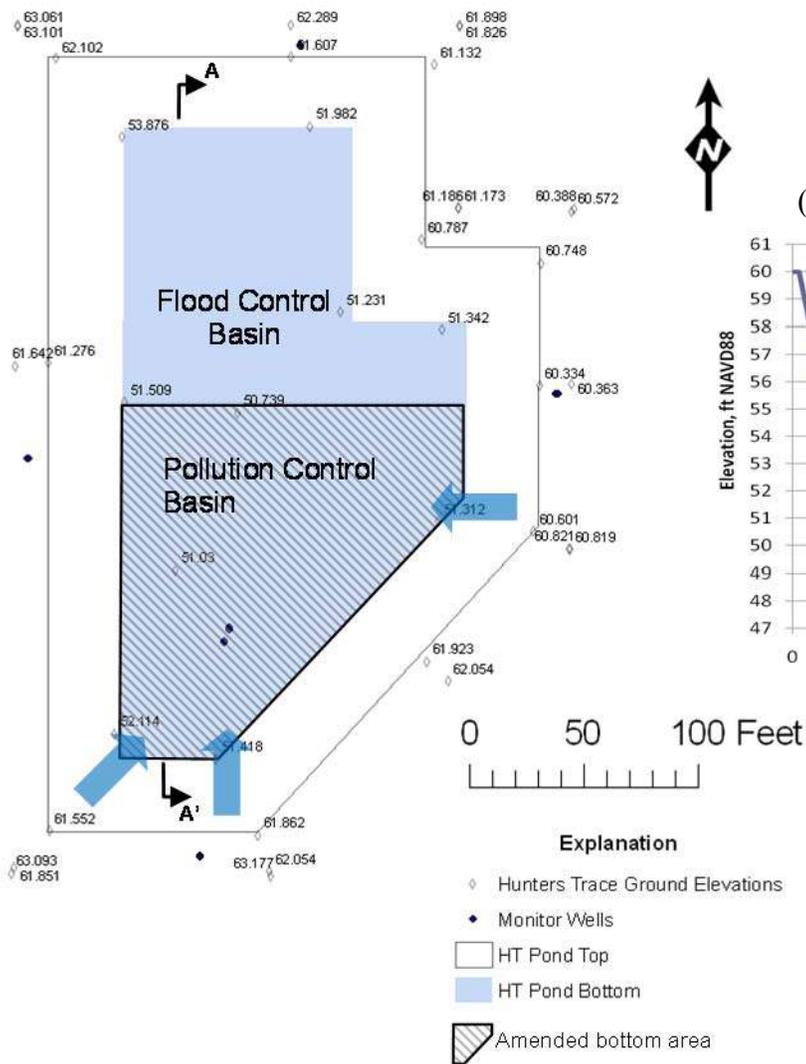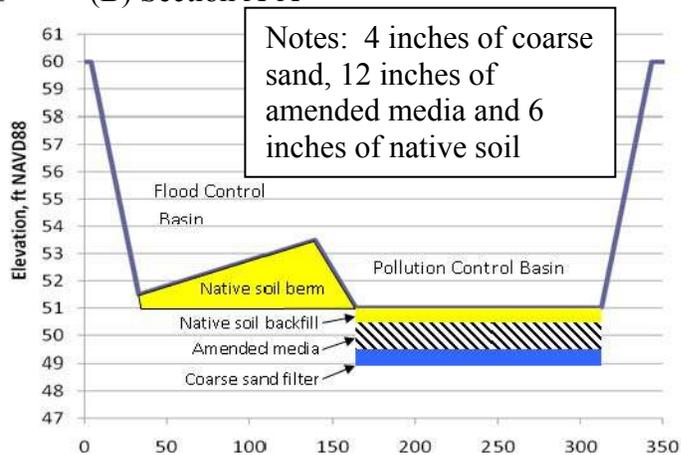
Figure 16 New integrated design at the Hunters Trace basin showing (a) plan view, and (b) cross-sectional view.

The pollution control basin was designed with a 2.5 foot high berm and an average area of about 17,300 square feet. The holding volume of the pollution control basin is about 1.0 Acre Feet. For a 4 acre effective impervious area (EIA) of the watershed, the runoff stored in the basin from the EIA is 3.0 inches ($1.0 \times 12/4$). Thus if the pollution control basin is empty, it can store the runoff from a 3.0 inch rainfall over the EIA. The mean annual daily rainfall for the maximum rainfall event is 4.2 inch (Rao, 1998).

Background monitoring data collected at the SO and HT sites, the results of which are described in Chapter 2, demonstrated two important factors affecting biogeochemical processes beneath the retention basins:

1) Aerobic conditions in the subsurface at the HT basin was the critical factor precluding nitrate reduction and thus causing nitrate leaching to ground water; and

2) Soil properties were an important control on surface/subsurface O_2 exchange, with the fine-grained soil at the SO basin inhibiting O_2 diffusion into the subsurface and the coarse-grained soil at the HT basin allowing O_2 diffusion into the subsurface.

The soil layer structure in the pollution control basin was designed to increase soil moisture, reduce O_2 diffusion into the subsurface, and increase sorption capacity while still maintaining an infiltration capacity near that of the original basin. Particle-size distributions of each sub layer are shown in Figure 17. The coarse sand layer (FDOT underdrain sand P2, Type V-1225644) is included to encourage rapid drainage of this thin layer to maintain a low moisture content. Because unsaturated soil hydraulic conductivity is directly and nonlinearly related to moisture content (Koorevaar et al. 1983), such a well drained layer will have a very low hydraulic conductivity and will inhibit drainage of an overlying fine-grained layer. The amended soil layer

target mix is 1:2:4 (by volume) of tire crumb to clay to sand. A mixture of tire crumb and native soils (1:4) was found to have no acute toxicity, even when the nutrient concentrations were as high as 50 mg/L of TN (Marinco Bioassay Laboratory, 2009). Tire crumb increases sorption capacity (Hossain et al., 2009), and clayey sand increases soil moisture retention. This mix of a commercial product is called Bold & Gold Stormwater and has the effect of increasing the moisture retention capacity of the soil beneath the pollution control basin because of its fine-grained texture (Figure 17). The SMRC for a preliminary amended soil media mix (tested during design of the pollution control basin) consisting of a 1:5 mixture (by volume) of tire crumb and clayey sand (Figure 18) demonstrates its greater moisture retention capacity over the native soil at the HT basin (Figure 5b). Additionally, due to the smaller size of the pollution control basin (approximately half the original area of the basin) and a lower rate of infiltration (as low as 0.25 inch/hour) relative to the native sandy soil of the site, water will remain in the pollution control basin for a longer time period for any given rainfall event. Thus the basin will remain wet longer than the original basin. Both the increased moisture retention capacity and the longer holding frequency will contribute to conditions more favorable for formation of anaerobic conditions beneath the pollution control basin. Lastly, the top sub layer consists of native topsoil excavated from the pollution control basin and later replaced. Due to the organic matter content and natural vegetation, this topsoil will provide a source of organic carbon to serve as an electron donor during denitrification or other biogeochemical processes. Laboratory testing of the amendment media indicates an estimated field infiltration rate of the amendment to be about 10–40% of the existing infiltration rate. Actual infiltration rates were measured after the amendment was added.
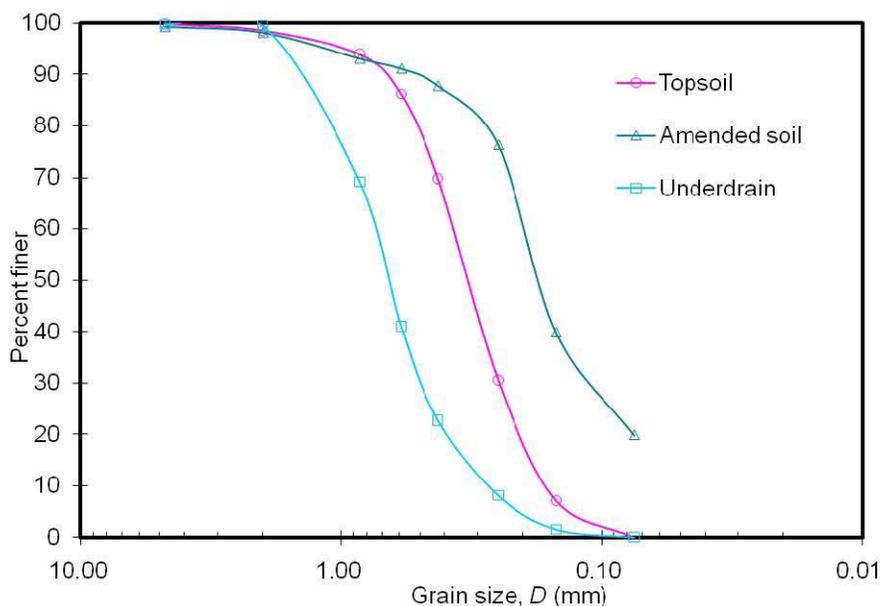
Figure 17 Particle-size distributions of soil sub layers for the new integrated design for the pollution control basin at the Hunters Trace basin.
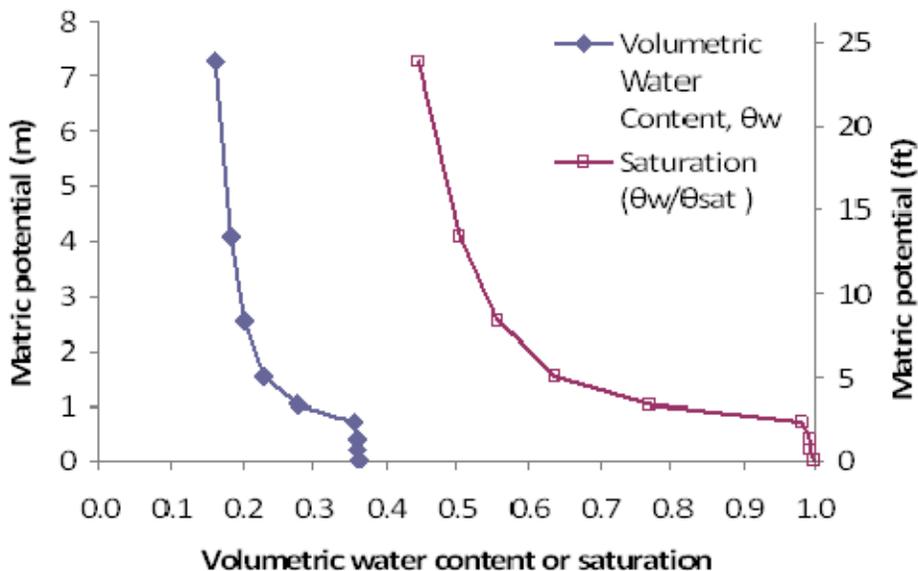
Figure 18 Soil moisture retention curve for a 1:5 mixture (by volume) of tire crumb and clayey sand similar to the amended soil layer used in the pollution control basin at the Hunters Trace basin.

Design Model Development and Calibration

In order to ensure that the hydraulic operation of the integrated basin design achieves the intended enhanced nutrient removal while maintaining the flood control requirements, a mass balance model was developed based on the following equation:

$$Q - F = \Delta S$$

where, Q is the runoff volume, which is the product of rainfall depth and effective impervious area (EIA) (conceptually, the EIA includes directly connected impervious area (DCIA) plus any pervious areas that may also contribute runoff); F is the infiltration volume, which is the product of infiltration rate and flooded area where flooded area is computed via a stage-area equation based on basin geometry; and ΔS is the change in storage volume, from which stage is computed via a stage-volume equation based on basin geometry.

The model was calibrated to measured field conditions August 21–26, 2008, which represents conditions during and after Tropical Storm Fay. During this period, 7.3 inches of rain fell, 6.1 inches of which occurred during the first 33 hours and can be attributed to the tropical storm. For comparison, Rao (1998) reported that the mean annual 24-hour maximum rainfall for central Marion County is 4.2 inches and the 10-year 24-hour maximum rainfall is about 6.3 inches. The model was implemented in Microsoft Excel. Because the basin geometry and rainfall are known, only two unknowns remain: EIA and infiltration rate. The Solver function was used to attain optimum parameter values by minimizing the root-mean-square error (RMSE) between

simulated and measured stage. The simulated stage closely matches the measured stage, with a mean error of 0.002 ft and a RMSE of 0.04 ft (Figure 19).
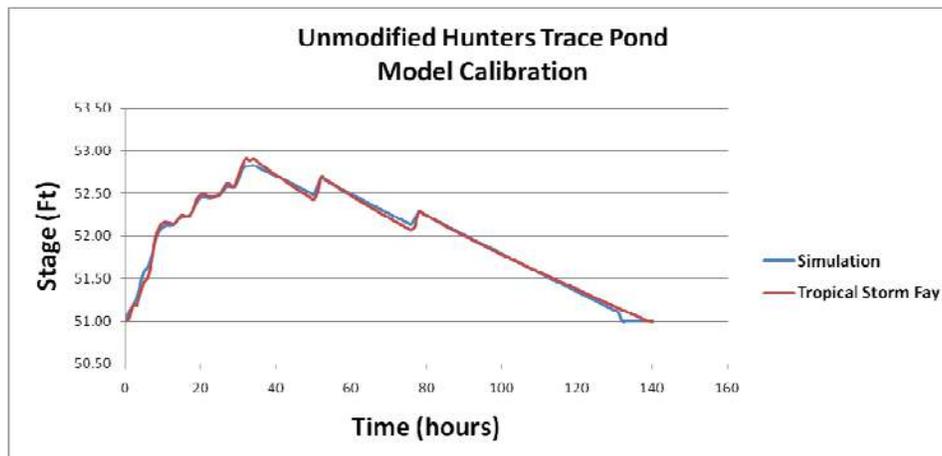
Figure 19 Measured and simulated stage at the Hunters Trace basin, August 21–26, 2008.

The optimum parameter values are reasonable based on comparisons with other data. The optimum EIA of 4.117 acres is slightly larger than the roadway area of 3.4 acres in the HT watershed, indicating that additional DCIA (e.g. driveways) and some pervious areas are likely contributing. The optimum infiltration rate of 0.289 in/hr falls in the range of values estimated from analysis of measured stage recession curves, which indicated infiltration rates ranging from 0.28 to 0.42 in/hr for large magnitude storms ranging from 1.8 to 6.1 inches.

Design Storm Simulations

Calibration results indicate good model performance, but a larger storm is required to adequately assess flood control performance. An 11-inch, 24-hour synthetic (type 2) design storm was selected, which represents a 100-year maximum rainfall for central Marion County.

The calibrated model was modified to represent the proposed modifications, thus revised stage-area and stage-volume equations were developed according to the geometry outlined in Figure 16. Since all three culverts enter the pollution control basin, the modified model was simulated to operate in a 3-step sequence. First, the pollution control basin fills. Second, at a depth of 2.5 ft, water overflows the berm and begins filling the flood control basin. Third, when the flood control basin fills (stage of 53.5 ft), the entire basin begins filling. At each of these three steps, the mass balance equation is solved for each respective sub volume: pollution control basin, flood control basin, and entire basin above stage 53.5 ft. An infiltration rate of 0.03 in/hr was specified for the bottom of the pollution control basin, which is the lowest expected infiltration rate for the amendment media and based on compacted laboratory tests. The existing infiltration rate of 0.289 in/hr was maintained for the flood control basin as well as the berm and side slope areas of the pollution control basin. Results indicate that the modified basin will stage higher (55.7 ft) than the unmodified basin (54.8 ft), but still 4.3 ft below the top of the basin (Figure 20).
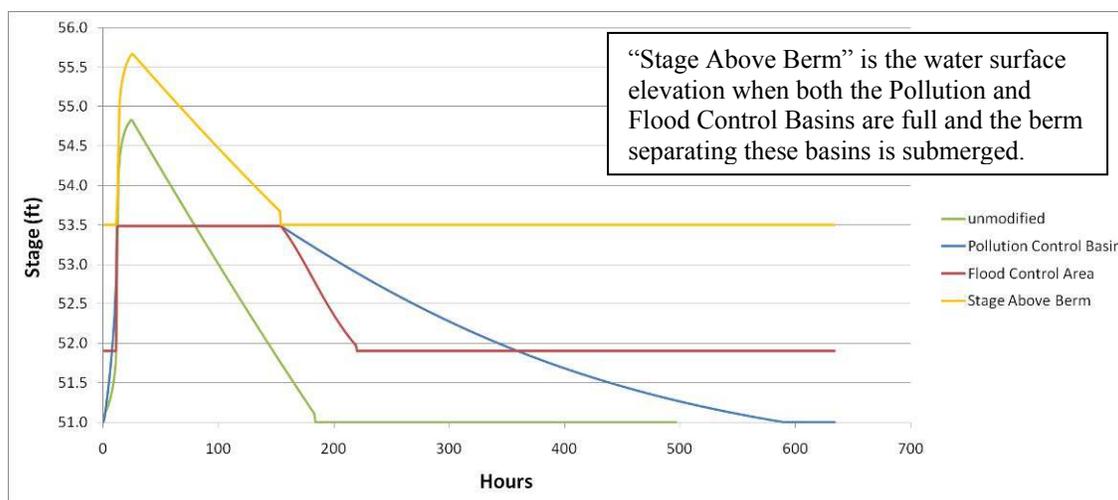
Figure 20 Simulated stage in the unmodified and modified Hunters Trace basin for a 100-year 24-hour synthetic (type 2) 11-inch storm assuming an infiltration rate of 0.03 in/hr for the pollution control basin.

Simulation of an isolated storm is not always an adequate test of basin performance because it implicitly assumes complete basin recovery during interevent dry periods. This likely is not a good assumption, especially considering the reduced infiltration rate in the pollution control basin and the closely spaced rainfall events common during the summer wet season. Therefore, the modified basin performance was simulated for a 2-year period (2004–2005) using rainfall measured at the Florida Automated Weather Network station in Citra, northern Marion County (http://fawn.ifas.ufl.edu/). This time period was chosen because it includes the unusually wet period during the summer and early fall of 2004 due to Hurricanes Charley, Frances, and Jeanne. To yield an even more conservative prediction, the 11-inch synthetic storm event was placed during the wet season on August 1, 2004, shortly before the occurrence of Hurricane Charley. Results indicate that the modified basin will stage higher (56.2 ft) than for the isolated storm event (55.7 ft), but still 3.8 ft below the top of the basin (Figure 21).
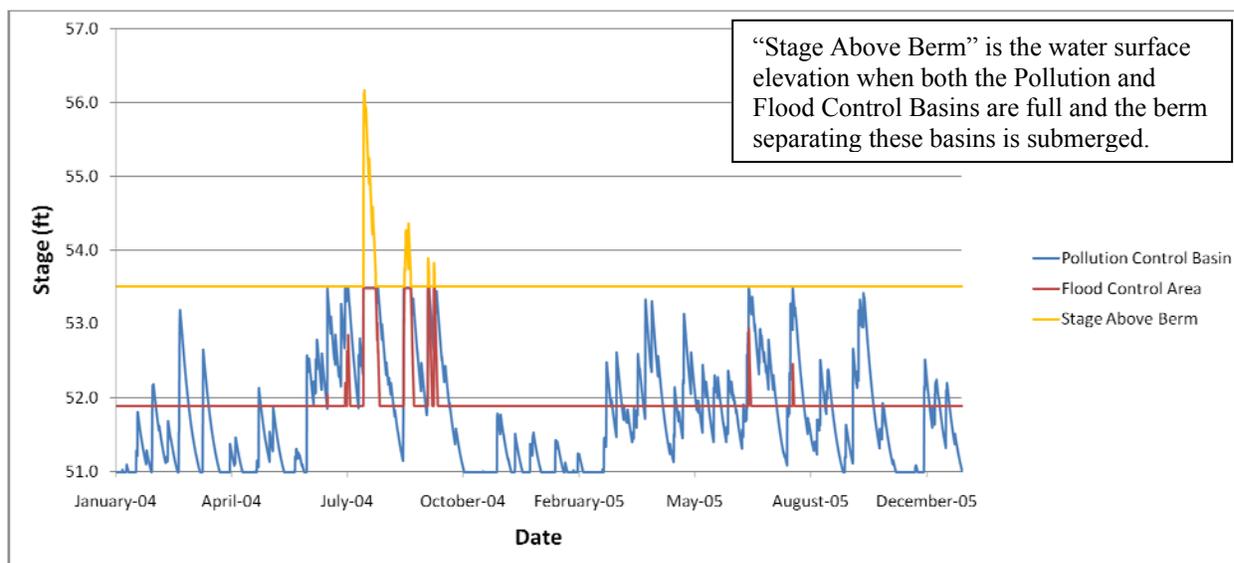
Figure 21 Simulated stage in the modified Hunters Trace basin based a 100-year 24-hour (11-inch) storm embedded in 2 years (2004–2005) of actual rainfall assuming an infiltration rate of 0.03 in/hr for the pollution control basin.

Simulated Hydraulic Performance

The model may be used to determine the volume of water infiltrating in the pollution control basin, thus giving as estimate of the treatment volume as a percentage of total runoff. This is a function of the infiltration rate assumed for the pollution control basin. The simulations presented above (Figures 20 and 21) are based on the minimum estimated infiltration rate of 0.03 in/hr, which results in 30% treatment volume with the pollution control basin remaining flooded for 80% of the 2004–2005 period. Alternatively, using the maximum estimated infiltration rate of 0.13 in/hr results in 68% treatment volume with the pollution control basin remaining flooded for 42% of the 2004–2005 period. Under these increased infiltration conditions, the peak stage reaches 55.7 ft (Figure 22).
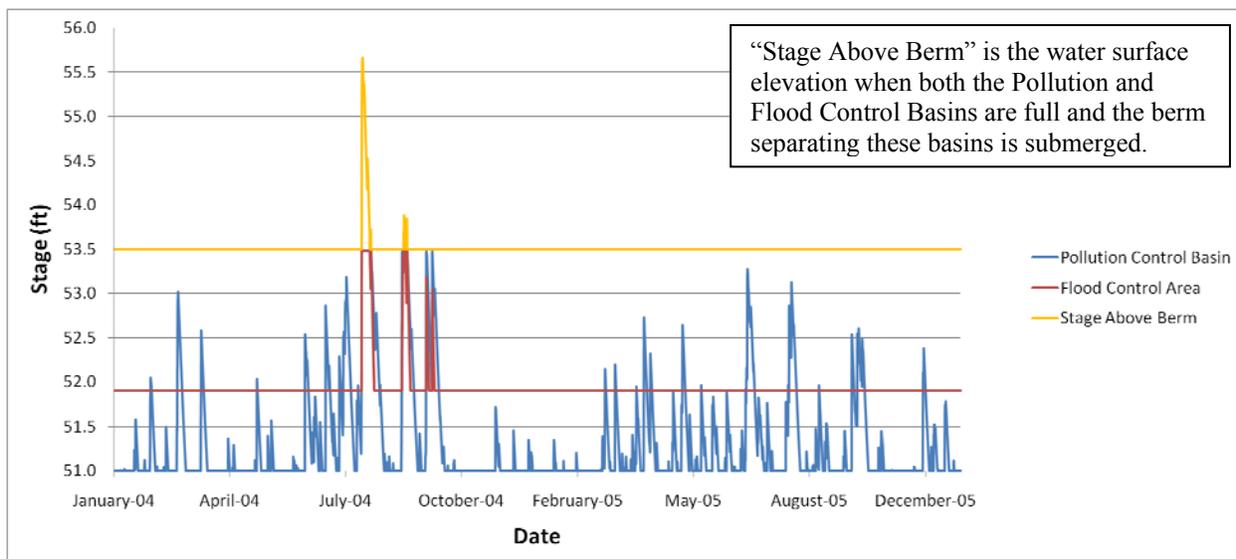
Figure 22 Simulated stage in the modified Hunters Trace basin based a 100-year 24-hour (11-inch) storm embedded in 2 years (2004–2005) of actual rainfall assuming an infiltration rate of 0.13 in/hr for the pollution control basin.

The simulations presented above indicate that implementation of the new integrated design at the HT basin will maintain the flood control capacity of the basin within acceptable limits. The modified basin is expected to maintain a peak stage of 56.2 ft during a 100-year 24-hour storm occurring during the summer wet season. The peak stage will leave 3.8 ft of freeboard below the lowest top of basin elevation, thus providing a margin of safety against decreased infiltration rates or larger runoff volumes.

Design and Construction of the Integrated Pollution Control Basin at Hunters Trace

The pollution control basin was designed to retain the runoff from a 3 inch event from an EIA of 4.1 acres. The time for recovery of this runoff volume at a 2.5 foot depth was 120 hours or 5 days. Construction of the new integrated design at the HT basin was completed November 3-6, 2009 in accordance with the specifications outlined in the Environmental Resource Permit approved by the St. Johns River Water Management District. An outline of the construction process is provided in Figure 23. The process is also deemed economical as construction and materials cost was only about $6.00 per square foot of basin bottom. This cost did not include profit and permit fees. There is minimal to no additional operation and maintenance cost, and operation, maintenance, and repairs are similar to those expected with existing retention systems.

1. Remove 6 inches of topsoil

2. Remove 16 inches of subsoil

3. Replace with 3 sub layers

4. Place 4-inch coarse sand layer

5. Mixing tire crumb & clayey sand

6. Place 12-inch amended soil layer

7. Place 6-inch topsoil layer

8. Final Integrated Design

Pollution Control Basin

Berm

Flood Control Basin

Figure 23 Construction of the new integrated design at the Hunters Trace basin.

CHAPTER 4: EVALUATION OF SOIL AUGMENTATION DESIGN

Introduction

Field monitoring was conducted to assess both the nutrient removal and hydraulic performance of the new integrated basin design using soil augmentation. Monitoring was conducted November 2009 – August 2010 in order to cover a variety of hydroclimatic conditions and all four seasons.

Objectives

In this chapter presented are the data collected at the HT basin during 2009–2010. The data are used to characterize the hydrologic and water quality conditions for the new integrated design. Next, these results are interpreted in order to identify and evaluate the natural processes (physical, chemical, and biological) that control the nitrogen cycle in soil and ground water beneath the pollution control basin. Lastly, a discussion of nitrate transport and fate and phosphorus data both before and after implementation of the new integrated design is presented.

Data Collection

Seven sampling events were conducted after construction of the new integrated design: November, early December, and mid December 2009 and January, March, April, and August 2010. Sampling included additional analytes not previously collected, namely $^{13}C/^{12}C$ ratios of dissolved inorganic carbon (DIC) and dissolved organic carbon (DOC) to look at carbon cycling; and N_2O and CH_4 (dissolved and soil gas) to look at nitrogen cycling and possible methanogenesis. Additionally, analyses performed during the background monitoring period were continued: nutrients, DOC, major ions, trace metals, nitrate isotopes ($\delta^{15}N$ and $\delta^{18}O$), water

isotopes (δ^2H and $\delta^{18}O$), dissolved gas concentrations, and $\delta^{15}N$ of N_2. Isotopic analysis of DIC and DOC samples was performed by the USGS Reston Stable Isotope Laboratory in Reston, VA, and analyzed on a carbon dioxide dual inlet isotope ratio mass spectrometer (Coplen, 1973; Revesz and Coplen, 2006). Carbon isotopic results are reported in per mil (‰) relative to VPDB (Vienna Peedee belemnite) and normalized (Coplen and others, 2006). N_2O and CH_4 analyses were performed by the research lab of R.L. Smith (U.S. Geological Survey, Boulder, CO) based on the method outlined by Antweiler et al. (2004) and Smith et al. (2005). Other water quality analyses were performed according to methods described in Chapter 2.

Hydrologic monitoring and soil analyses were performed. Continuous hydrologic monitoring was continued to assess hydraulic performance of the new integrated design. Soil moisture and temperature probes were placed at the midpoint of the amended soil layer (0.3 m depth) and at the midpoint of the coarse sand layer (0.5 m depth). The deepest set of soil moisture and temperature probes remained in the native soil at a depth of 0.9 m. Three sets of soil samples were collected (January, April, and August 2010) and analyzed for C and N contents and denitrifier activity by real-time PCR. Hydrologic monitoring and soil analyses were performed according to the methods described in Chapter 2.

Hydrologic and Soil Data

Hydrologic monitoring during the post-amendment period indicates frequent water in the Pollution Control Basin (Figure 24). Because the Pollution Control Basin is approximately half the original area of the basin, water ponds deeper for any given rainfall event and thus the basin stays flooded longer than the original basin. The more frequent water in the basin combined with

the fine-grained texture of the amended soil layer causes higher soil moisture contents (0.3-m probe, Figure 24), leading to conditions more favorable for denitrification.
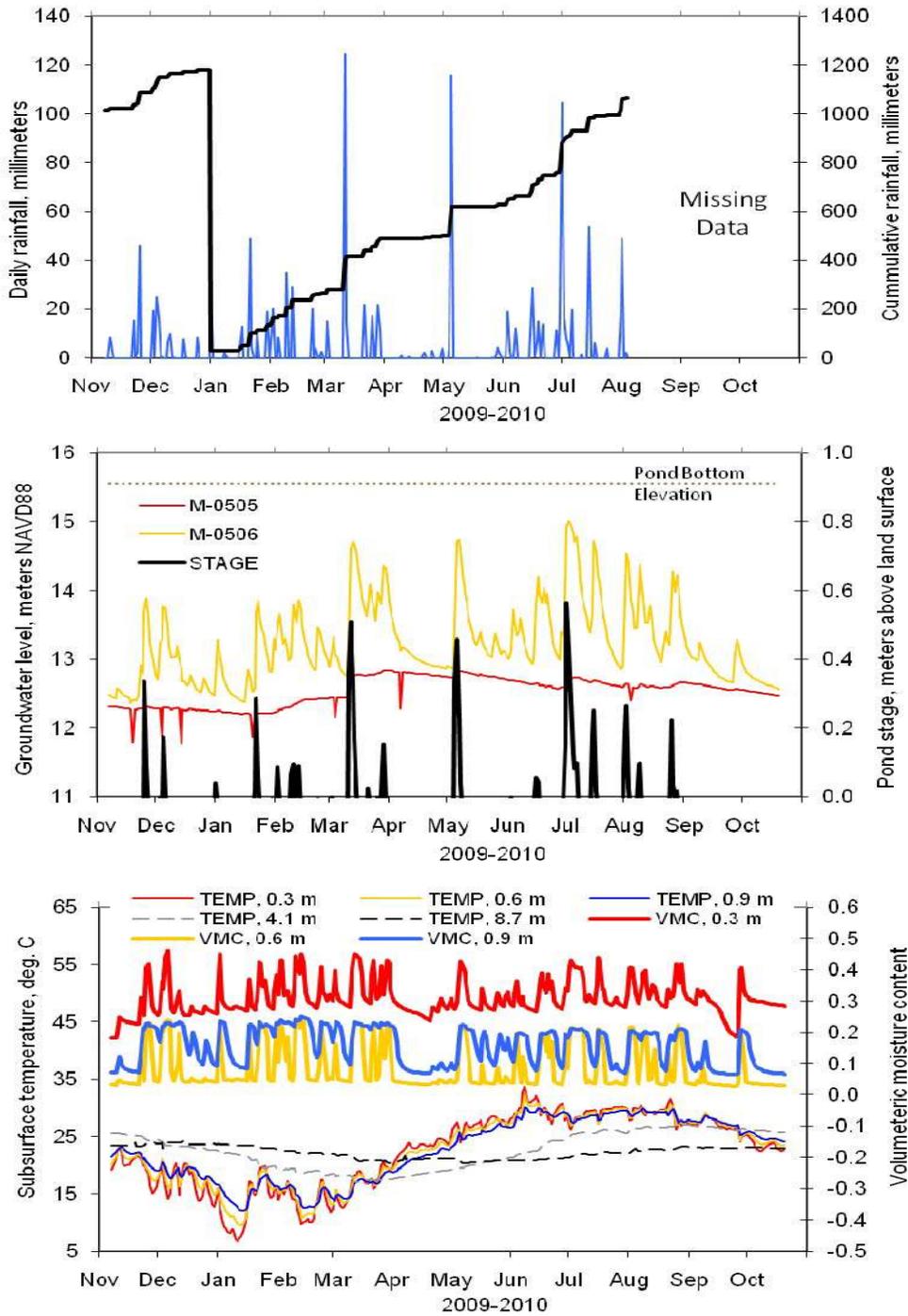
Figure 24 Hydrologic monitoring for the new integrated design at the Hunters Trace basin.

The large storm event in March 2010 (Figure 24) resulted in overtopping of the berm, flooding of the Flood Control Basin, and moderate erosion on the downstream (north) side of the berm. The berm was repaired to its original dimensions, seeded with grass, and an erosion control blanket installed along the entire downstream side (Figure 25). Subsequent large storm events in May and July 2010 resulted in overtopping of the berm (Figure 24), but no erosion occurred.

Figure 25 New integrated design at the Hunters Trace basin (Pollution Control Basin is in background; Flood Control Basin is in foreground) after placement of erosion control blanket showing good performance and absence of erosion after 3.7-inch storm.

Rainfall and basin stage data (Figure 24) indicate that the Pollution Control Basin holds about a 3-inch storm before overtopping (as designed). Analysis of basin stage recession curves both before and after the new integrated design indicates essentially no change in limiting infiltration rate, averaging about 0.34 in/hr (Table 2). Note that for the original basin there were some rates exceeding 1 in/hr, but the other four values were within the range of infiltration rates for the new design. This likely is related to the antecedent moisture content of the soil. For the

original basin, the higher rates occurred when the soil was dry, which was commonly the case for the well drained sandy soil (Figure 4b); the lower rates prevailed during large events when the soil remained wet. In contrast, for the new integrated design the soil remains relatively wet (Figure 24), thus the infiltration rates remain very similar to those for the original basin under relatively wet antecedent moisture conditions. Considering the range of computed values and that possible future decreases could occur, a limiting infiltration rate of 0.25 in/hr is recommended for simulations given similar subsoil conditions. Using the 2004–2005 rainfall with the EIA of 4.1 acres and an infiltration rate of 0.25 in/hr with the simulation model described in Chapter 3, results in an annual capture in the pollution control basin of 86% of the yearly runoff volume. The average infiltration rate after amendment is 0.34 in/hr.

Table 2 Infiltration rates at the Hunters Trace basin before and after amendment and calculated from pond stage data

Date	Rain (in)	Duration (hr)	Infiltration Rate (in/hr)
BEFORE AMENDMENT			
16-Dec-07	1.48	3.17	2.16*
21-Feb-08	0.36	1.67	1.50*
23-Feb-08	1.82	5.33	0.35
15-Jul-08	1.97	1.33	0.42
22-Aug-08 1st estimate	6.12	33.08	0.34
22-Aug-08 2nd estimate	6.12	33.08	0.29
AFTER AMENDMENT			
25-Nov-09	1.69	1.33	0.37
17-Jan-10	0.67	2.64	0.41
21-Jan-10	1.91	5.83	0.35
11-Mar-10	4.83	6.25	0.26
21-Mar-10	0.86	6.17	0.30

* indicates soil was dry for at least one foot into the basin before runoff.

Soil C contents generally are similar for samples collected before and after the amendment (Figure 26). The elevated soil solids TC contents for the amended soil layer (0.3-m depth samples) in January, April, and August 2010 are indicative of the tire crumbs. It should be noted that the soil solids OC contents reflect little of the tire crumb because the standard procedure used for OC analyses of soils (Walkley and Black, 1934) cannot digest the tire fragments. In contrast, soil solids TC is performed by combustion-oxidation at 1000°C and does measure the C content of the tire fragments. Therefore, soil solids IC contents for the amended soil layer are bias high because IC is computed as the difference between TC and OC.
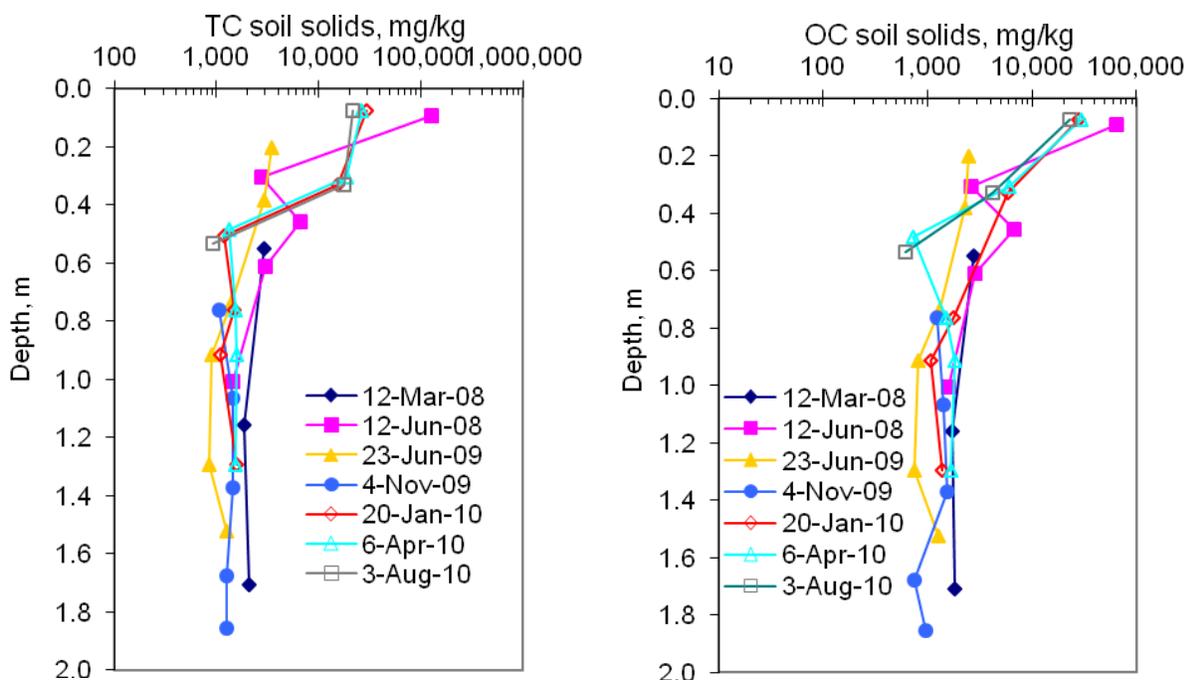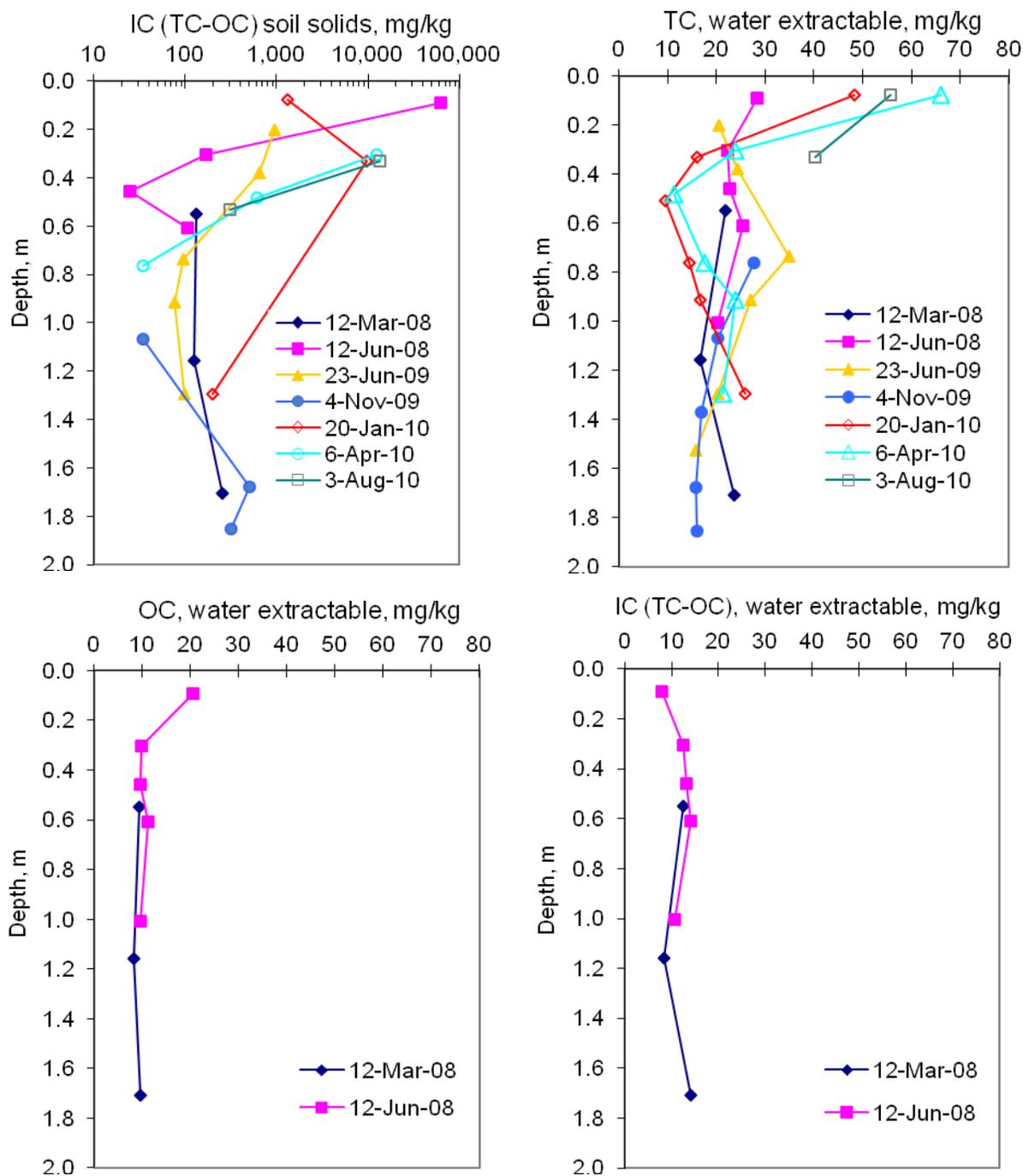
Figure 26 Soil solid and water extractable total carbon (TC), organic carbon (OC), and inorganic carbon (IC) contents at the Hunter's Trace stormwater infiltration basin.

Soil N contents differ for samples collected before and after the new integrated design (Figure 27). Soil solids TN is higher in the amended soil layer than the native soil sampled in 2008–2009 at the same depth, although concentrations fall within the range of values at other depths. Soil solids TN are lowest in the coarse sand layer as expected for a clean quartz sand. In the topsoil and native subsoil, solids TN contents are similar for samples collected before and after the new integrated design. Water extractable NH_4^+ is lower for the January and April 2010 samples in the amended soil and coarse sand layers, but at similar levels in the topsoil and native subsoil. Most notable are differences in water extractable NO_x ($NO_3^-+NO_2^-$). All water extractable NO_x contents were below the method detection limit for samples collected below the topsoil layer after construction of the new integrated design. For January and April 2010, soil samples were collected at depths of 0.1, 0.3, 0.5, 0.8, 0.9, and 1.3 m; for August 2010, soil samples were collected at depths of 0.1, 0.3, and 0.5 m. Samples collected at depths below 0.1 m had water extractable and KCl extractable NO_x below the method detection limit for January and April 2010. For August 2010, samples collected at depths below 0.1 m had KCl extractable NO_x below the method detection limit (water extractable NO_x and NH_4^+ were not analyzed due to limited sample availability). In contrast, water extractable NO_x was 0.08–2.3 mg/kg and KCl extractable NO_x was 0.08–3.0 mg/kg at depths below 0.1 m for samples collected prior to construction of the new integrated design.
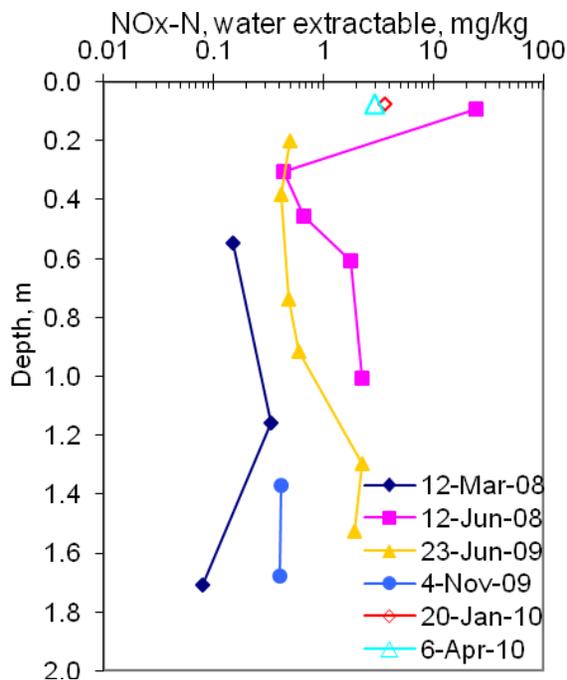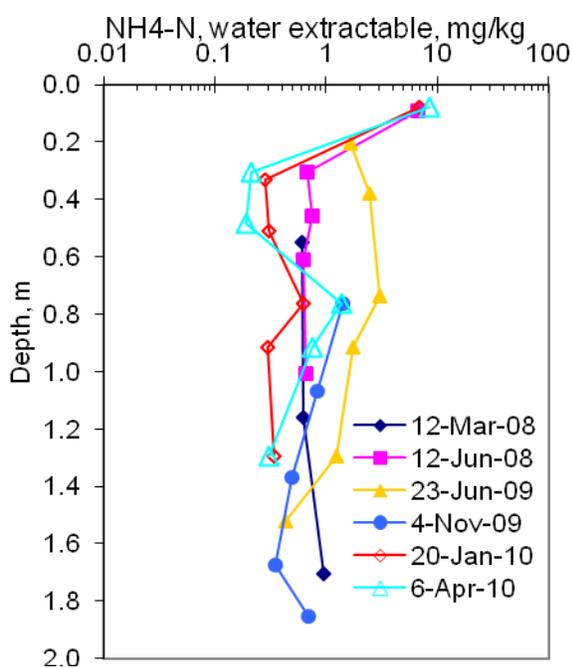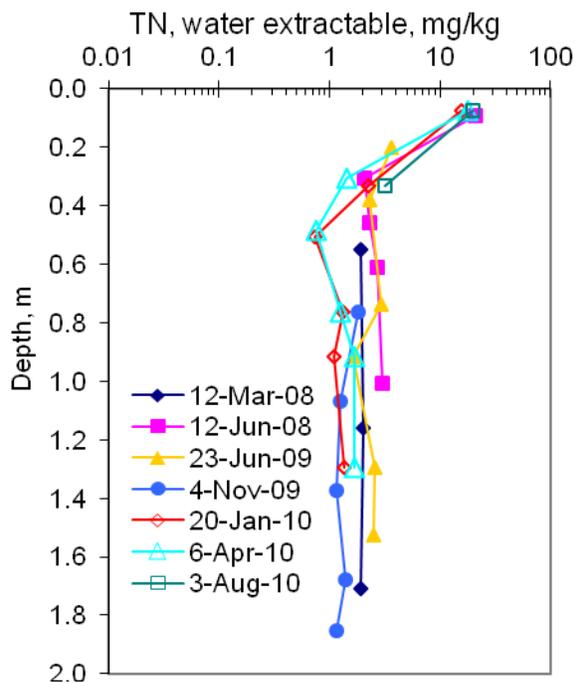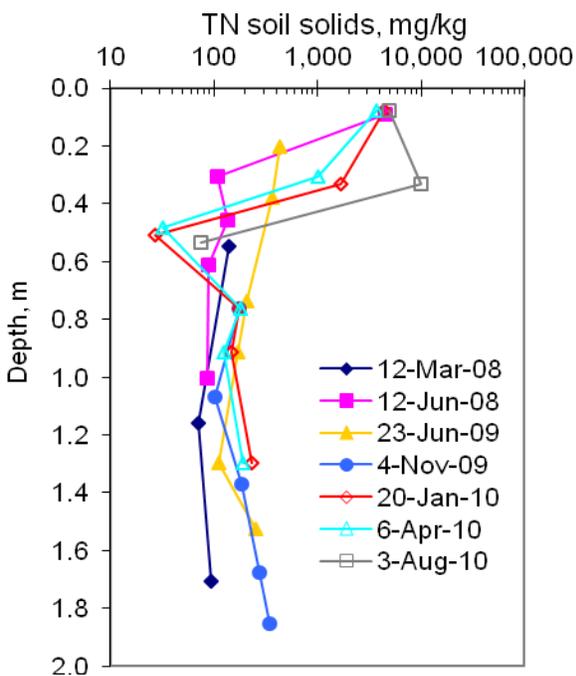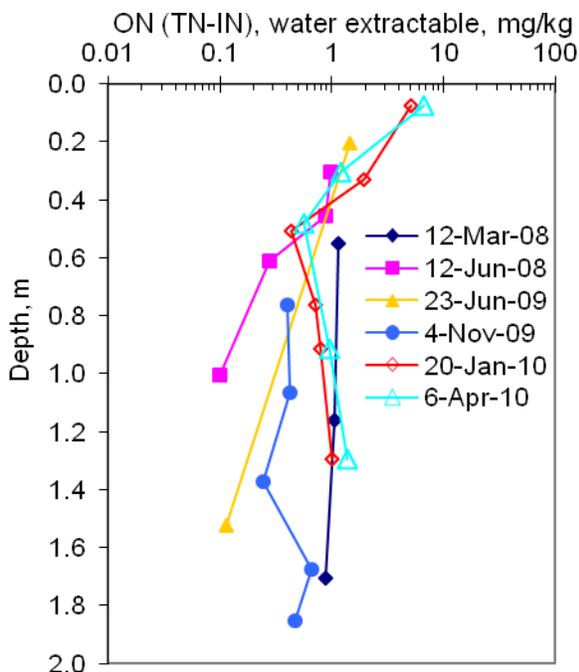
Figure 27 Soil solid and water extractable total nitrogen (TN) and soil water extractable ammonium nitrogen (NH4+), nitrate plus nitrite (NOx), and organic nitrogen (ON) at the Hunter's Trace stormwater infiltration basin. January and April 2010 samples collected at 0.3, 0.5, 0.8, 0.9, and 1.3 m depths were below the method detection limit.

Water Quality Data

Dissolved nitrogen in the vadose zone and shallow ground water at the HT basin is almost exclusively in the NO_3^- form throughout the entire monitoring period June 2007–August 2010 (Figure 28). Dissolved nitrogen in stormwater was predominantly in the organic form; particulate and colloidal nitrogen (greater than 0.45 µm) are at times an important constituent of the total nitrogen in stormwater (Figure 28). Short-term temporal variations in soil water and ground water are likely due to changing hydroclimatic conditions and variable nitrogen concentrations in runoff, although a long-term downward trend is apparent at several depths. The long-term trend is most evident in the shallow ground water (well M-0506, Figure 28) because

there naturally is an increasing integration of higher frequency "signals" with increasing depth. This integration effect likely is due to a combination of mixing and physicochemical and biological reactions such as sorption, nitrification, and denitrification. Therefore, reductions in NO_3^- concentrations after November 2009 at the HT basin are due to variations in nitrogen input (via stormwater infiltration) as well as natural variations and the effects of the new integrated design. The change reduction in nitrogen in the vadose zone (lysimeters in Figure 28) is obvious and implies that the reduction of nitrogen primarily occurred before percolating water entered the well water. These reductions in the vadose zone are most likely due to physiochemical and biological factors, as the following discussion describes.
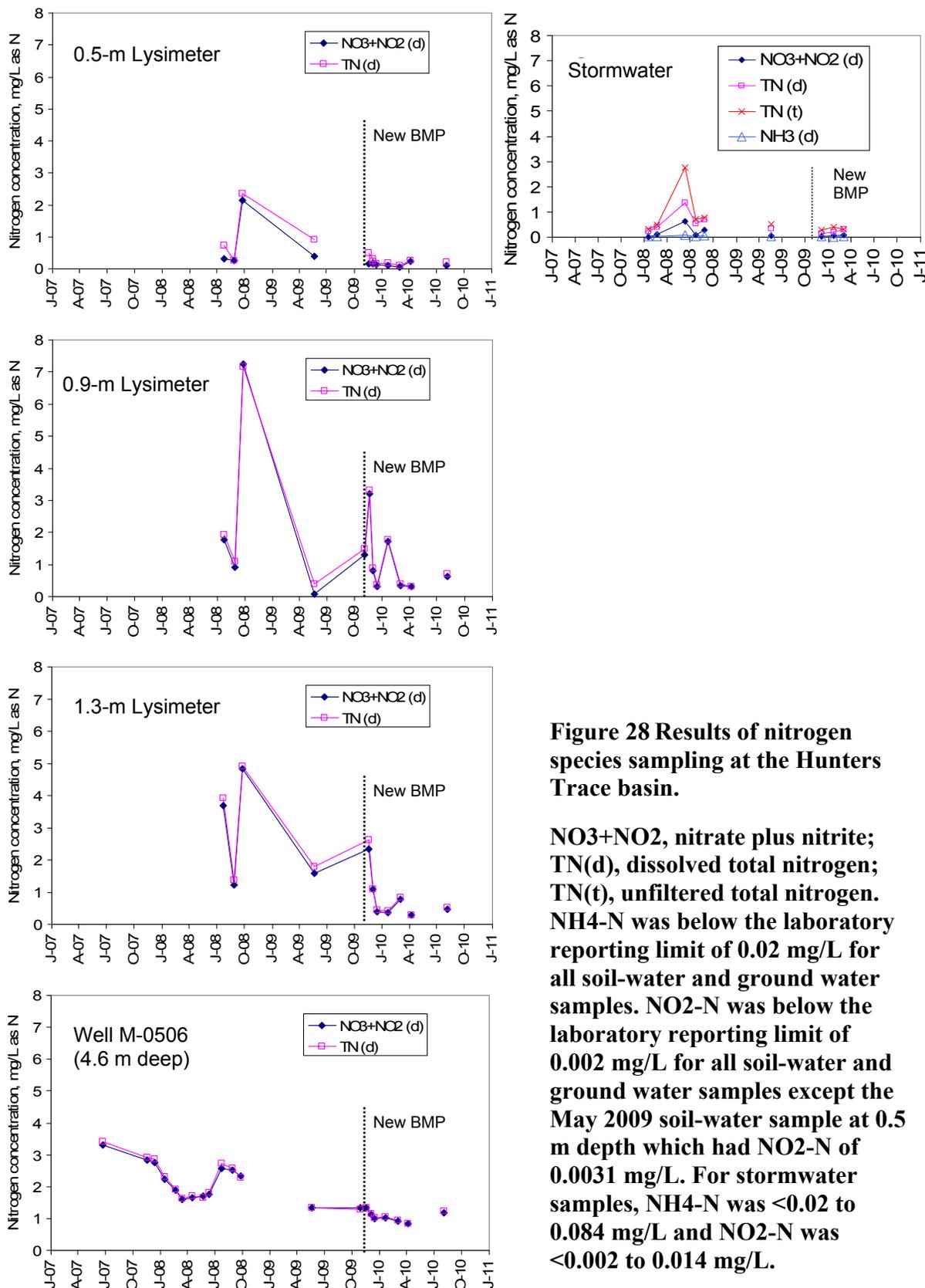
Figure 28 Results of nitrogen species sampling at the Hunters Trace basin.

NO3+NO2, nitrate plus nitrite; TN(d), dissolved total nitrogen; TN(t), unfiltered total nitrogen. NH4-N was below the laboratory reporting limit of 0.02 mg/L for all soil-water and ground water samples. NO2-N was below the laboratory reporting limit of 0.002 mg/L for all soil-water and ground water samples except the May 2009 soil-water sample at 0.5 m depth which had NO2-N of 0.0031 mg/L. For stormwater samples, NH4-N was <0.02 to 0.084 mg/L and NO2-N was <0.002 to 0.014 mg/L.

To provide additional insight into reaction based reductions in NO_3^-, such as denitrification, occurring after the new integrated design was implemented, several additional types of data were examined: soil gases, dissolved gases, stable isotopes, and denitrifier activity. Analysis of these data can provide independent evidence of NO_3^- reactions that cannot be derived by examination of nitrogen species concentrations alone, which often is confounded by mixing (with water of low or zero nitrate concentration) or variations in NO_3^- input into the subsurface.

The results of gas sampling during the first three sample events after construction of the new integrated design are shown in Figure 29. These results indicate the presence of N_2O above ambient atmospheric levels (~0.3 ppmv) suggesting denitrification is occurring. Also, the presence of CH_4 above ambient atmospheric levels (~1.7 ppmv) suggests methanogenesis is occurring (Figure 29). Since denitrification and methanogenesis both require low oxygen conditions yet the vadose zone generally is aerobic (Figure 29), these processes likely are occurring in anoxic microsites or occur cyclically during periods when the soil is wet or saturated and oxygen levels are low (Christensen et al., 1990a,b; Parkin, 1987; Koba et al., 1997). Additionally, DO concentrations in the shallow ground water have been decreasing since December 2009, reaching a minimum level of 2.7 mg/L in August 2010 (Figure 30).

Analysis of dissolved N_2 and Ar in shallow ground water (well M-0506) does not indicate the presence of excess N_2. This suggests that denitrification is not occurring in the shallow ground water or, if it were occurring, excess N_2 was lost by degassing into the vadose zone. Even though DO has been decreasing during much of the time after construction of the new integrated design (Figure 30), it still is above the maximum DO level of 2 mg/L sometimes reported for aquifers experiencing documented denitrification (McMahon and Chapelle, 2007). However, if

denitrification were occurring in the vadose zone, as suggested by soil gas results, excess N_2 probably would not be transported downward to the water table. Therefore, the absence of excess N_2 in ground water, even though it was an important piece of evidence for denitrification at the SO basin, does not preclude the possibility that denitrification is occurring elsewhere in the subsurface.
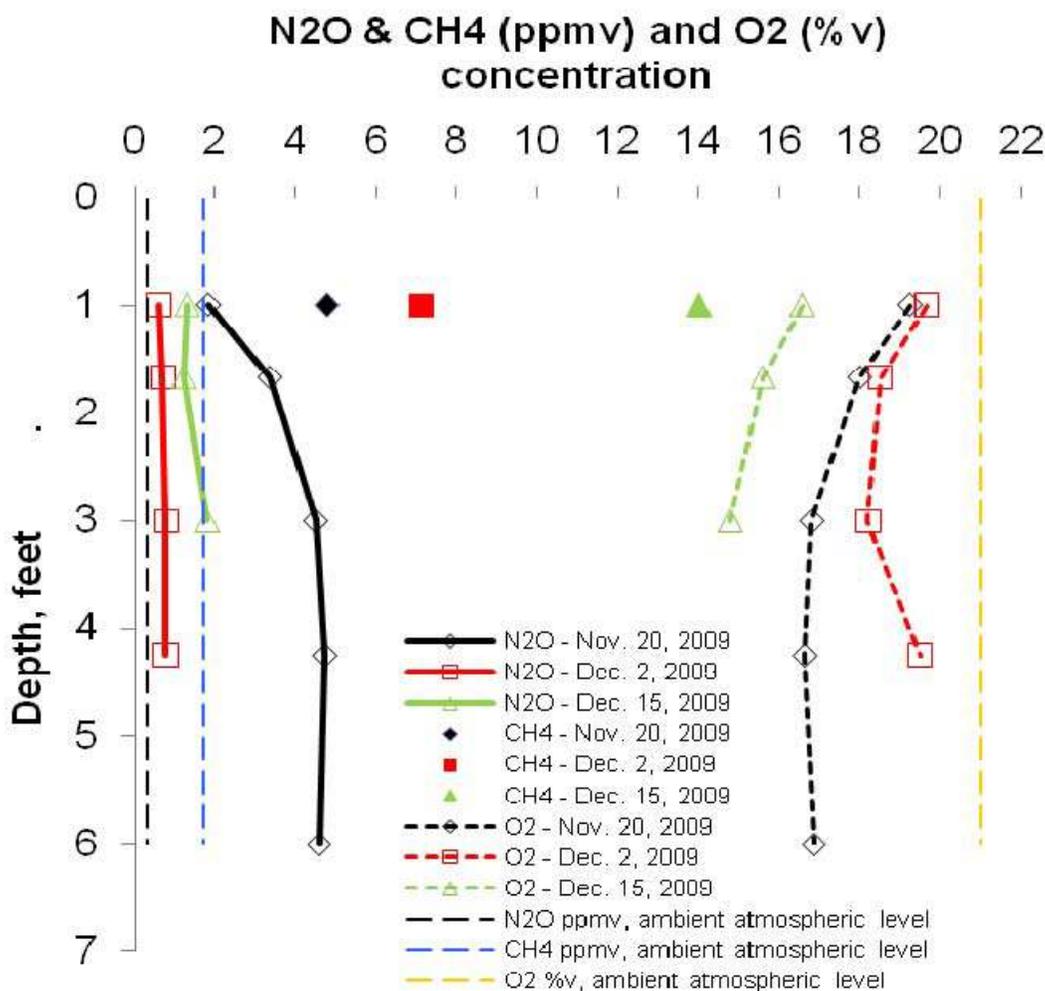
Figure 29 Soil gas sampling results at the Hunters Trace basin.
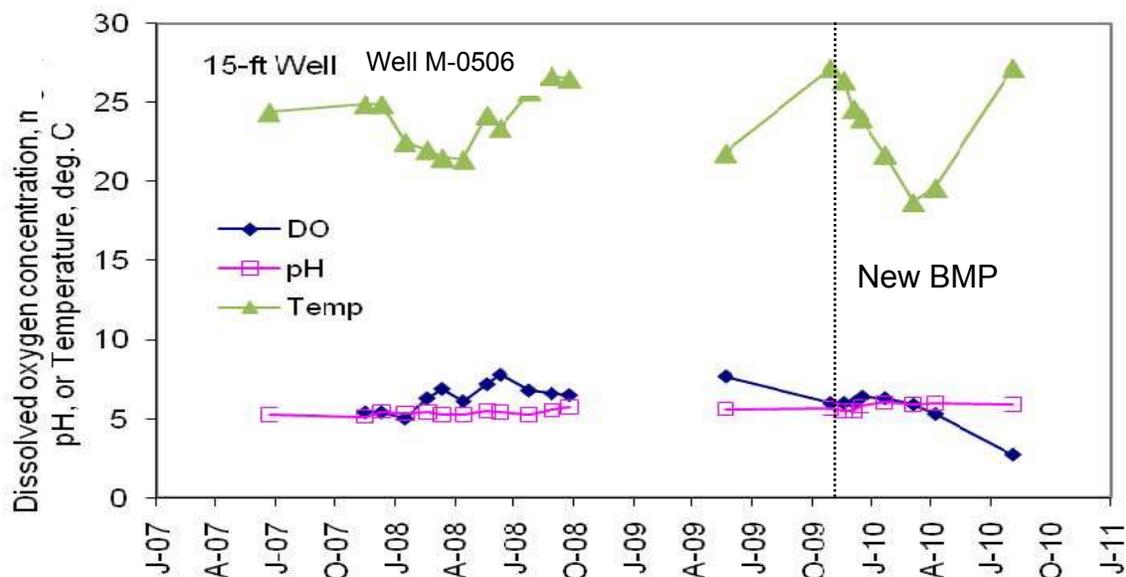
Figure 30 Dissolved oxygen, pH, and temperature of shallow ground water (well M-0506) at the Hunters Trace basin.

Isotope data collected after construction of the new integrated design provides evidence of denitrification when considered in combination with other data. The slight but consistent upward trends in the $\delta^{15}N[NO_3^-]$ and $\delta^{15}N[N_2]$ (Figure 31) are consistent with enrichment in the heavy ^{15}N isotope that would occur if denitrifiers were metabolizing the NO_3^- consisting of light ^{14}N. It is important to note that variations in the isotopic composition of the NO_3^- source will affect the isotopic composition of the residual NO_3^- and N_2. Therefore, deviations of $\delta^{15}N[N_2]$ on both the low side and the high side of air-saturated-water values could be a result of denitrification (Figure 32), depending on the progress of the reaction (it starts out producing light N_2, then evolves to higher values as the reaction proceeds). The single relatively high value of

$\delta^{15}N[N_2]$ in August 2010 may be the result of an isotopically heavy NO_3^- source, a denitrification reaction that proceeded to completion (NO_3^- source depleted), or some combination of these factors. The August 2010 sample is the sample most likely to indicate denitrification, and its $\delta^{15}N[N_2]$ is similar to values at the SO basin where multiple indicators confirmed denitrification was occurring (Figure 32).
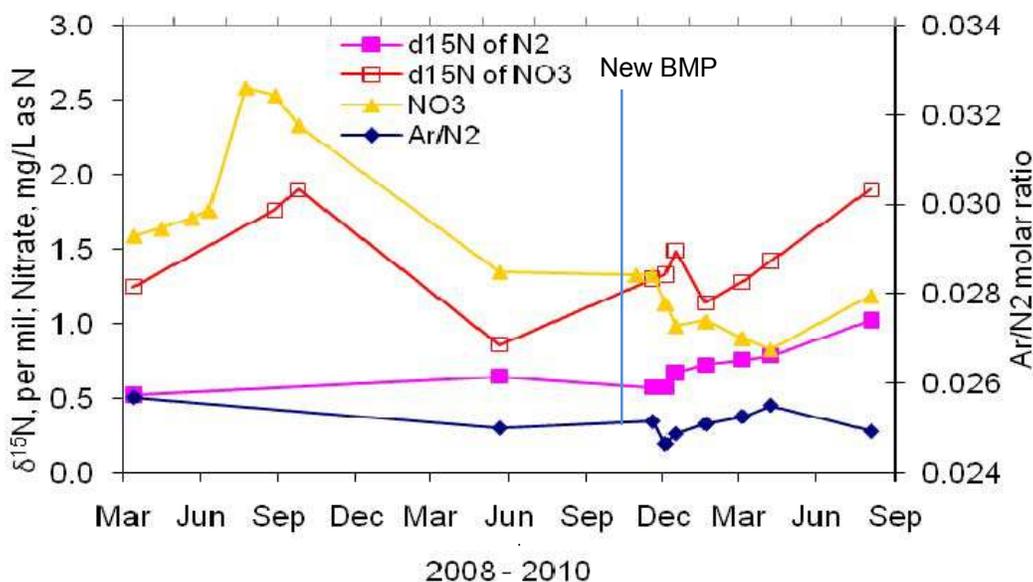
Figure 31 Nitrogen stable isotope results at the Hunters Trace basin for shallow ground water (well M-0506).
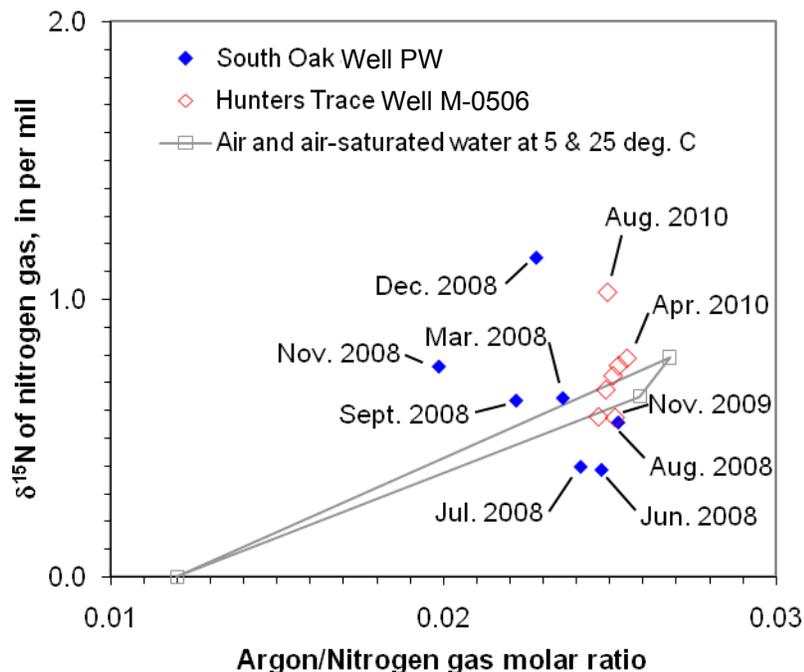
Figure 32 Comparison of isotope data for dissolved nitrogen gas at the South Oak basin and the new integrated design at the Hunters Trace basin.

δ^{13}C[DIC] results suggest oxidation of soil organic matter (Figure 33). DIC comprises aqueous CO_2 and alkalinity, which for the pH values at the HT site (Figure 30) is predominantly HCO_3^-. In March 2010, alkalinity began increasing steadily and δ^{13}C[DIC] began decreasing (Figure 33). This is consistent with microbial mediated oxidation of OC to DIC (CO_2 and HCO_3^-) because DIC of biogenic origin will be depleted in ^{13}C resulting in more negative values of δ^{13}C[DIC] (Li et al., 2005). This oxidation of OC may be coupled with NO_3^- reduction via denitrification.
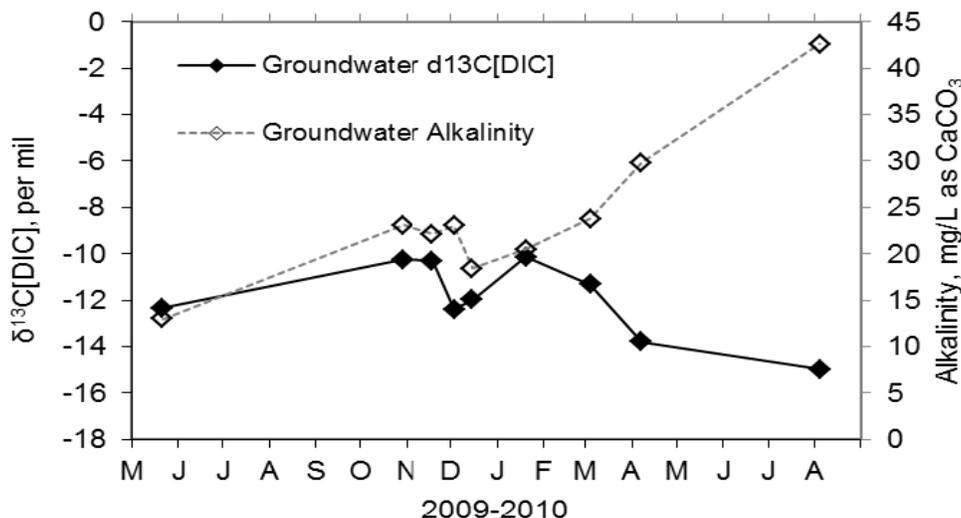
Figure 33 Carbon stable isotope results at the Hunters Trace basin.

Biological Data

Results of the real-time PCR analyses indicate the presence of denitrifying bacteria, which is inferred from nitrite reductase gene density. At the HT basin, two sets of soil samples for PCR analysis were collected prior to construction of the new integrated design and three sets were collected after construction. Denitrifier activity was somewhat lower after construction at similar soil depths (Figure 34), but this may be expected due to the disruption of construction and the time required for microbial acclimation and growth as well as possible natural spatial and temporal variations. Due to the completely different soil environments before and after construction and the limited number of samples, it is more appropriate to note the change in denitrifier activity only in the new integrated design (Figure 34). In the new integrated design, denitrifiers are concentrated in the amendment layer, indicating the media is conducive to their growth. Furthermore, the denitrifier density has increased, starting at 3.6×10^4 gene copies/g in

the media mixed onsite before placement in the ground to 1.5×10^5 gene copies/g in August 2010, suggesting denitrifiers are acclimating to the new environment. This increase in denitrifier activity occurred during the period when $\delta^{15}N[NO_3^-]$ and $\delta^{15}N[N_2]$ were increasing (Figure 31) and dissolved oxygen concentrations were decreasing (Figure 30); all three of these trends are qualitatively consistent with denitrification.
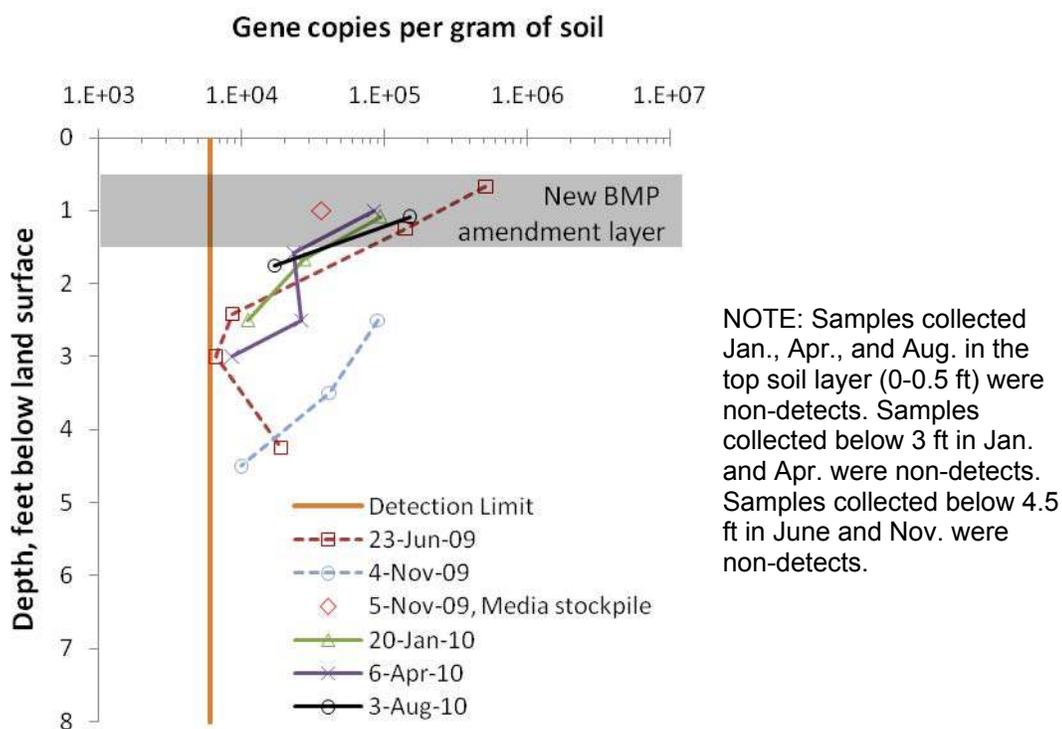
Figure 34 Denitrifier activity inferred from nitrite reductase gene density measured by real-time PCR at the Hunters Trace basin.

Nitrate Transport and Fate

The transport and fate of NO_3^- in the subsurface is governed by a combination of conservative mixing and physical, chemical, and biological reactions. Understanding these varied mechanisms is important to understanding the effectiveness of the new BMP at the

Hunters Trace basin. Examination of conservative species, such as chloride (Cl) and bromide (Br), help differentiate reaction based physiochemical and biological processes from conservative mixing.

Monitoring at Hunters Trace 2007–2010 has shown a long-term downward trend in NO_3^- concentration in the shallow ground water (well M-0506). Nitrogen is nearly exclusively in the NO_3^- form, and moderate seasonal variation is evident in the background trend (Figure 35). During this same time period, an exponential decline in Cl concentration is apparent (Figure 35). Similar downward trends in Br concentration existed before and after new BMP construction; however, a substantial increase in Br occurred November 2009 through January 2010 following construction of the new integrated design, suggesting a possible source of Br in the amended soil layer to which the ground water chemistry was equilibrating. The increase in Cl relative to Br in August 2010 is likely due to infiltration of fertilizer impacted stormwater because Cl is a common anion in fertilizer, whereas Br is not. The similar slopes of the Cl and Br trends are strongly suggestive of conservative mixing.
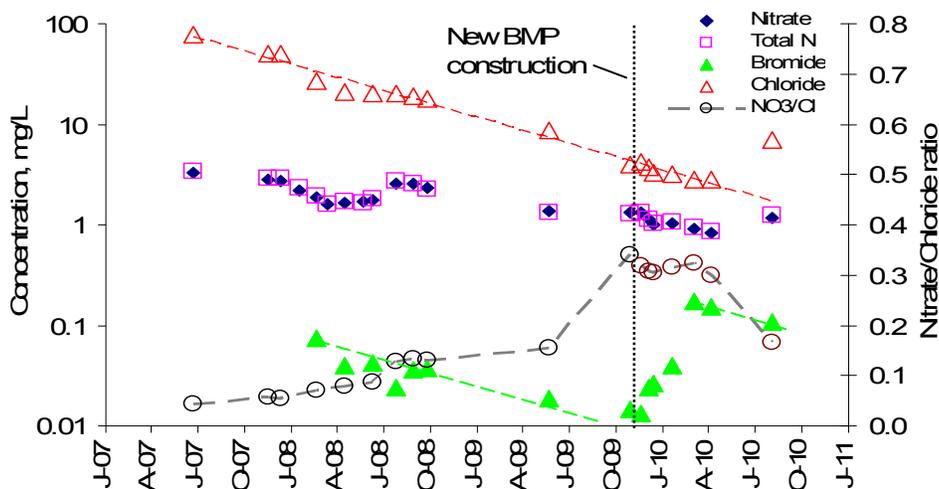
Figure 35 Comparison of chloride, bromide, nitrate, and total nitrogen concentrations at the Hunters Trace well M-0506. Dashed lines for chloride and bromide approximate conservative mixing-based trends.

NO_3^- concentrations can be affected by mixing (with water of different nitrate concentration) and a variety of chemical reactions that generally are biologically mediated (nitrification, denitrification, dissimilatory reduction to ammonium, microbial assimilation, or plant uptake). In contrast, Cl and Br generally are considered to be transported conservatively in the subsurface, that is, moving at the same rate as infiltrating water or ground water. Therefore, examination of these data in combination can give insight into NO_3^- variations due to processes other than conservative mixing, that is, the net effects of reaction-based processes and source inputs. NO_3^-/Cl ratios were analyzed because Cl is expected to be present and to act as a conservative tracer in fertilizer impacted stormwater runoff; whereas, Br was not present in stormwater runoff in measureable concentrations (laboratory reporting limit for Br is 0.02 mg/L). A change in slope of the NO_3^-/Cl ratio indicates a change in the relation between the two values due to NO_3^- reaction or changes in source inputs:

- A positive NO_3^-/Cl ratio slope indicates NO_3^- is decreasing slower or increasing faster than Cl due to nitrification, NO_3^- input increased relative to Cl, or Cl input decreased relative to NO_3^-;

- A negative NO_3^-/Cl ratio slope indicates NO_3^- is increasing slower or decreasing faster than Cl, possibly due to reaction (for example, denitrification), NO_3^- input decreased relative to Cl, or Cl input increased relative to NO_3^-; and

- A zero NO_3^-/Cl slope indicates NO_3^- and Cl are changing at the same rate due to conservative mixing, and the reaction kinetics for NO_3^- remain relative the same over time.

Inflection points in the NO_3^-/Cl ratio occurred near the time when the new BMP was constructed and again in March 2010 (Figure 35). These inflection points indicate times when fundamental changes (from positive to zero slope and from zero to negative slope) occurred in NO_3^- concentrations relative to Cl, suggesting changes in NO_3^- reactions, NO_3^- and Cl inputs, or some combination of these factors. The consistent exponential decline in Cl both before and after construction of the new integrated design suggests that changes in NO_3^- reactions or NO_3^- input, rather than Cl input changes, are the primary reasons for these changes in NO_3^-/Cl ratio slopes.

In order to quantify the difference in NO_3^- concentration associated with the NO_3^-/Cl ratio slope changes, a "reconstructed" NO_3^- time series was computed based on the fractional change in Cl concentration. This reconstructed concentration represents the NO_3^- concentration that would have occurred if only conservative mixing and NO_3^-/Cl mass input variations were affecting concentrations. This is based on two assumptions: (1) transport of Cl is conservative; and (2) there is no subsurface source of Cl. The first assumption implies that a fractional change in NO_3^- will equal the fractional change in Cl, which is expected to be a valid assumption given the low anion exchange capacity of the HT soils (Appendix B). The second assumption is also expected to be valid given the mineralogy of subsurface sediments and the lack of dissolved Cl sources. Even though residences in Hunters Trace are served by septic tanks, a possible source of dissolved Cl, the water table gradients beneath the basin were nearly always outward, ranging from -0.00059 to 0.047 m/m (negative values inward, positive values outward). The infiltration of fertilizer impacted stormwater runoff probably is the predominant input of Cl mass into the subsurface due to the low concentration of Cl in precipitation (0.2 and 0.6 mg/L for samples collected May and December 2009, respectively).

For each sample event, a reconstructed NO_3^- concentration was computed as follows:

$$NO_{3,R}{}^i = (NO_{3,M}{}^{i-1})\Delta Cl + NO_{3,M}{}^{i-1} \tag{1}$$

$$\Delta Cl = (Cl^i - Cl^{i-1})/Cl^{i-1} \tag{2}$$

where,

$NO_{3,R}{}^i$ is reconstructed nitrate concentration for current sampling event;

$NO_{3,M}{}^{i-1}$ is measured nitrate concentration for preceding sampling event;

ΔCl is fractional change in chloride concentration;

Cl^i is chloride concentration for current sampling event; and

Cl^{i-1} is chloride concentration for preceding sampling event.

This yields an incrementally reconstructed NO_3^- time series showing what NO_3^- concentrations would have been due to conservative mixing or NO_3^-/Cl mass input variations for only the time period between current and preceding sampling events. The percent difference in NO_3^- concentration between measured and reconstructed values ($\%\Delta NO_{3,M-R}$) is computed as follows:

$$\%\Delta NO_{3,M-R} = 100(NO_{3,M} - NO_{3,R})/NO_{3,M} \tag{3}$$

$\%\Delta NO_{3,M-R}$ represents a percentage measure of the net effects of NO_3^- reaction and changes in NO_3^-/Cl inputs. If additionally it is assumed that Cl input is relatively consistent, then $\%\Delta NO_{3,M-R}$ represents the net effects of NO_3^- reaction and NO_3^- input variations only. This assumption is supported by the consistent exponential decline in Cl experienced throughout the study period, with the exception of the relatively large increase that occurred August 2010 (Figure 35). Therefore, positive values of $\%\Delta NO_{3,M-R}$ represent a reaction gain or input increase in NO_3^- and negative values of $\%\Delta NO_{3,M-R}$ represent a reaction loss or input decrease in NO_3^-. Values of $\%\Delta NO_{3,M-R}$ near zero indicate NO_3^- was being transported conservatively, thus any

observed changes in NO_3^- may be attributed to mixing with water of different nitrate concentration..

Prior to construction of the new integrated design at Hunters Trace, NO_3^- transport was dominated by nitrification or NO_3^- input increases with isolated periods of conservative movement possibly influenced by ephemeral reaction losses as indicated by $\%\Delta NO_{3,M-R}$ values ranging from −3 to 120% (Figure 36). In contrast, from November 2009 to April 2010 after construction of the new integrated design, NO_3^- was controlled by intermittent periods of slight reaction losses and nitrification as indicated by $\%\Delta NO_{3,M-R}$ values ranging from −8 to 4% (Figure 36). However, the August 2010 sample indicated an increase in NO_3^- considerably less than that expected based on the Cl increase, yielding a $\%\Delta NO_{3,M-R}$ value of −45% (Figure 36). This indicates that in the absence of any NO_3^- reaction or input decrease, the NO_3^- concentration would have been 2.12 mg/L rather than 1.18 mg/L, suggesting nearly half (0.94 mg/L) was lost. An increase in NO_3^- input is expected in late spring to early summer, as suggested by samples collected in 2007–2009, which would coincide with the start of the summer growing season, thus the large $\%\Delta NO_{3,M-R}$ decrease is probably reaction based, possibly due to denitrification.
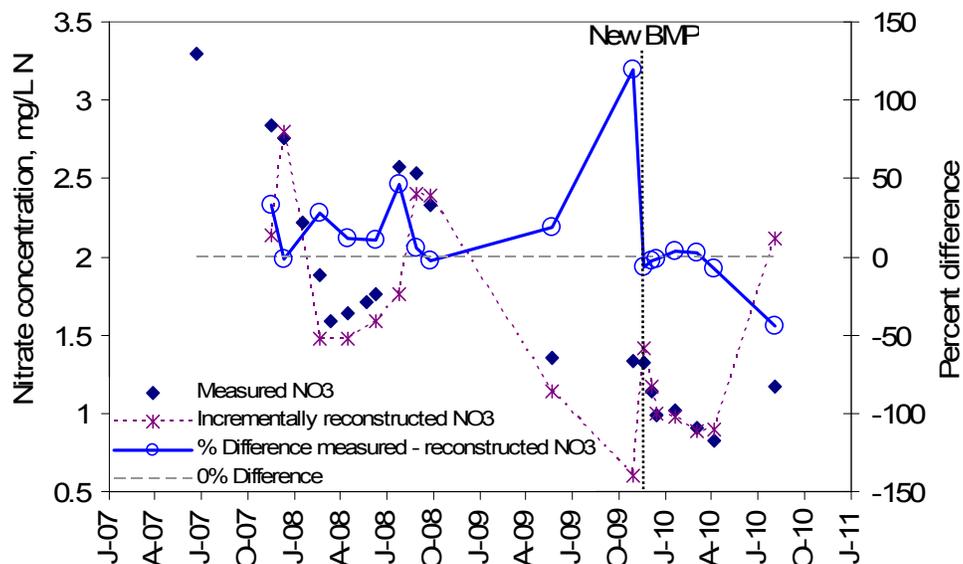
Figure 36 Measured and incrementally reconstructed NO_3^- concentrations and the incremental percentage differences assumed to be attributable to NO_3^- reactions or NO_3^- input variations at the Hunters Trace well M-0506. Positive percentages indicate NO_3^- gains and negative percentages indicate NO_3^- losses.

The effects of conservative transport can be accumulated by replacing the second term $(NO_{3,M}{}^{i-1})$ in equation (1) with the reconstructed NO_3^- concentration for the preceding sampling event $(NO_{3,R}{}^{i-1})$:

$$NO_{3,R}{}^{i} = (NO_{3,M}{}^{i-1})\Delta Cl + NO_{3,R}{}^{i-1} \tag{4}$$

This yields a completely reconstructed NO_3^- time series showing what NO_3^- concentrations would have been if only conservative mixing had occurred during the study period (Figure 37). In contrast, the incrementally reconstructed NO_3^- time series in Figure 36 reflects the *incremental* difference between sampling events due to conservative mixing or NO_3^- input variations. Two reconstructed NO_3^- time series are shown in Figure 37 by applying equation (4) relative to the first sample of the study period (June 22, 2007) and relative to the sample collected the week prior to construction of the new integrated design (October 29, 2009). The first time series indicates what NO_3^- concentrations would have been if only conservative

mixing had occurred during the *entire* study period; whereas the second time series indicates what NO_3^- concentrations would have been if only conservative mixing had occurred *after* construction of the new integrated design. Note that both of the completely reconstructed conservative mixing-based NO_3^- time series mimic that of Cl. The reconstructed NO_3^- time series for the entire study period is substantially lower than the measured NO_3^- (Figure 37). This large difference is primarily due to the cumulative effects of positive percentage differences indicated in Figure 36, presumably due to nitrification or NO_3^- input increases prior to construction of the new integrated design. In contrast, the reconstructed NO_3^- time series for the new integrated design is approximately equal to measured NO_3^- except for the August 4, 2010 sample (Figure 37). This similarity is due to the cumulative effects of small positive and negative percentage differences indicated in Figure 36, suggesting conservative mixing effects were predominant from November 2009 to April 2010 for the new integrated design; whereas, in August 2010, denitrification may have caused the measured NO_3^- to be substantially lower than the reconstructed NO_3^-. Another important difference before and after construction of the new integrated design is the prevalence of pre-construction increases in NO_3^- percentage differences and the absence of post-construction increases (Figure 36). This is suggestive of reduced nitrification after construction of the new integrated design and was concurrent with increased soil moisture (Figure 24) and less aerobic conditions (Figure 30), both of which are conditions less favorable for nitrification.
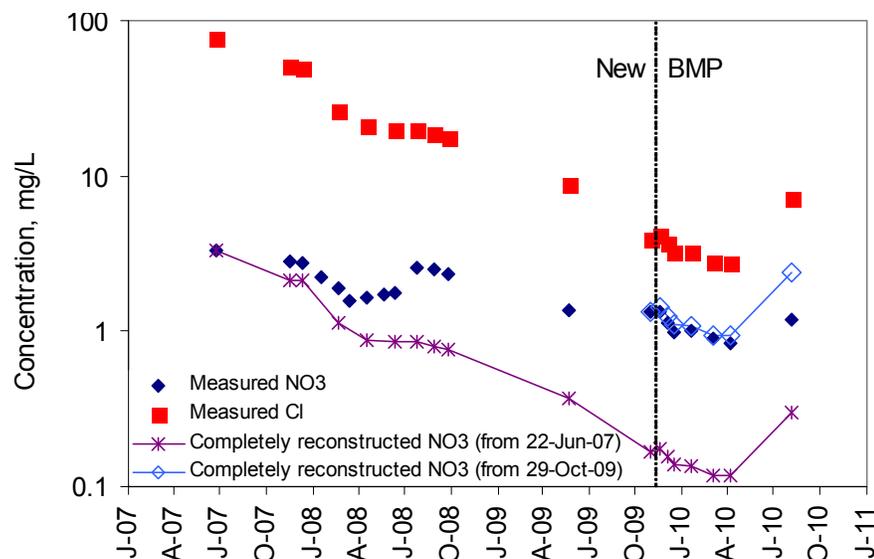
Figure 37 Measured NO3⁻ and Cl concentrations and completely reconstructed NO₃⁻ concentrations at the Hunters Trace well M-0506.

Decreases in NO_3^- in shallow ground water beneath the Pollution Control Basin as inferred by comparison with Cl (Figure 36) could be caused by denitrification, dissimilatory nitrate reduction to ammonium (DNRA), microbial assimilation, plant uptake, or some combination of these processes. Microbial assimilation generally is not a major sink for NO_3^- and plant uptake probably was not substantially different before or after construction of the new integrated design. Soil gas, NO_3^- and N_2 isotopes, and denitrifier activity by real-time PCR provide results consistent with denitrification. Possible DNRA is suggested by a KCl extractable NH_4^+ of 5.9 mg/kg in the amended soil layer in August 2010, which is approximately four times greater than amended soil layer samples collected in January and March 2010. Under such dynamic conditions of rapid infiltration beneath a retention basin, net water quality effects in the shallow ground water would be related to the intensity and duration of denitrification and mixing ratios with non-denitrified water. The water chemistry, soil and dissolved gas, and isotopic analyses at the HT site suggest that NO_3^- losses are attributable to denitrification, which likely is

intermittent, and possibly to DNRA. These data also indicate that the physicochemical and biological processes leading to NO_3^- losses were occurring primarily in the vadose zone. Intermittent denitrification likely is supported by the increased soil moisture conditions of the Pollution Control Basin and resultant reductions in surface/subsurface oxygen exchange. The amended soil (BAM) layer likely contributed to these conditions favorable for denitrification.

Phosphorus Data

Total dissolved phosphorus (TDP and TP(d) in Figures 38, 39 and 43) at the HT basin was nearly exclusively in the orthophosphate (PO_4^{3-}) form (Figure 38). In soil water, TDP showed a generally downward trend throughout the entire study period, although notable decreases occur shortly after construction of the new integrated design (see lysimeters in Figure 38). Comparison of concentrations data for TDP in soil water collected indicate 70–90% reductions in median TDP from pre-construction (June 2007–October 2009) to post-construction (November 2009–August 2010), see Figure 39. TDP decreases may be due to conservative mixing, sorption, precipitation, microbial assimilation, or some combination of these processes. The lowest TDP occurred in the 1.5-ft deep lysimeter, which spans the lower portion of the amended soil (BAM) layer and the entire coarse sand layer. This reduction of TDP (and PO_4^{3-} since TDP is predominantly in this form) is consistent with sorption likely due to the tire crumb and clay content of the amended soil layer, although also may be partly due to lower P concentrations in the stormwater during this period (Figure 38).

Hossain et al. (2009) report removal efficiencies exceeding 75% for both TDP and PO_4^{3-} for a sorption media comprising 50% sand, 20% limestone, 15% sawdust, and 15% tire crumb. It is further noted that this removal and the associated kinetics were with no clay particles, leading

to the idea that the other constituents of the mix were important for dissolved phosphorus removal. However the mix Hossain used had low soil moisture residuals. Large changes in TDP are not evident in shallow (well M-0506) or deep (well M-0505) ground water beneath the Hunters Trace basin before and after construction of the new integrated design (Figure 39). However, TDP was consistently very low in well M-0506 (Figure 38) during the entire study period, suggesting much of the TDP may be removed naturally by the native sediments that increase significantly in clay content (from <5% to >40% clay-size particles) at a depth of approximately 5 ft. PO_4^{3-}/Cl^- ratios were examined to elucidate PO_4^{3-} variations attributable to the net effects of reaction-based processes and source inputs using the same methodology as applied for NO_3^- in the previous section. PO_4^{3-}/Cl^- ratios for shallow groundwater (well M-0506) show similar trends to NO_3^-/Cl^- ratios (Figure 35). Reconstructed concentrations generally indicate increasing PO_4^{3-} prior to construction of the new integrated design and conservative transport or PO_4^{3-} losses afterwards. The high TDP concentrations in well M-0505 (Figure 39) are most likely due to the prevalence of phosphate minerals confirmed by x-ray diffraction analyses of the sediments at this depth.
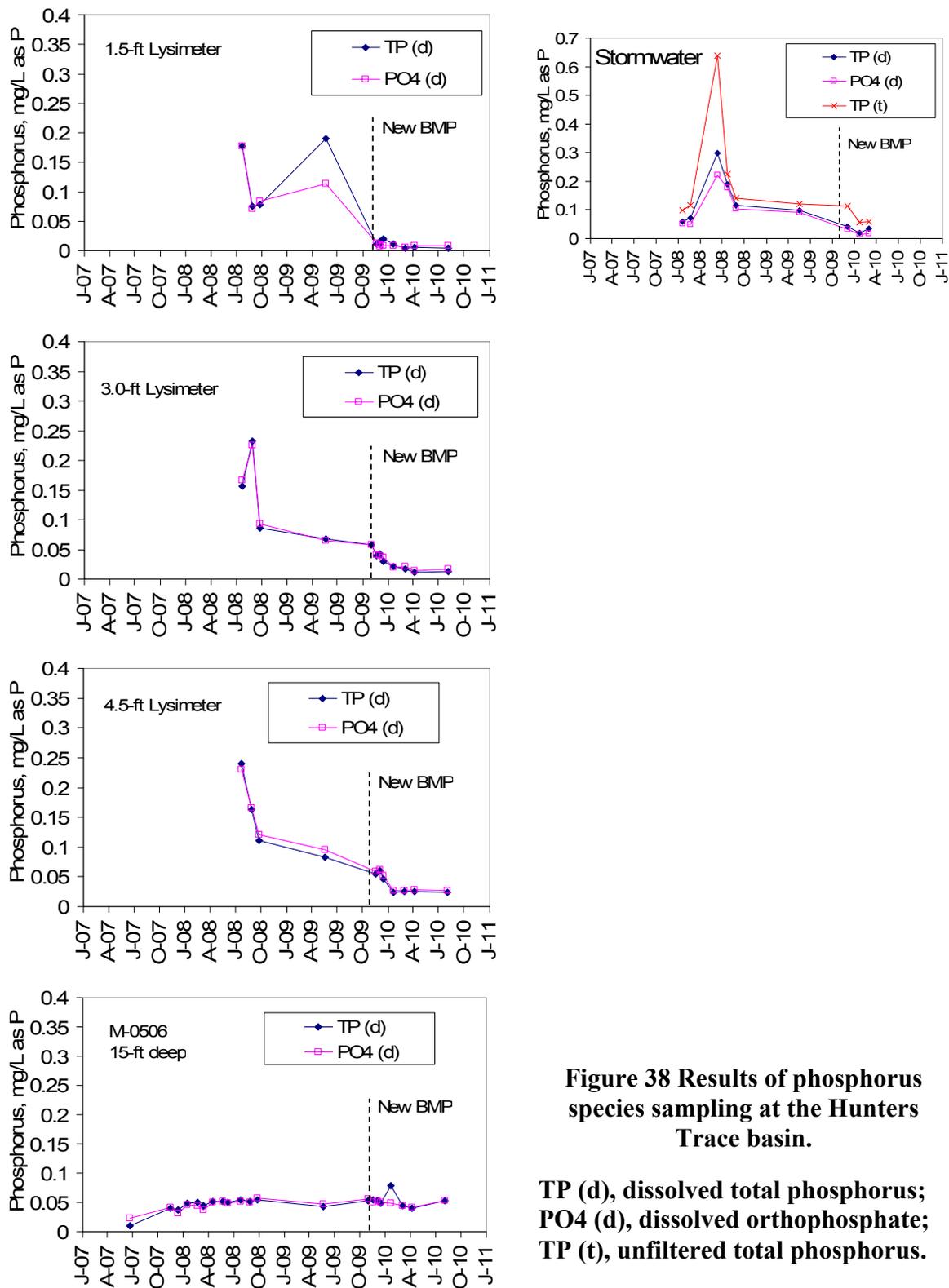
Figure 38 Results of phosphorus species sampling at the Hunters Trace basin.

TP (d), dissolved total phosphorus; PO4 (d), dissolved orthophosphate; TP (t), unfiltered total phosphorus.
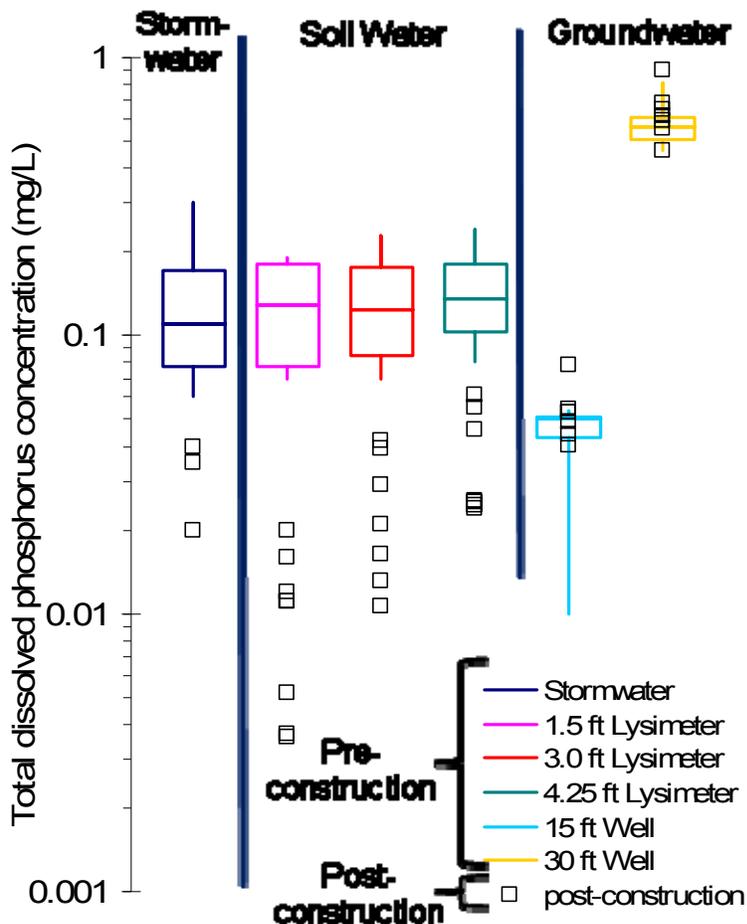
Figure 39 Total dissolved phosphorus concentrations at the Hunters Trace basin before and after construction of the new integrated design.

Verification of Hydrologic and Water Quality Performance

The rainfall in the Marion County area was low than usual during the early part of 2011. To verify if the new integrated design can continue to infiltrate and remove nitrogen during the low rainfall, additional data were collected for pond depth, rainfall, infiltration rates, and water quality to gain a confidence in the pond performance with time. This time period for data collection was from January through October 2011.
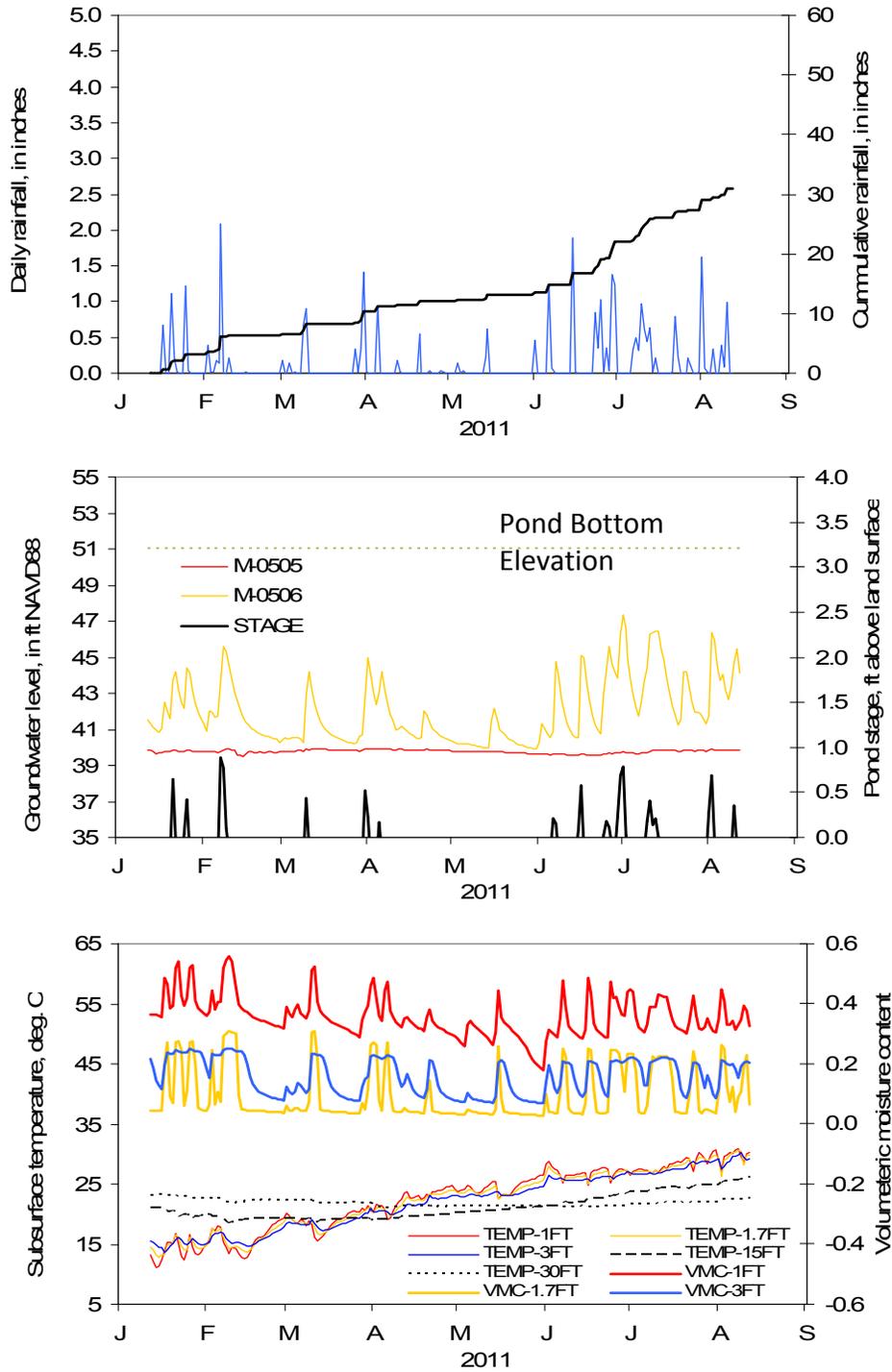
Figure 40 Hydrologic monitoring for the new integrated design at the Hunters Trace basin in the verification 2011 time period.

Hydrologic monitoring data in Figure 40 indicates one-fourth decrease of cumulative rainfall in the Pollution Control Basin compared to the same period in 2010 (Figure 24). The Maximum daily rainfall was 2.1 inches in 2011 while that was 5.0 inches in 2010. The HT pollution control area of the basin was fully saturated 13 times for more than one day from January through August. There was an overflow of the berm in early October for which infiltration data were recorded. Soil moisture is measured by the volumetric moisture content as shown in Figure 40. Moreover, the similar and high range of soil moisture at the top of the pollution control layer (VMC-1FT in Figure 40) confirms that moisture is still available for bacterial action between runoff events.

Actual operating infiltration rates after the soil amendment and during the verification period calculated from basin water recession depth data of Figure 40 are listed in Table 3, with the additional October event.

Table 3 Operating infiltration rates computed from pond stage recession curves

Date	Rainfall (in)	Duration (hr)	Infiltration (in/hr)
21-Jan-11	1.31	6.1	0.35
25-Jan-11	1.22	4.6	0.36
7-Feb-11	2.21	20.4	0.34
31-Mar-11	1.42	6.8	0.40
6-Jun-11	1.22	1.7	0.44
9-Oct-11	6.30	~10	0.34

The average actual operating infiltration rate in 2011 is 0.37 in/hr (Table 3) and the average rate during 2009-2010 after the amendment is 0.34 in/hr (Table 2). Thus, the infiltration

rates during "wet" years 2009-2010, and the infiltration rate during 2011 (verification period) was approximately the same at an average of about 0.35 in/hr.

To measure the infiltration rate for the different media layers in the pollution control basin, four 1-foot diameter embedded ring infiltrometer kits (ERIK) are installed near monitoring well M-0506 at different depths: 7 inches, 17 inches, 19 inches and 27 inches which corresponded to the top of amendment soil, top of coarse sand, middle of coarse sand and parent soil, respectively. In addition, the double-ring is used for the infiltration rate measurement at the surface. Figure 41 (a) shows that the limiting infiltration rate gradually increased with depth up to the top of the coarse sand and then decreased to 0.76 in/hr at the parent soil layer. This compares to the limiting infiltration rate average of 0.38 in/hr as measured from the actual recession curves of pond depth data. Thus the rate from the embedded ring infiltrometer at the parent soil level is twice the actual amount. The double ring infiltrometer produced similar results in the parent soil at the surface compared to the embedded ring at 27 inch depth. The higher rate with the infiltrometer is most likely because there is greater ability for counter current gas flow in the infiltrometer to release soil gas pressure, whereas when the overall pond is flooded soil gas can become trapped and impede infiltration. Also note that the double ring infiltrometer has to be embedded into the parent soil so there is no leakages (> 2 inches in this application).
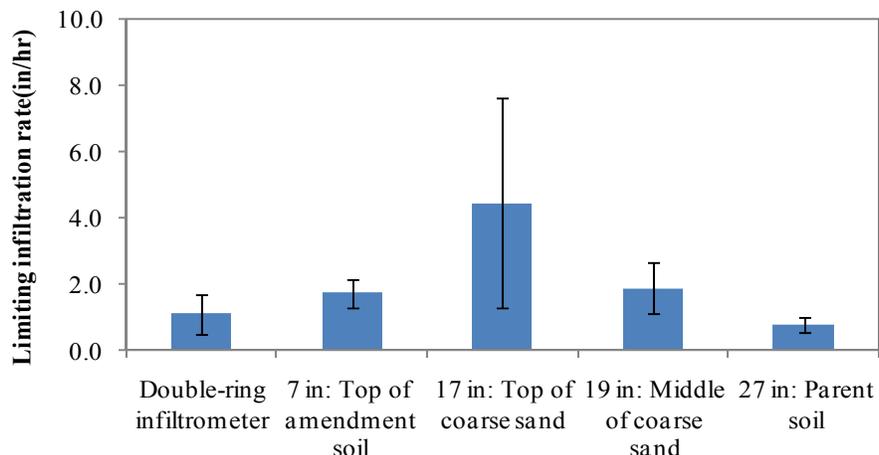
Figure 41a Average limiting infiltration rates at different depths in 2011.

From Figure 41 (b), it is apparent that the limiting infiltration rate of coarse sand layer ascended in the dry season of 2011 and decreased in the wet season while little influence of weather on the limiting infiltration rate was observed in other layers. Thus the results of infiltration rate tests during the verification period are highly consistent with the original data on infiltration rates during 2009-2010. In addition, before using a soil amendment, the infiltration rates must be reported and documented to insure proper drain times for the a retention basin
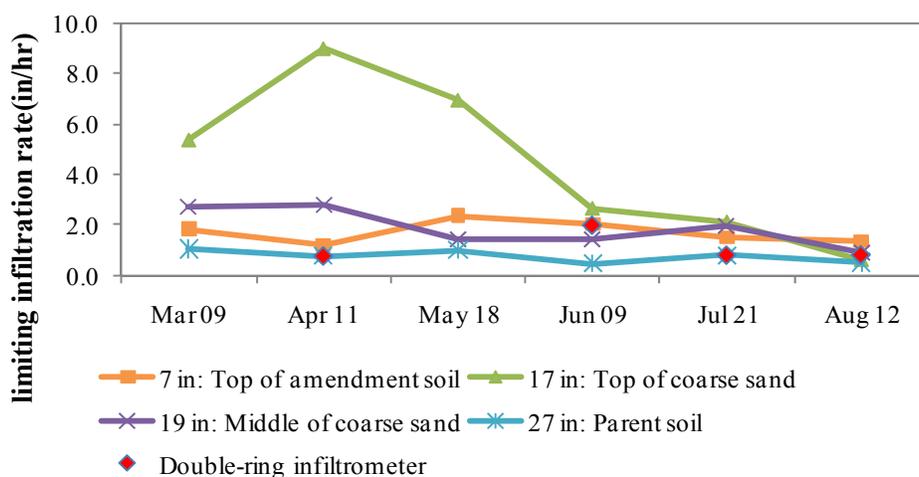
Figure 41b Time-series limiting infiltration rates at different depths in 2011.

Similar to the previous post amendment analysis, chloride concentration in shallow groundwater beneath the basin is low and NO_3^-/Cl ratio is relatively stable. Nitrogen species are primarily dissolved N, in which NO_3^- form contributes greater than 82% on average, and generally presented a downward trend throughout the validation period during 2011 (Figure 42a). The average TN concentration during the verification period (1.05 mg/L) remained almost the same as that (1.08 mg/L) before the verification period and after BMP construction (Nov 2009 – Aug 2010), which was about half of the TN concentration (2.17 mg/L) during pre-construction period. Thus, the system continues to maintain a decrease in nitrogen. Additionally, after BMP construction, chloride concentration in shallow groundwater beneath the basin stays low and has a moderate seasonal variation trend (Figure 42b). Evident positive slopes in NO_3^-/Cl occurred prior to November 2009 (Figure 35), when the new integrated design was implemented, suggesting a more thorough nitrification in the native soil layers. After that, NO_3^-/Cl ratio kept relatively stable for months, meanwhile, denitrifying bacteria gradually acclimated to the new environment and exponentially increased in the amended soil (BAM) layer concurrent with the drop in DO level until NO_3^- losses became dominant and then caused a negative slope of NO_3^-/Cl ratio (Figures 35 and 42b). Up to August 2011, NOx/Cl ratio decreased from an average of 0.31 (Nov 2009 – Apr. 2010) to average of 0.21 (Aug. 2010– Aug. 2011) which also indicates that a new equilibrium in ground water has been formed and the relative contribution of NOx to Cl has stabilized. It is important to note the NOx/Cl ratio in ground water (sampled from well M-0506 with a screened depth of 10.2 to 15.2 ft, Table 1) reflects the effects of stormwater percolation through the overlying BAM layer (depth of 0.5 to 1.0 ft, Figure 16), thus a stable NOx/Cl ratio during the verification period suggests nitrate losses in the BAM layer were similar in 2011 to those occurring in August 2010. Additionally, the *absence* of substantial increases in

NOx/Cl ratio after the new BMP was implemented (Figure 42b), compared to increases prior to the new BMP (Figure 35), suggests positive nitrate mitigation behavior (removal of nitrate) for the new integrated design. Additional evidence as to removal of nitrates in wet conditions is the sample collection in the pollution control basin in June 2011 when there was about 0.5 foot deep water and at the end of rain event. The data (see Figure 42b) reflect a decrease in nitrates and a decrease in the NOx/Cl ratio. Thus, assuming Cl is not decreasing, NOx must be decreasing, and leading to a conclusion that wet BAM conditions most likely increase nitrate removal
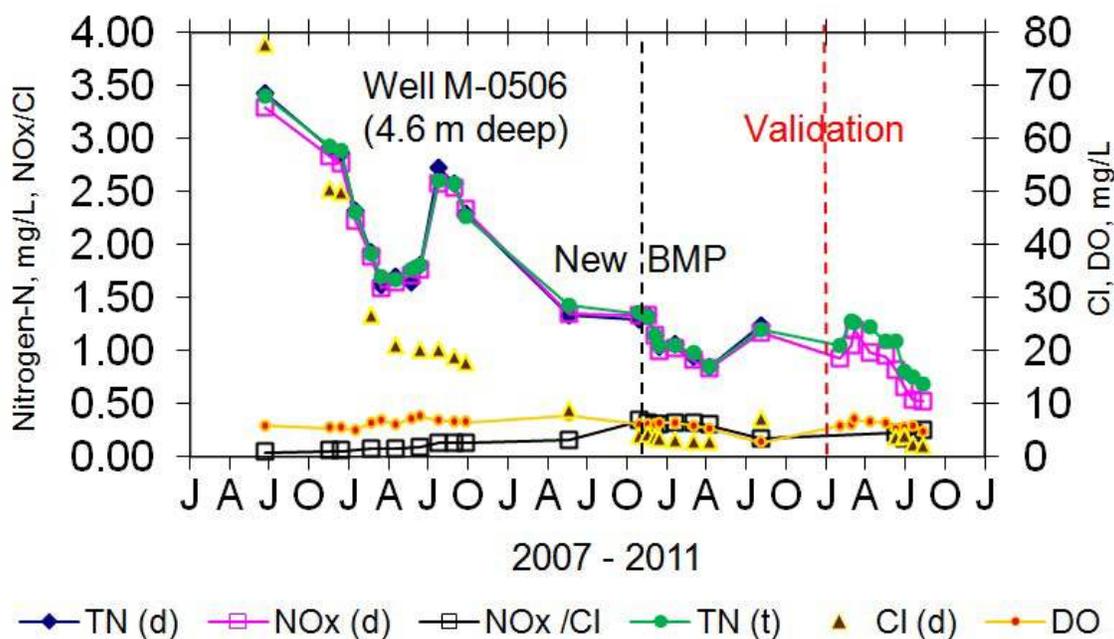
Figure 42a Nitrogen species, chloride, and dissolved oxygen concentrations in groundwater during whole experimental period
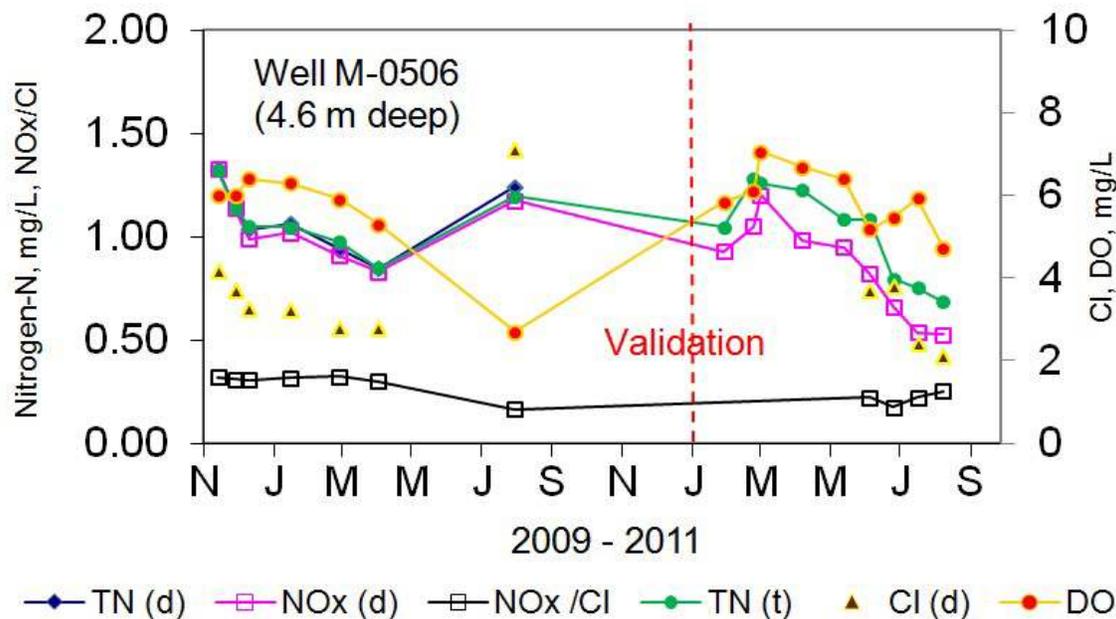
Figure 43b Nitrogen species, chloride, and dissolved oxygen concentrations in groundwater after BMP construction

During the verification period, orthophosphate (PO_4^{3-}) was generally below 0.08 mg/L in groundwater as was the same as before the amendment. Total phosphorus was measured also during the verification period and the particulate and colloidal P (greater than 0.45 μm), were at times a significant constituent of the total P in shallow groundwater. Such pattern is normally observed in stormwater especially during drought conditions when watershed phosphorus loadings do increase before a runoff event. This runoff water is then primarily the water which is sampled in the wells. In Figure 43 shown are phosphorus species with pH and Chloride in the validation period relative to the other sampling periods.
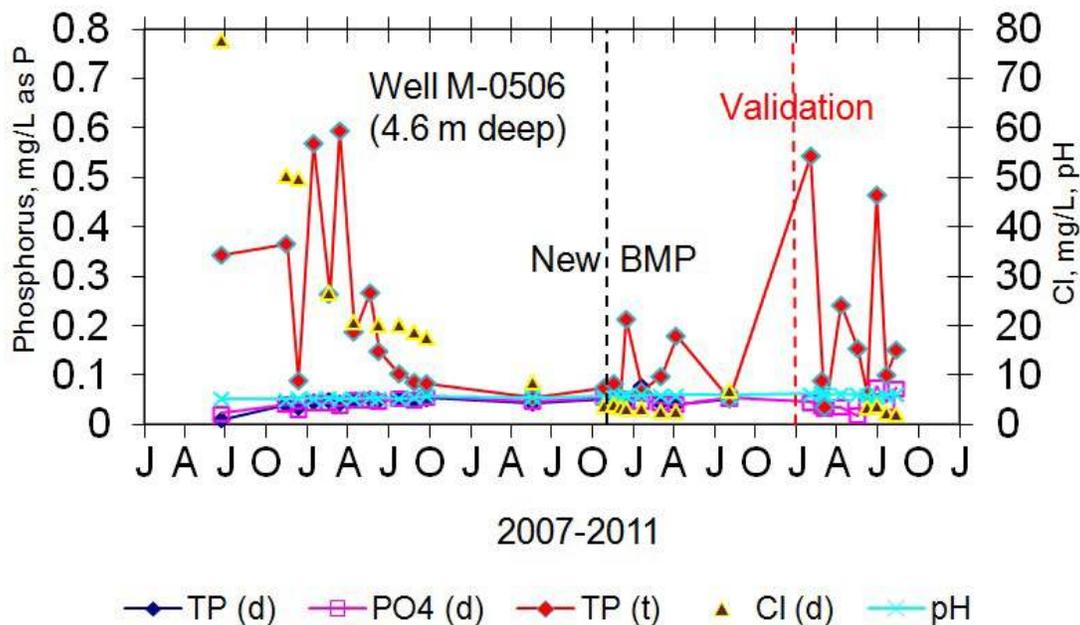
Figure 44 Phosphorus species and chloride concentrations and pH in groundwater

The number of denitrifier gene copies per gram of soil, during the verification phase, continues to be present at approximately the same density as previously measured, although increases over time are noted in the BAM layer (Figure 44). The data on Aug 12th 2011 show a typical zigzag pattern along the soil profile. That is, no denitrifying bacteria is found in the basin top soil layer before and after BMP construction and a decrease beneath the soil amended layers is noted. For the top soil layer, an exception for denitrifier gene copies at the surface from the seven sampling dates is on Jul 21st 2011 probably due to the full saturation for days in mid-July. Below the top soil layer, the number of gene copies always thrives in the BAM layer, drops in the sand layer and then returns to different states in the parent soil due to different wet conditions. The reason may be related to the relatively high residual moisture content in the

BAM layer which provides a nurturing environment for the denitrifying bacteria growth. The sand layer usually had lower soil moisture than the other layers.

It should also be noted that the number of copies in the BAM layer are greater than those in the stockpile of media before construction. This may be because of the residual moisture content of the amended layer. The stock pile had a tendency to lose moisture as it was exposed to the atmosphere. These gene copies for denitrifying organisms provide additional justification for the removal of nitrogen.
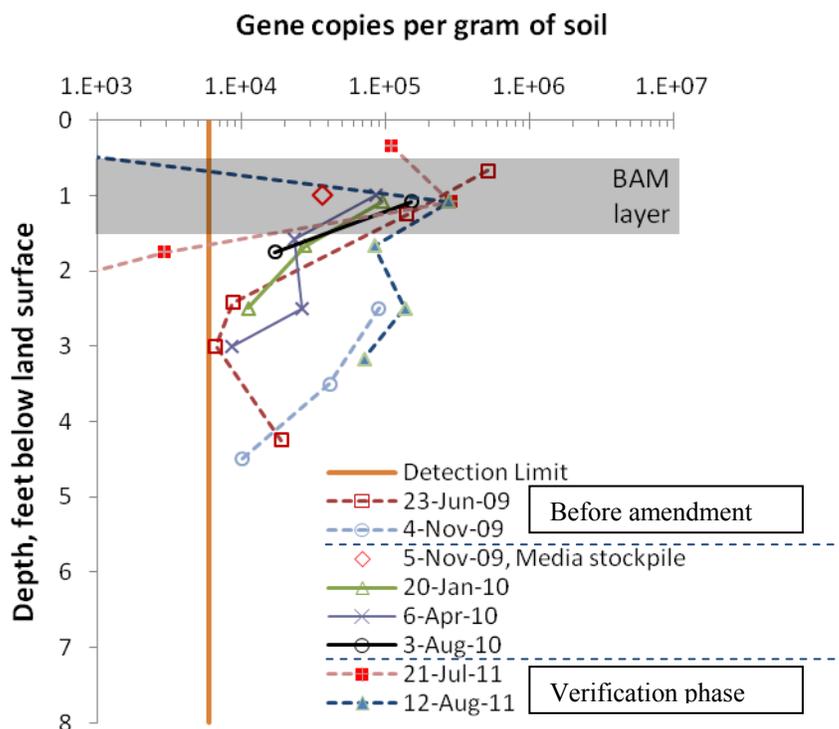
Figure 45 Verification Phase Denitrifier activity inferred from nitrite reductase gene density measured by real-time PCR at the Hunters Trace basin.

CHAPTER 5: CONCLUSIONS AND RECOMMENDATIONS

Summary

A wide variety of hydrologic, soil, water chemistry, isotope, dissolved gas, and microbiological data were analyzed to provide a quantitative process-based understanding of denitrification and other biogeochemical processes occurring beneath the South Oak (SO) and Hunters Trace (HT) retention basins in Marion County, Florida. At the SO site, cyclic variations were present in many important redox sensitive constituents in the shallow ground water system, such as DO, NO_3^-, Mn, Fe, and DOC. These cyclic variations coincide with generally wet and dry hydroclimatic conditions, with oxidizing conditions occurring at the beginning of wet periods followed by reducing conditions. The presence of subsurface O_2 was a key factor controlling the biogeochemical processes, such that when O_2 was present the C cycle was limited to aerobic oxidation of OC, and the N cycle was effectively limited to ammonification, nitrification, and assimilation. However, once DO was depleted, the O_2 cycle was truncated thus allowing anoxic conditions to prevail and anaerobic oxidation of OC. Therefore, DOC provided by a large solid-phase reservoir of OC served as the predominant electron donor for NO_3^-, Mn, and Fe reduction, even progressing to methanogenesis during highly reducing conditions caused by prolonged surface water retention. At the HT site, advection-dominated transport of NO_3^- prevailed due to the persistent aerobic conditions and permeable soils.

The presence or absence of DO in the subsurface at the SO site was strongly controlled by soil texture. The fine-grained soil maintained a generally high water table, and even as the underlying water table dropped the vadose zone remained wet or nearly saturated during

prolonged dry periods (saturations exceeding 70%). A fine textured soil that remains wet during prolonged dry periods will promote anoxic conditions because: (1) the diffusion coefficient of O_2 through water is 10^4–10^5 times less than through air; and (2) the gas diffusion coefficient in soil is proportional to the square of the volumetric gas-phase content (Jin and Jury, 1996). A fine-grained soil remains wet for extended periods because of capillary wicking and adhesion of soil water in the narrow pores (Koorevaar et al. 1983). Based on the measured soil moisture contents and SMRCs at each site, soils that maintain a water saturation greater than 90% (conversely, a gas-phase fraction less than 10%) are expected to significantly inhibit surface/subsurface O_2 exchange, thus helping to produce denitrifying conditions.

The contrasting conditions at the SO and HT sites provide valuable insight into natural biogeochemical processes beneath stormwater infiltration basins in subtropical environments and the salient factors that affect these processes. Hossain et al. (2009) describes the application of functionalized soil amendments for mitigating ground water quality impacts of stormwater infiltration basins, with emphasis on reducing NO_3^- leaching. Combining such soil amendments with replication of the soil and biogeochemical conditions documented at the SO site may lead to a new stormwater infiltration design for improving ground water quality.

Construction of the new integrated design at the HT basin was performed November 3-6, 2009 in accordance with the specifications outlined in the Environmental Resource Permit approved by the St. Johns River Water Management District. The alternative design implemented at the HT basin is based on combining functionalized soil layers to replicate the soil and biogeochemical conditions documented at the SO site. This design involves integrating pollution and flood control basins into a single retention basin. Several important criteria were outlined and the integrated design was developed to meet these:

1) Maintain the flood control capacity of the original retention basin;

2) Reduce the NO_3^- loading to ground water by implementing a passive pollution control technology that promotes potentially self-sustaining natural biogeochemical processes for NO_3^- removal; and

3) Maximize economic feasibility by minimizing design and construction costs and maintain operation and maintenance costs comparable to existing retention basin designs.

The process is also deemed economical as construction and materials cost was only about $6.00 per square foot of basin bottom. This cost did not include profit and permit fees. There is minimal to no additional operation and maintenance cost, and operation, maintenance, and repairs are similar to those expected with existing retention basins.

Field monitoring was conducted to assess both the nutrient removal and hydraulic performance of the new integrated basin design. Monitoring was conducted November 2009 – August 2010 in order to cover a variety of hydroclimatic conditions and all four seasons. Decreases in NO_3^- of up to 45% in shallow ground water beneath the Pollution Control Basin, as inferred by comparison with Cl, could be caused by denitrification, dissimilatory nitrate reduction to ammonium (DNRA), microbial assimilation, plant uptake, or some combination of these processes. Microbial assimilation generally is not a major sink for NO_3^- and plant uptake probably was not substantially different before or after construction of the new integrated design. Soil gas, NO_3^- and N_2 isotopes, and denitrifier activity by real-time PCR provide results consistent with denitrification. Possible DNRA is suggested by increased KCl extractable NH_4^+ in the amended soil layer in August 2010 compared to samples collected in January and March

2010. Under such dynamic conditions of rapid infiltration beneath a retention basin, net water quality effects in the shallow ground water would be related to the intensity and duration of denitrification and mixing ratios with non-denitrified water. The water chemistry, soil and dissolved gas, and isotopic analyses at the HT basin after construction of the new integrated design suggest that NO_3^- losses are attributable to both denitrification, which probably is intermittent, and possibly DNRA. Intermittent denitrification likely is supported by the increased soil moisture conditions of the Pollution Control Basin and resultant reductions in surface/subsurface oxygen exchange. Substantial decreases exceeding 70% for both TDP and PO_4^{3-} occurred in the vadose zone beneath the Pollution Control Basin both within and below the amended soil layer. These reductions in P concentrations are consistent with sorption likely due to the tire crumb and clay content of the amended soil layer, and similar results were reported by Hossain et al. (2009) for a sorption media comprising 50% sand, 20% limestone, 15% sawdust, and 15% tire crumb. However, P reductions in the vadose zone may also be partly due to lower P concentrations in the stormwater that occurred after construction of the new integrated design.

Conclusions

First and foremost, the SO basin did remove nitrogen from the stormwater and the unmodified HT basin did not. Because of the success due primarily to the soil conditions in the SO basin bottom, the soil conditions were replicated for a modified HT basin design. Thus, within this publication is information that demonstrates and promotes a design to remove nitrogen using soil amendments for stormwater retention basins. For the HT basin, the original design was most likely (permit not available but runoff calculations are available) based on holding the runoff from the 25 year/24 hour rain event with a 3 inch/hour infiltration rate. When the HT basin was modified to provide an area for pollution control as well as an area for flood

control but using only the runoff from an EIA of 4.1 acres, the volume of the basin was sufficient for the 100 year rain event and the infiltration rates as measured in the basin were used. The original design also left a free board of about 2.5 foot or room for additional storage, possibly for the 100 year storm event, but that could not be verified. For most retention basins similar in design to Hunters Trace, the basin area or volume will most likely be sufficient because not all of the amended pond volume is used for infiltration or there remains a portion of the pond volume that will continue to infiltrate at a higher rate during large runoff events.

The water quality measurement data after modification shows a basin that does remove nitrogen before it enters the ground water. Thus, an integrated pollution and flood control design was achieved that can function to remove nitrogen within this type of existing retention basin design. For newly constructed basins, the design can also be used. A limiting infiltration rate of 0.25 in/hr is recommended for design purposes using the soil augmentation design of this work. Monitoring of the storage after storm events at HT basin supports this statement. The design information can be used to promote and educate builders, engineers, scientists, private citizens, government officials, and students on the benefits of an alternative design to reduce nitrate movement into the ground water from retention systems by integrating pollution and flood control at a single site without substantially increasing the size of a retention basin designed for a 100-year storm event.

Furthermore, it should be understood that the soil augmentation used in this research for nitrogen removal also can be applied in an off line retention treatment system. The idea of bottom soil augmentation can be used in any retention system including underground retention, exfiltration systems, or swales. It is anticipated that the soil augmentation will better protect

ground water quality by enhancing nitrogen removal, as well as to demonstrate an environmental awareness and cost savings relative to other methods.

Another benefit of the soil augmentation is the use of Florida naturally occurring soils and blending them with recycled materials. The process is also deemed economical as the conversion of the Hunters Trace basin initial cost was only about $6.00 per square foot of basin bottom. This cost did not include profit and permit fees. There is minimal to no additional operation and maintenance cost, and operation, maintenance, and repairs are similar to those expected with existing retention basins.

Recommendations

It is recommended that the information in this report be used as a learning tool for the design of stormwater retention systems in the State of Florida and especially in Karst sensitive areas, springsheds, or where ground water quality is a concern. The installation of soil augmentation is not difficult and common existing construction methods are used. The soil augmentation used at the Hunters Trace basin should be considered for other retention basins and for low impact development management methods.

Design recommendations for an integrated pollution and flood control basin are:

1. The soil augmentation materials used in this research should be specified as one option to remove nitrogen and phosphorus in retention basins. Specifications on soil augmentation blend would include the following: 1:2:4 mix of tire crumb to clay to sand by volume, an infiltration rate of 0.25 inch/hour or less, organic content less than 5% by volume, unit weight of no more than 90 pounds/cubic foot at maximum compaction, and a minimum of 40-50% soil saturation (percentage of water-filled void space).

2. An objective of a pollution control basin is to capture a fraction of the runoff water and remove the pollutants before discharging to a ground water or surface water area. For small areas, there may be a first flush event which means that the early part of runoff may (but not always) have the greatest amount of pollution mass relative to the total runoff. Thus, the pollution control basin should be located before a flood control basin. This will permit the capture and infiltration of the largest portion of pollution during a runoff event.

3. For design of an infiltration basin, there are two commonly used procedures. The first assumes that infiltration will occur but does not account for it during the runoff event. With the average rainfall duration of Florida storms being around 1.5 hours, not accounting for infiltration during runoff appears to be a reasonable approach since in a short runoff time period (say on the average about 3 hours), the amount infiltrated is not a significant part of the total when considering an infiltration rate of 0.25 in/hr, and there are other design parameter estimates that may influence the results more significantly such as the EIA. For this design, the depth of the basin depends on the drainage time. If the basin has to be drained in 72 hours, then the maximum depth of the pollution control basin is 1.5 feet [(.25 in/hr / 12 in/ft) × 72hr)]. This may be attainable for on-site retention of water in swales and bioretention areas. However for regional basins, the depth of storage may need to be deeper or the 72 hour constraint changed to 120 hours. For the HT basin, a 120 hour recovery time is calculated. At the regional level and from the experience of both the SO and HT basins, there is water in storage for time periods longer than 72 hours for storm events greater than 3 inches. Results at the SO and HT basins indicate that an increase in the 72 hour constraint on drainage will promote

conditions more favorable for nitrogen removal. Thus for regional basins, it is recommended that the basin be designed using a simulation procedure and a 120 hour recovery period.

4. The second design procedure uses a simulation given a rainfall record and data on the infiltration rates. This assumes that there are accurate or at least reasonable support data for rainfall and for infiltration rates over time. The infiltration basin at Hunters Trace was designed using a mass-balance simulation of rainfall and a limiting infiltration rate from actual operation of the pollution control basin over time. From the simulation, the fraction of yearly water infiltrated is calculated. The simulation is an option for design. However for basins not constructed, the availability of infiltration data is limiting and sometimes not accurate. For the HT basin, the amended soils had a limiting rate of (0.25 in/hr) and was higher than the compacted laboratory estimates (0.03 - 0.13 in/hr). Using the simulation model of this work with 2004–2005 rainfall and an infiltration rate of 0.25 in/hr, a 3 inch storage volume will reduce the annual runoff by 86%. Thus, storage of runoff from 3 inches of rainfall is recommended for design to attain at least 85% retention. The pollution control basin storage is calculated as 3 inches times the EIA. The EIA is calculated using the design rain event.

5. For an integrated pollution and flood control basin, the berm separating the basins should be designed to minimize erosion of the berm. This can be achieved using a shallow side slope (1v:10h was used for the HT basin) and erosion control protection. The berm height for the HT integrated basin was 2.5 feet above the basin bottom.

6. The subsurface soil percolation rates must exceed 0.25 inch/hour so that there will be no decrease in the amended layer infiltration and percolation rates.

While nitrogen reduction is achieved by the new integrated design for a relatively low cost, several areas where further research would be beneficial were identified. Further monitoring of nitrogen species, major element, and dissolved oxygen concentrations at monthly to quarterly intervals would provide valuable data on long-term sustainability of the nitrogen removing capabilities. Continued hydrologic monitoring and denitrifier quantification by real-time PCR would provide opportunities for better understanding of the physical and microbial processes controlling the environmental effectiveness of the new integrated design. Such additional data would promote future development and refinement of design guidelines for functionalized soil augmentation that may be applied under a wide range of environmental conditions.

REFERENCES

Aeschbach-Hertig, W., El-Gamal, H., Wieser, M., and Palcsu, L., 2008, Modeling of excess air and degassing in ground water by equilibrium partitioning with a gas phase: Water Resources Research, v. 44, W08449.

Antweiler, R.C., R.L. Smith, M.A. Voytek, J.K. Böhlke, and K.D. Richards. 2004. Water Quality Data from two Agricultural Drainage Basins in Northwestern Indiana and Northeastern Illinois: I. Lagrangian and Synoptic Data, 1999-2002: U.S. Geological Survey Open-File Report 2004-1317. 206 p.

Braker G, Fesefeldt A, Witzel KP. 1998. Development of PCR primer systems for amplification of nitrite reductase genes (nirK and nirS) to detect denitrifying bacteria in environmental samples. Appl Environ Microbiol 64:3769–3775

Bohlke, J.K., Harvey, J.W., and Voytek, M.A., 2004, Reach-scale isotope tracer experiment to quantify denitrification and related processes in a nitrate-rich stream, midcontinent United States, Limnol. Oceanogr., 49(3), 821–838

Busenberg, E., Plummer, L.N., and Bartholomay, R.C., 2001, Estimated age and source of the young fraction of ground water at the Idaho National Engineering and Environmental Laboratory. U.S. Geological Survey Water-Resources Investigations Report 01-4265 (DOE/ID-22177), 144p.

Casciotti, K.L., Sigman, D.M., Galanter Hastings, M., Böhlke, J.K., and Hilkert, A., 2002, Measurement of the oxygen isotopic composition of nitrate in seawater and freshwater using the denitrifier method: Analytical Chemistry, v. 74, p. 4905-4912.

Chapelle, F.H., P.B. McMahon, N.M. Dubrovsky, R.F. Fujii, E.T. Oaksford, and D.A. Vroblesky. 1995. Deducing the distribution of terminal electron-accepting processes in hydrologically diverse ground water systems. Water Resources Research 31, no. 2: 359–371.

Christensen, S., S. Simkins, and J.M. Tiedje, 1990a, Spatial Variation in Denitrification: Dependency of Activity Centers on the Soil Environment, Soil Science Society of America Journal 54:1608-1613

Christensen, S., S. Simkins, and J.M. Tiedje, 1990b, Temporal Patterns of Soil Denitrification: Their Stability and Causes, Soil Science Society of America Journal 54:1614-1618

Clark, I.D., and Fritz, Peter, 1997, Environmental Isotopes in Hydrogeology: Boca Raton, FL, CRC Press, 328 p.

Coplen, T. B., 1973, A double focusing, double collecting mass spectrometer for light stable isotope ratio analysis: International Journal Mass Spectrometry and Ion Physics, v. 11, p. 37-40.

Coplen, T.B., Böhlke, J.K., and Casciotti, K., 2004, Using dual-bacterial denitrification to improve delta 15N determinations of nitrates containing mass-independent 17O: Rapid Communications in Mass Spectrometry, v. 18, p. 245-250.

Coplen, T.B., Brand, W.A., Gehre, M., Gröning, M., Meijer, H. A. J., Toman, B, and Verkouteren, R. M., 2006, New guidelines for delta 13C measurements: Analytical Chemistry, v. 78, p. 2439-2441.

Coplen, T.B., A.L. Herczeg, and C. Barnes, 2000, Isotope Engineering—Using stable isotopes of the water molecule to solve practical problems, in Cook, P.G, and Herczeg, A.L. (eds.), Environmental tracers in subsurface hydrology: Boston, MA, Kluwer Academic Publishers, p. 79-110.

Coplen, T. B., Wildman, J. D. and Chen, J., 1991. Improvements in the Gaseous Hydrogen-Water Equilibration Technique for Hydrogen Isotope Ratio Analysis, Analytical Chemistry, v. 63, p. 910-912.

Craig, H., 1961, Isotopic variations in meteoric waters: Science, v. 133, p. 1702-1703.

Harper, H.H., and Herr, J.L., 1993, Treatment efficiencies of detention with filtration systems: St. Johns River Water Management District Special Publication SJ93-SP12, 263 p., 25 appendices.

Harris, W.G., V.W. Carlisle, and S.L. Chesser. 1987. Clay mineralogy as related to morphology of Florida soils with sandy epipedons. Soil Sci. Soc. Am. J. 51:1673-1677.

Hossain, F., Chang, N. & Wanielista, M. 2009. Modeling kinetics and isotherms of functionalized filter media for nutrient removal from stormwater dry ponds. Environmental Progress & Sustainable Energy, doi: 10.1002/ep.10415.

Jacobs, J., J. Mecikalski, and S. Paech. 2008. Satellite-based solar radiation, net radiation, and potential and reference evapotranspiration estimates over Florida. Technical report, University of New Hampshire, Department of Civil Engineering, Durham, NH, 138 p.

Jin, Y.J., and Jury, W.A., 1996, Characterizing the dependence of gas diffusion coefficient on soil properties: Soil Science Society of America Journal, v. 60, p. 66-71.

Kendall, Carol, 1998, Tracing nitrogen sources and cycling in catchments, in Kendall, Carol, and McDonnell, J.J. (eds.), Isotope tracers in catchment hydrology: Amsterdam, The Netherlands, Elsevier, p. 519-576.

Kendall, Carol, and Aravena, R., 2000, Nitrate isotopes in ground water systems, in Cook, P.G, and Herczeg, A.L. (eds.), Environmental tracers in subsurface hydrology: Boston, MA, Kluwer Academic Publishers, p. 261-297.

Koba, K., N. Tokuchi, E. Wada, T. Nakajima, and G. Iwatsubo. 1997. Intermittent denitrification: The application of a 15N natural abundance method to a forested ecosystem. Geochim. Cosmochim. Acta 61:5043–5050.

Korom, S.F. 1992. Natural denitrification in the saturated zone: A review. Water Resour. Res. 28:1657–1668.

Koorevaar, P., Menelik, G., and Dirksen C., 1983, Elements of soil physics: Amsterdam, Elsevier, 230 p.

Li, S.L., C.Q. Liu, F.X. Tao, Y.C. Lang, and G.L. Han. 2005. Carbon Biogeochemistry of Ground Water, Guiyang, Southwest China: Ground Water 43(4):494–499.

Marinco Bioassay Laboratory. 2009. Report # 090146, Sarasota Florida, February.

Mariotti, A., A. Landreau, and B. Simon. 1988. 15N isotope biogeochemistry and natural denitrification process in ground water: Application to the chalk aquifer of northern France. Geochimica et Cosmochimica Acta, 52:1869-1878.

McMahon, P.B., and F.H. Chapelle. 2007. Redox processes and water quality of selected principal aquifer systems. Ground Water 46: 259–271. doi: 10.1111/j.1745-6584.2007.00385.x

Naujock, L. 2008, Development of Hydraulic and Soil Properties for Soil Amendments and Native Soils for Retention Ponds in Marion County, Florida. MS Thesis, University of Central Florida, Orlando Fl.

O'Reilly, A.M., Chang, N.B., and Wanielista, M.P., 2007, Data mining analysis of nitrate occurrence in ground water in central and northeast Florida and an overview of stormwater best management practices for nitrate control, *in* 9th Biennial Stormwater Research and Watershed Management Conference, Proceedings May 2-3, 2007, Orlando, Fla. University of Central Florida Stormwater Management Academy, Orlando, Fla.

Parkin, T.B., 1987, Soil Microsites as a Source of Denitrification Variability, Soil Science Society of America Journal, 51:1194-1199

Pennell, K.D. 2002. Specific Surface Area. In Methods of Soil Analysis: Part 4 – Physical Methods. Madison, Wisconsin: Soil Science Society of America, Inc.

Phelps, G.G., 2004, Chemistry of ground water in the Silver Springs basin, Florida, with emphasis on nitrate: U.S. Geological Survey Scientific Investigations Report 2004-5144.

Rao, D.V., 1988, Rainfall Analysis for Northeast Florida Part VI: 24-Hour to 96-Hour Maximum Rainfall for Return Periods 10 Years, 25 Years, and 100 Years: St. Johns River Water Management District Technical Publication 88-3, 47 p.

Révész, Kinga, and Casciatti, Karen, 2007, Determination of the delta ($^{15}N/^{14}N$) and delta ($^{18}O/^{16}O$) of nitrates in water: RSIL Lab Code 2900, chap. C17 of Révész, Kinga, and Coplen, Tyler B., eds., Methods of the Reston Stable Isotope Laboratory: Reston, Virginia, U.S. Geological Survey, Techniques and Methods, book 10, sec. C, chap. 17, 24 p.

Révész, K., and Coplen, T.B., eds., 2006, Methods of the Reston Stable Isotope Laboratory: U.S. Geological Survey Techniques and Methods, book 10.

Révész, Kinga, and Coplen, T.B., 2008a, Determination of the delta ($^{2}H/^{1}H$) of water: RSIL lab code 1574, chap. C1 of Révész, Kinga, and Coplen, T.B., eds., Methods of the Reston Stable Isotope Laboratory: U.S. Geological Survey Techniques and Methods 10–C1, 27 p.

St. Johns River Water Management District, 2005, Applicants Handbook: Regulation of stormwater management systems: Palatka, Florida, 287 p.

Seitzinger, S.P., J. Harrison, J.K. Böhlke, A.F. Bouwman, R.R. Lowrance, B.J. Peterson, C.R. Tobias, and G. van Drecht. 2006. Denitrification across landscapes and waterscapes: A synthesis. Ecol. Appl. 16:2064–2090.

Schiffer, D.M., 1988, Effects of three highway-runoff detention methods on water quality of the surficial aquifer system in central Florida: Water-Resources Investigations Report 88-4170, 79 p.

Schipper, L.A., and Vojvodic-Vukovic, Maja, 2000, Nitrate removal from ground water and denitrification rates in a porous treatment wall amended with sawdust: Ecological Engineering, v. 14, no. 3, p. 269-278.

Schipper, L.A., and Vojvodic-Vukovic, Maja, 2001, Five years of nitrate removal, denitrification and carbon dynamics in a denitrification wall: Water Research, v. 35, no.14, p. 3473-3477.

Schipper, L.A., Barkle, G.F., Hadfield, J.C., Vojvodic-Vukovic, Maja, and Burgess, C.P., 2004, Hydraulic constraints on the performance of a ground water denitrification wall for nitrate removal from shallow ground water: Journal of Contaminant Hydrology, v. 69, no. 3, p. 263-279.

Shaddox, T.W., 2004, Investigation of soil amendments for use in golf course putting green construction: PhD dissertation, University of Florida, 123 p.

Smith, R.L., S.P. Buckwalter, D.A. Repert, and D.N. Miller. 2005. Small-scale, hydrogen-oxidizing-denitrifying bioreactor for treatment of nitrate-contaminated drinking water. Water Research 39, 2014-2023.

Spechler, R.S., and Halford, K.J., 2001, Hydrogeology, water quality, and simulated effects of ground-water withdrawals from the Floridan aquifer system, Seminole County and vicinity, Florida: Water-Resources Investigations Report 01-4182, 116 p.

Tiedje, J.M. Weaver, RW, S. Angle, P. Bottomley, D. Bezdicek, S. Smith, A. Tabatabi, and A. Wollum (eds.) Methods of soil analysis. Part 2: Microbiological and biochemical properties, ASA, SSSA, CSSA, Madison, WI.

U.S. Geological Survey, 1998, National field manual for the collection of water quality data: U.S. Geological Survey Techniques of Water-Resources Investigations, book 9, chaps. A1–A9, 2 v., variously paged. (Also available at http://water.usgs.gov/owq/FieldManual/)

Vogel, J.C., A.S. Talma, and T.H.E. Heaton. 1981. Gaseous nitrogen as evidence for denitrification in ground water. J. Hydrol. 50:191–200.

Walkley A. and I. A. Black. 1934. An examination of Degtjareff method for determining soil organic matter and a proposed modification of the chromic acid titration method. Soil Sci. 37: 29-38.

Wallenstein, M.D., D.D. Myrold, M. Firestone, AND M. Voytek. 2006. Environmental controls on denitrifying communities and denitrification rates: Insights from molecular methods. Ecological Applications, 16(6): 2143–2152

Wang, H.D., W.G. Harris, and T.L. Yuan. 1989. Phosphate minerals in some Florida phosphatic soils. Soil and Crop Soc. Fla. Proc. 48:49-55.

Wanielista, M.P., and Hardin, Mike, 2006, Stormwater management assessment of green roofs with irrigation: Proceedings of the 2nd Biennial Stormwater Management Research Symposium, May 4-5, 2006, Orlando, Florida, p. 153-163.

Wanielista, M.P., and Hulstein, Ewoud, 2006, Stormwater irrigation volume I: Evapotranspiration and nitrate reduction after biofiltration to reduce health risks: Stormwater Management Academy, University of Central Florida, 101 p.

Wanielista, M.P., Miller, Robert, and Pernezny, Ben, 2006, Stormwater irrigation volume II: Cyanobacteria counts with toxin concentrations in stormwater ponds and after biofiltration to reduce health risks: Stormwater Management Academy, University of Central Florida, 108 p.

Wilde, F.D. and Radtke, D.B., 1998, Field measurements, in National field manual for the collection of water-quality data: U.S. Geological Survey Techniques of Water-Resources Investigations, book 9, chap. A6.

Xuan, Z., N.B. Chang, A. Daranpob, and M. Wanielista. 2009. Initial Test of a Subsurface Constructed Wetland with Green Sorption Media for Nutrient Removal in On-site Wastewater Treatment Systems. Water Qual Expo Health (2009) 1: 159–169 DOI 10.1007/s12403-009-0015-6

.

APPENDICES

Appendix A: Laboratory method reporting limits.

Type	Analyte	Reporting Limit	Units
Nitrogen	Nitrogen, ammonia, filtered	0.02	mg/L
	Nitrogen, nitrite, filtered	0.002	mg/L
	Nitrogen, nitrite + nitrate, filtered	0.016	mg/L
	Total nitrogen (NH3+NO2+NO3+Organic), filtered	0.06	mg/L
	Total nitrogen (NH3+NO2+NO3+Organic), unfiltered	0.06	mg/L
Phosphorus	Phosphorus, filtered	0.006	mg/L
	Phosphorus, phosphate, ortho, filtered	0.006	mg/L
	Phosphorus, unfiltered	0.008	mg/L
Trace Metals	Nickel, filtered	0.06	ug/L
	Nickel, unfiltered	0.16	ug/L
	Copper, filtered	0.4	ug/L
	Copper, unfiltered	1.2	ug/L
	Zinc, filtered	0.6	ug/L
	Zinc, unfiltered	2	ug/L
	Lead, filtered	0.12	ug/L
	Lead, unfiltered	0.06	ug/L
	Chromium, filtered	0.12	ug/L
	Chromium, unfiltered	0.6	ug/L
	Cadmium, filtered	0.04	ug/L
	Cadmium, unfiltered	0.018	ug/L
Electron Donors	Manganese, filtered	0.2	ug/L
	Manganese, unfiltered	0.6	ug/L
	Iron, filtered	2	ug/L
	Iron, unfiltered	2	ug/L
	Sulfate, filtered	0.18	mg/L
	Organic carbon, dissolved	0.4	mg/L
	Organic carbon, total	0.4	mg/L
Major Ions	Calcium, filtered	0.02	mg/L
	Calcium, unfiltered	0.014	mg/L
	Magnesium, filtered	0.014	mg/L
	Magnesium, unfiltered	0.002	mg/L
	Potassium, filtered	0.04	mg/L
	Potassium, unfiltered	0.16	mg/L
	Sodium, filtered	0.2	mg/L
	Sodium, unfiltered	0.5	mg/L
	Chloride, filtered	0.12	mg/L
	Boron, filtered	1.8	ug/L
	Solids, residue, 105 deg C, total, gravimetric	10	mg/L
	Solids, residue, 180 deg C, dissolved, gravimetric (TDS)	10	mg/L

Appendix B: Soil chemical characteristics. EC, electrical conductivity; CEC, cation exchange capacity; AEC, anion exchange capacity; AAO, acid-ammonium-oxalate extraction; CDB, citrate-dithionite-bicarbonate extraction.

Basin Site	Well	Depth (m)	Sand (%)	Silt (%)	Clay (%)	pH	EC (ds/m)	CEC (cmol/kg)	AEC (cmol/kg)	Al AAO (mg/kg)	Fe AAO (mg/kg)	P AAO (mg/kg)	Al CDB (mg/kg)	Fe CDB (mg/kg)	P CDB (mg/kg)
HT	M-0506	0.8	98.9	0.9	0.2	6.4	0.04	2.2	1.5	514	570	59	309	845	29
HT	M-0506	1.8	59.3	0.3	40.5	6.8	0.17	4.0	1.2	1040	250	145	626	308	37
HT	M-0506	3.6	48.1	6.3	45.6	6.5	0.08	9.0	1.5	2830	779	723	1700	961	86
HT	M-0506	6.1	54.2	9.2	36.7	6.4	0.05	8.1	2.0	1750	1140	590	1850	1750	85
HT	M-0506	8.2	45.8	12.1	42.1	6.5	0.07	16	0.8	2430	1910	10200	676	737	142
HT	M-0506	9.7	37.6	11.3	51.2	6.5	0.05	19	1.0	1060	882	13400	504	3470	111
HT	M-0507	8.2	43.0	10.8	46.3	6.4	0.03	20	0.1	4470	4820	10400	1320	5220	262
HT	M-0508	8.2	95.3	2.5	2.3	6.2	0.02	1.1	5.2	1060	191	187	695	258	30
HT	M-0509	8.2	63.1	7.1	29.9	6.4	0.05	3.5	1.6	2950	1270	10500	614	495	106
HT	M-0510	8.1	14.1	8.1	77.9	6.5	0.02	17	0.3	8190	11500	1060	6820	39200	370
SO	M-0511	0.7	58.8	11.5	29.8	7.2	0.18	30	4.6	3130	4360	3600	1330	5750	522
SO	M-0511	1.8	52.3	7.3	40.4	7.0	0.06	17	2.1	3540	3220	1470	1280	4200	598
SO	M-0511	3.0	7.5	38.0	54.6	5.5	0.18	52	0.4	5780	19800	2550	3390	22000	1050
SO	M-0511	5.1	36.6	17.5	46.0	5.6	0.13	33	0.4	1570	2610	634	3310	2930	189
SO	M-0511	8.2	54.8	3.9	41.4	5.5	0.10	15	0.8	2340	1850	7710	805	2970	214
SO	PW	0.5	84.5	8.9	6.6	--	--	--	--	1290	944	--	1050	627	--
SO	PW	0.9	55.8	5.8	38.4	--	--	--	--	3000	2040	--	1890	1330	--
SO	PW	1.5	20.2	7.4	72.4	6.3	0.05	42	1.9	9350	7020	3500	2630	3300	686
SO	PW	2.4	66.1	6.5	27.5	5.5	0.03	9.1	2.5	1850	5630	1440	2490	1980	853
SO	M-0513	6.7	18.3	18.4	63.4	5.8	0.09	34	0.8	2760	2550	13500	1230	1600	351
SO	M-0514	3.0	67.1	1.9	31.1	5.1	0.07	7.7	2.9	2550	478	888	1450	331	221
SO	M-0515	3.6	56.8	5.0	38.2	5.2	0.08	16.4	2.6	4220	1360	1450	2530	951	542
SO	M-0516	3.3	62.4	5.9	31.8	6.0	0.12	17	2.2	3300	4040	2860	1910	2220	1550
SO	M-0521	3.0	68.5	2.0	29.5	5.8	0.07	7	2.5	2990	2010	1350	1880	1370	499

Appendix C: Grant Information

Original Grant Budget $ 315,601

Original Match Budget $ 500,000

Budget Revisions $ 75,000

Actual Grant Expenditures $ 359,307.74

Actual Match Expenditures $ 500,000.00

Total actual cost $ 859,307.74